論文 / 著書情報
Article / Book Information

題目(和文)	
Title(English)	Development of Pneumatic Booster Valve with Energy Recovery
著者(和文)	イムジョンハ
Author(English)	Jongha Lim
出典(和文)	学位:博士(工学), 学位授与機関:東京工業大学, 報告番号:甲第11509号, 授与年月日:2020年3月26日, 学位の種別:課程博士, 審査員:只野 耕太郎,石田 忠,金 俊完,沖野 晃俊,吉田 和弘
Citation(English)	Degree:Doctor (Engineering), Conferring organization: Tokyo Institute of Technology, Report number:甲第11509号, Conferred date:2020/3/26, Degree Type:Course doctor, Examiner:,,,,
学位種別(和文)	博士論文
Type(English)	Doctoral Thesis

Tokyo Institute of Technology

2020 doctoral thesis

Development of Pneumatic Booster Valve with Energy Recovery

Human Centered Science and Biomedical Engineering,

Doctoral Program

17D10105 Jongha Lim

Adviser: Kotaro Tadano

Contents

Nomenclature

A	[m2]	Area
b_1	[Yen/m]	Price per unit length of an air cylinder
b_2	[Yen]	Basic price
c	[kg/s]	Viscous friction coefficient
e	[-]	Energy saving ratio
E	[J]	Energy
E_e	[Wh]	Electric energy consumption
E_v	[Yen/m^3]	Electricity charge per unit volume
f	[N]	Friction force
f_s	[N]	Static friction force
G	[kg/s]	Mass flow rate
k_e	[-]	Recovery ratio
k_p	[-]	Boost ratio
k_r	[-]	Area ratio
k_v	[-]	Effective consumption rate
l	[m]	Length of a stroke
m	[kg]	Mass of gas
M	[-]	Motor load factor
n	[-]	Number of strokes
N	[-]	Total number of stroke with no dead volume
$\widehat{N}$	[-]	Total number of stroke with dead volume

p	[Pa]	Pressure
$\bar{p}$	[Pa]	Average pressure
p_{T}	[Pa]	Pressure of air tank with no dead volume
$\hat{p}_{\mathrm{T}}$	[Pa]	Pressure of air tank with dead volume
P	[W]	Air power
q	[-]	A ratio that PBV or PBV-R is necessary
Q	[L/min(ANR)]	Flow rate
R	[J/kg K]	Ideal gas constant
s	[km]	Lifespan of an air cylinder
t	[s]	Time
T	[K]	Temperature
u	[m/s]	Velocity
v	[m^3]	Dead volume
V	[m^3]	Volume
w_c	[Yen]	Cost loss
w_d	[Yen]	Cost of an air cylinder
W	[J]	Work
x	[m]	Distance
α	[-]	Dead volume rate
η	[-]	Energy efficiency
κ	[-]	Specific heat ratio

subscript

a	Atmosphere
all	The entire
b	Boost cylinder
$b1/b2$	Boost Chamber 1/2
comp	Air compressor
D	Drive cylinder
$d1/d2$	Drive chamber 1/2
e	Expansion cylinder
$e1/e2$	Expansion chamber 1/2
in	Inlet/Input
ideal	Ideal
n	*n*th
out	Outlet/Output
PBV	Value of pneumatic booster valve
PBVR	Value of pneumatic booster valve with energy recovery
s	Supply
T	Air tank

Chapter 1

Introduction

1.1 Pneumatic Systems

Pneumatic systems are extensively used for relatively high power-to-weight and cleaner and lower cost than hydraulic systems in industries, such as robot, manufacturing industry and environment management systems [1,2,3]. For example, beverage plants, as shown in Fig.1-1(a), and sewage treatment plants, as shown in Fig.1-1(b), also utilize pneumatic systems for keeping the factories clean even in operation and generating a lot of air, respectively [4,5]. Moreover, in automobile industry, as shown in Fig.1-1(c), and semiconductor industry, as shown in Fig.1-1(d), which are one of major industries in the world, pneumatic systems are indispensable to many manufacturing processes [9]. The pneumatic system is closely related to our

(a) Beverage plant

(b) Sewage treatment plant

(c) Automobile Plant

(d) Semiconductor plant

Fig.1-1. Plants utilizing pneumatic systems [6,7,8,9] lives, especially in the field of robot. Due to the advantage explained above, pneumatic systems are also applied to surgical robots. As shown in Fig.1-2(a), Riverfield inc. has developed EMARO, which is the world's first pneumatically driven endoscope manipulator robot [10]. Also, several studies have suggested and developed rehabilitation wearable robots by using pneumatic system e.g. wearable glove for rehabilitation by Xiloyannis, M. *et al.*, as shown in Fig.1-2(b) [11,12,13]. Furthermore, humanoid robots and rescue robots that adopted pneumatic systems, as shown in Fig.1-2(c) and Fig.1-2(d), have been developed by Kurumaya, S. *et al.* and Tsukagoshi, H. *et al.*, respectively [14,15].

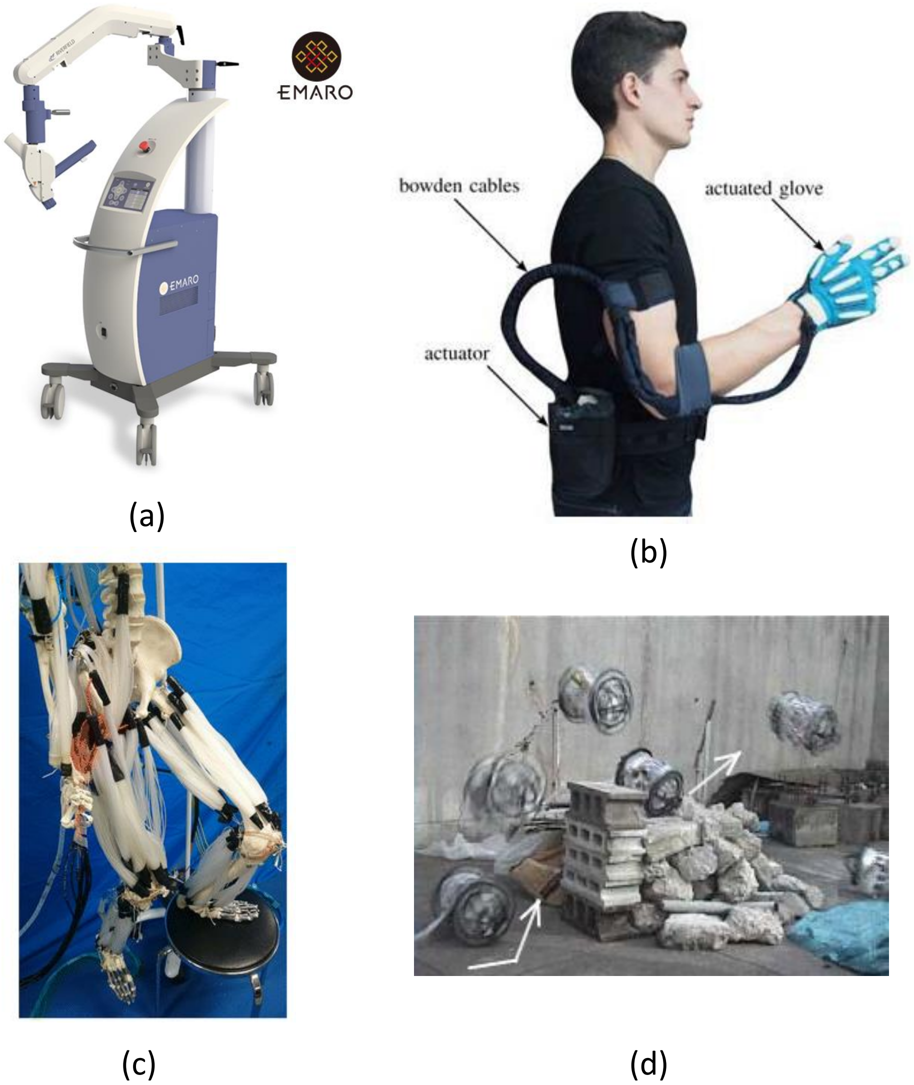

Fig.1-2. Application of pneumatic system to (a) surgical robot, (b) rehabilitation wearable robot, (c) humanoid robot and (d) rescue robot [10,13,14,15]

In recent years, the demands of pneumatic systems have been rapidly increasing. As represented in Fig.1-3, manufacturing output of both automobile and semiconductor in Japan rises 7% and 40% in the last 5 years, respectively, which causes an 64.5% increase of manufacturing output of pneumatic device in the last 7 years, according to the report of Japan Fluid Power Association [16,17,18]. Electric energy consumption of pneumatic systems has also increased as the demands of pneumatic systems have increased. According to a report, industrial electric energy consumption accounts for 36% of total electricity [19]. Furthermore, as shown in Fig.1-4, the electric energy consumption of pneumatic compressors accounts for 14 % of total industrial electric energy consumption in Japan, while it accounts for up to 30 % in many countries [20,21,22,23]. Meanwhile, "Kyoto Protocol", which is an international treaty extending the 1992 United Nations Framework Convention on Climate Change, encourages major countries to reduce greenhouse gas emission [24]. Also, The Paris Agreement, which is an agreement within the United Nations Framework Convention on Climate Change (UNFCCC), has been signed in 2016 for dealing with greenhouse-gas-emissions mitigation, adaptation, and finance [25]. Furthermore, "the Law on

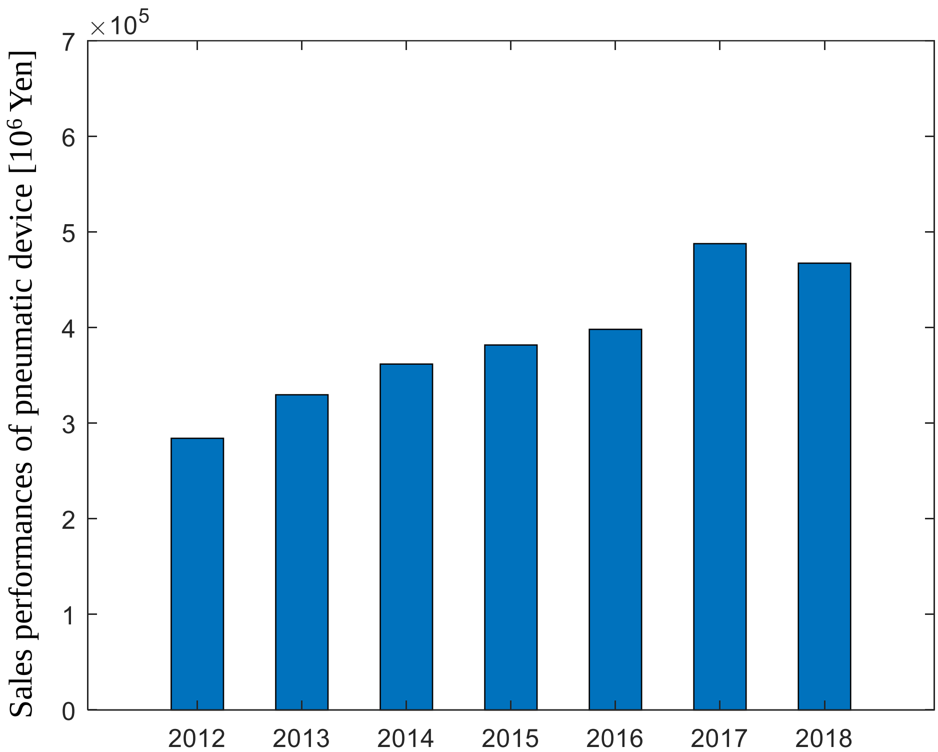

Fig.1-3. Annual sales performance of pneumatic device in Japan [18]

Rationalization of Energy Consumption", which is a decree of Japan enforced in 1979, has imposed a duty of reducing energy consumption upon industrial facilities [26]. Thus, electric energy consumption of pneumatic systems has to be inevitably reduced in many factories.

Many previous studies have been carried out for energy conservation of pneumatic systems. Rinoshika *et al.* showed that an energy saving method for pneumatic conveying systems they proposed can save power consumption of up to 34 percent [27]. Yang *et al.* suggested that a method of pneumatic drive system by using by-pass valve control can improve energy efficiency of up to 28 percent [28]. A research indicated that a control method for pneumatic servo systems they suggested can save 10 percent energy, by Al-Dakkan *et al* [29]. Also, Harris *et al.* and Ke *et al.* proposed a method of energy optimization for pneumatic actuator systems that can reduce use of 29 % compressed air [30,31]. However, one of the easiest method that can save electric energy consumption of pneumatic system without any device and control is to reduce pressure of air compressor. According to a report, as represented in Fig.1-5, at least 8% of electric energy used by a compressor operating can be conserved for every 0.1 MPa the pressure is reduced [32]. For this reason, many plants have attempted to reduce the air supply pressure, especially one automobile plant changed its air pressure from 0.6 MPa to 0.35 MPa, which led more than 20 % electric energy conservation.

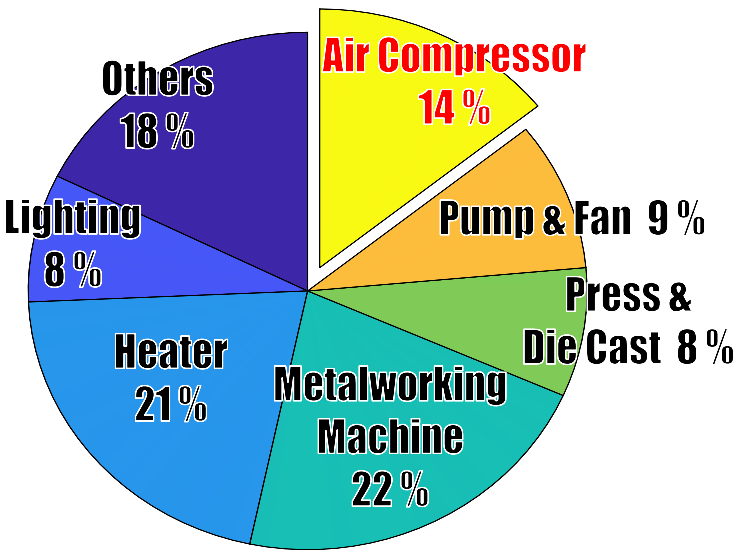

Fig.1-4. Details of electricity in a factory [20]

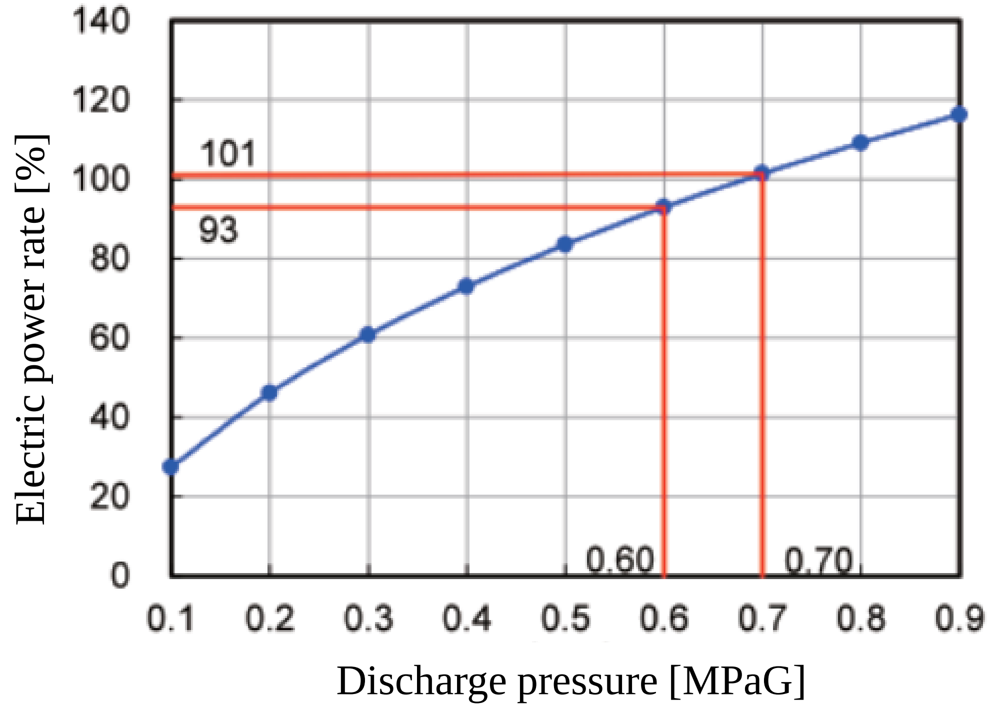

Fig.1-5. Relationship between discharge pressure and electric power [32]

However, although this is one of the simplest way for energy saving, it causes some problems in cases where factories need a high force e.g. a production process, short takt time, or press system. As shown in Fig.1-6(a), if supply pressure decreases from 0.6 MPa to 0.35 MPa, many processes in a plant operate without any trouble, while some processes is not able to be carried out with 0.35 MPa supply pressure. Thus, as shown in Fig.1-6(b), it is necessary for the processes that need high-pressure air to install air boosters partly in order to solve the trouble.

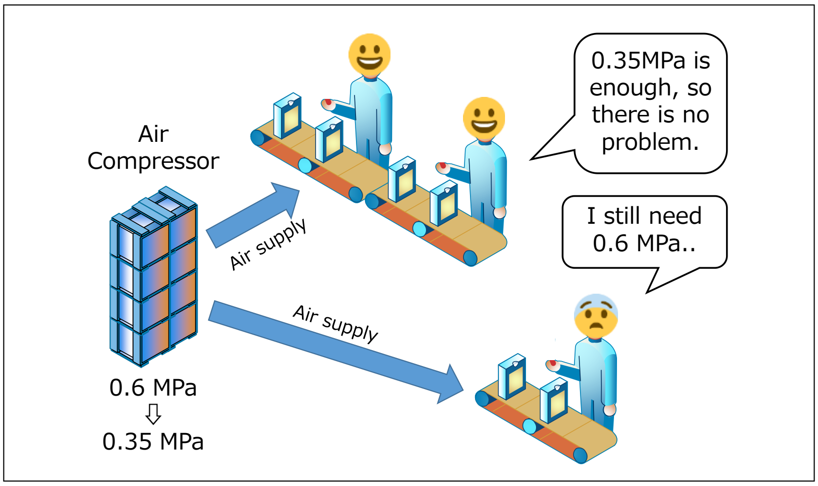

(a) A problem caused by decreased supply pressure

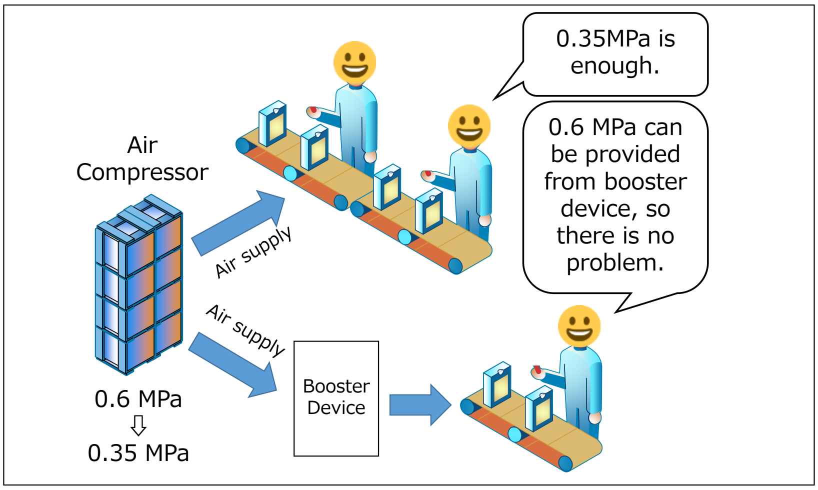

(b) A problem solved by adding a booster device

Fig.1-6. A problem caused by decreased supply pressure and solution

1.2 Development of Pneumatic Booster Valve

1.2.1 Proposition of Various Pneumatic Booster Valve

As mentioned above, local air boosters are needed for plants who reduced supply pressure. One of the idea what we can consider is to apply small air compressors to the process that need high-pressure air. For instance, compared with a big air compressor manufactured by ANEST IWATA as represented in Fig.1-7(a), which is usually used for a main compressor, one small air compressor manufactured by MAX shown in Fig.1-7(b) is generally less than 5 kW, while the main compressor consumes electric energy of more than 100 kW [33,34]. Thus, if the number of little air compressor for boosting air pressure partially is small when supply pressure is reduced, this solution is effective because a relatively enormous amount of electrical energy can be conserved. However, if the number of small air compressor reaches a certain value, the energy consumption of additional air compressors becomes bigger than the energy saved by reducing the supply pressure. Thus, we cannot say it is a general method for boosting air partly.

Another idea is to use a device that boosts air pressure without using electricity. According to resultant force, the air pressure in the small chamber called 'boost

(a) (b)

Fig.1-7. (a) Large main air compressor and (b) small air compressor [33,34] chamber' can be higher than initial state by pushing a piston from the other chamber called 'drive chamber'. With this principle, many booster devices have been proposed by patents. One-way booster devices have been suggested as Fig.1-8(a), which had been the most common method until 1980s [35]. This device, however, has problems that the boost chamber is too small and it takes much time to boost because the volume of compressed air made by each stroke is small. Moreover, the one-way booster device adopted one-way boosting process and the other way is not related to boosting process. To solve these problems, many patents had been presented to improve the booster device. One of the boost devices proposed by a patent is 'two-way booster device' that has improved the process of one-way booster device, as shown in Fig.1-8(b) [36]. The two-way booster device is literally a booster device that boosting process occurs in both ways by installing two boost chambers on both sides. The two-way booster device can reduce the boosting time to half. Nevertheless, this proposition still has problems that boost chambers are small that the boosting time is long, as well as the energy loss from drive chambers. Other patents have suggested the methods that improve the previous booster devices, but these are difficult to apply to booster devices due to complexity and a lot of additional components [37,38,39,40].

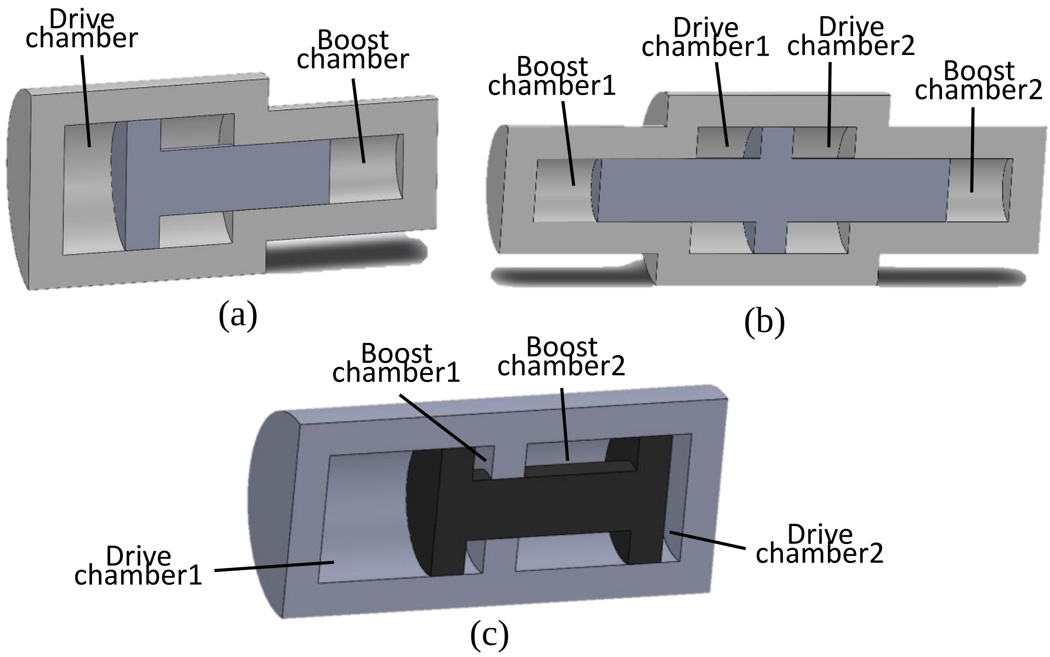

Fig.1-8. (a) one-way booster device, (b) two-way booster device and (c) pneumatic booster valve. [35,36,41]

Fig.1-9. (a) Symmetric pneumatic booster valve and (b) asymmetric pneumatic booster valve [44]

One of the methods that has markedly improved efficiency of the booster devices is suggested by K. Kishimoto [41]. The inventor proposed a new-shaped booster device as shown in Fig.1-8(c), also known as pneumatic booster valve (PBV). The PBV is, unlike the previous booster devices, has two pistons, two drive chambers and two boost chambers. This structure is able to make volumes of both chambers almost the same, which can greatly reduce the boosting time. Furthermore, the PBV exhausts only half of compressed air due to one more drive chamber, while the previous booster devices exhaust the entire compressed air. Thus, it is considered that the PBV is energetically more efficient than the previous booster devices. Many researchers have validated the PBV and the previous device has been superseded by the PBV that has been developed into product by SMC corporation, as represented in Fig.1-9(a), from 1990s [42,44]. Moreover, asymmetric PBV which has been presented by patent can boost the air four time, while previous PBV is symmetric and able to boost twice [43]. This asymmetric PBV has also been verified its validation by Shi *et al.* and developed into product by SMC corporation, as shown in Fig.1-9(b) [45].

1.2.2 Proposition of Pneumatic Booster Valve with Energy Recovery

Since PBV solves the problem caused by reducing supply pressure, PBV is effective in reducing electric energy consumption of an air compressor. However, PBV exhausts part of high-pressure air during the process, which causes energy loss, i.e., there is still room for improving the energy efficiency. To improve the energy efficiency, two methods can be considered: to apply the method of improving energy efficiency of an air cylinder or PBV. Stephan et al. studied to improve energy efficiency of pneumatic cylinders by using several extra solenoid valves and a controller [46]. Shi et al. carried out numerical research that PBV can be improved in terms of energy efficiency by using two extra solenoid valves and a controller [47,48]. However, those methods need extra components, which can make manufacturing cost higher, and use electrical energy, which can disturb improvement of energy efficiency. To supplement the weaknesses and to improve energy efficiency of PBV, Kagawa et al. proposed pneumatic booster valve with energy recovery (PBV-R) by patent [49]. Principle of PBV-R is similar to that of PBV, although the structure of PBV-R has one more air cylinder called 'Expansion Cylinder'. As shown in Fig.1-10, the Expansion Cylinder of PBV-R recovers and reuses high-pressure air exhausted from PBV without any solenoid valve and controller. Also, Yang et al. has shown the results of numerical simulation that energy efficiency of PBV-R is greater than that of PBV [50,51,52]. However, those results are from numerical simulation, which was carried out under several assumptions, e.g., there is no dead volume, temperature of the air in a tank is constant, etc. Those assumptions on numerical simulations generally make different results from actual experiment. Furthermore, even though simulation is implemented with no assumption, it is well-known that numerical simulations usually do not coincide with experimental result in fluid dynamics, especially gas dynamics and aerodynamics that deal with compressible fluid [53]. In the case of PBV or PBV-R, it can be considered as airflow in several closed systems that are comprised of two chambers and pipe, although the previous studies have not taken the pipe into consideration, which causes pressure drop. If it is steady flow and Reynolds number is constant, the pressure drop that is directly proportional to Darcy friction factor can be calculated [54,55,56,57,58]. Normally, however, unsteady flow occurs inside of PBV or PBV-R, which makes Reynolds number not constant and Darcy friction factor difficult to find. Several researchers have carried out numerical analysis of such closed systems and established the method of simulation of pneumatic systems including pipe [59,60]. However, since the studies show unneglectable errors between the result of the simulation and that of the experiment, experimental verification of validation of

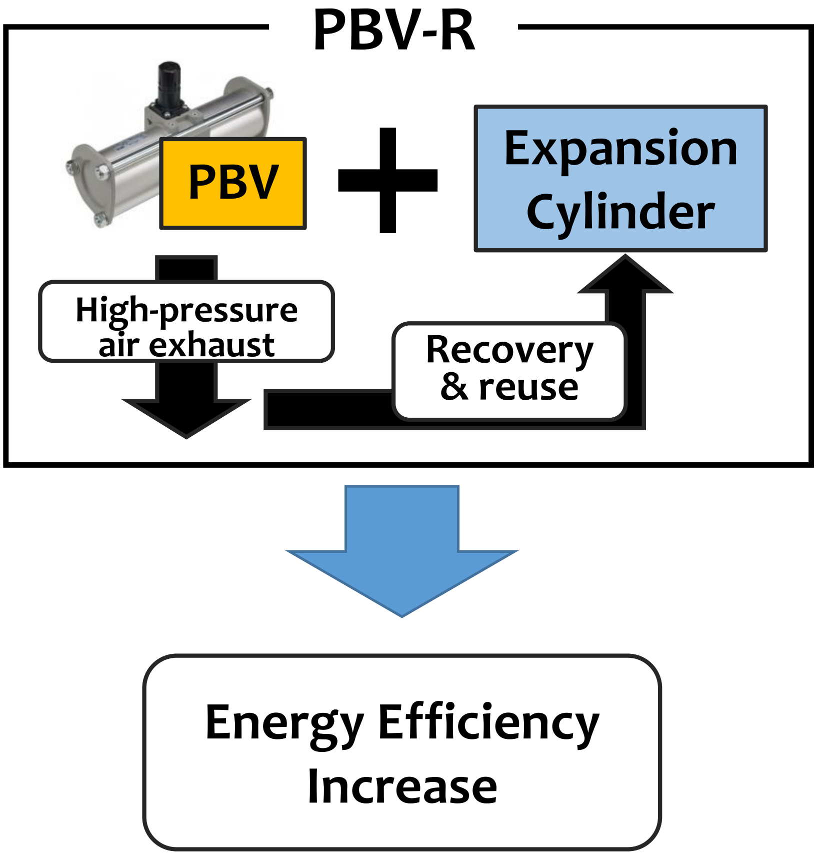

Fig.1-10. Concept of PBV-R.

PBV-R is required for precise results.

1.3 Purpose of this Thesis

As mentioned above, PBV-R is more efficient than PBV. Nevertheless, verification by an experiment is the most accurate method in fluid dynamics. Therefore, the first purpose of this thesis is to verify experimental validation of PBV.

Next, it is necessary to investigate the geometric design of PBV-R that maximizes performances, e.g. energy efficiency and boost ratio by experiment. For PBV-R, both area ratio and stroke length, for example, are two of the most important geometric parameters. According to previous studies, area ratio highly affects the performances of PBV-R, while stroke length does not have any effect on PBV-R [50,51,52]. However, as the explanation above, those results include some assumptions, i.e., those have not been verified by experimental validation. Therefore, in this thesis, we vary some geometric parameters and investigate how much effect do the parameters have on the performances of PBV-R.

Finally, we make prototype of PBV-R and compare the performances of both PBV and PBV-R. The conditions of the experiments above, e.g. dead volume and a diameter of pipe, are not the same as that of a real product. Therefore, it is necessary to make a prototype of PBV-R that is similar to a finished product and prove that the performances of PBV-R are better than that of PBV.

1.4 Structure of This Thesis

The structure of this research is shown is Fig.1-11. There are four chapters as following:

In Chapter 2, we make an experimental apparatus for examining both PBV and PBV-R. Then, using the apparatus, we measure and compare efficiency, boost ratio, and air consumption of PBV and PBV-R. In addition, because PBV-R has one additional cylinder for recovering and reusing energy, we investigate how much efficiency is improved by the expansion cylinder.

In Chapter 3, we make another experimental apparatus for examining PBV-R. Then, with this apparatus, we implement experiments on different conditions, i.e., various area ratios and stroke lengths, and verify how the performances of PBV-R change as the geometric parameters change. Also, we discuss the reason why do the stroke lengths have effect on the energy efficiency of PBV-R.

In Chapter 4, we make a prototype of PBV-R. Then, we compare the performances of both the prototype of PBV-R and PBV on the market. Moreover, by using these results, we carry out a calculation how much energy consumption and carbon dioxide are reduced by applying PBV-R in order to understand effects of PBV-R on the whole industry in Japan.

In Chapter 5, conclusion of this research are listed.

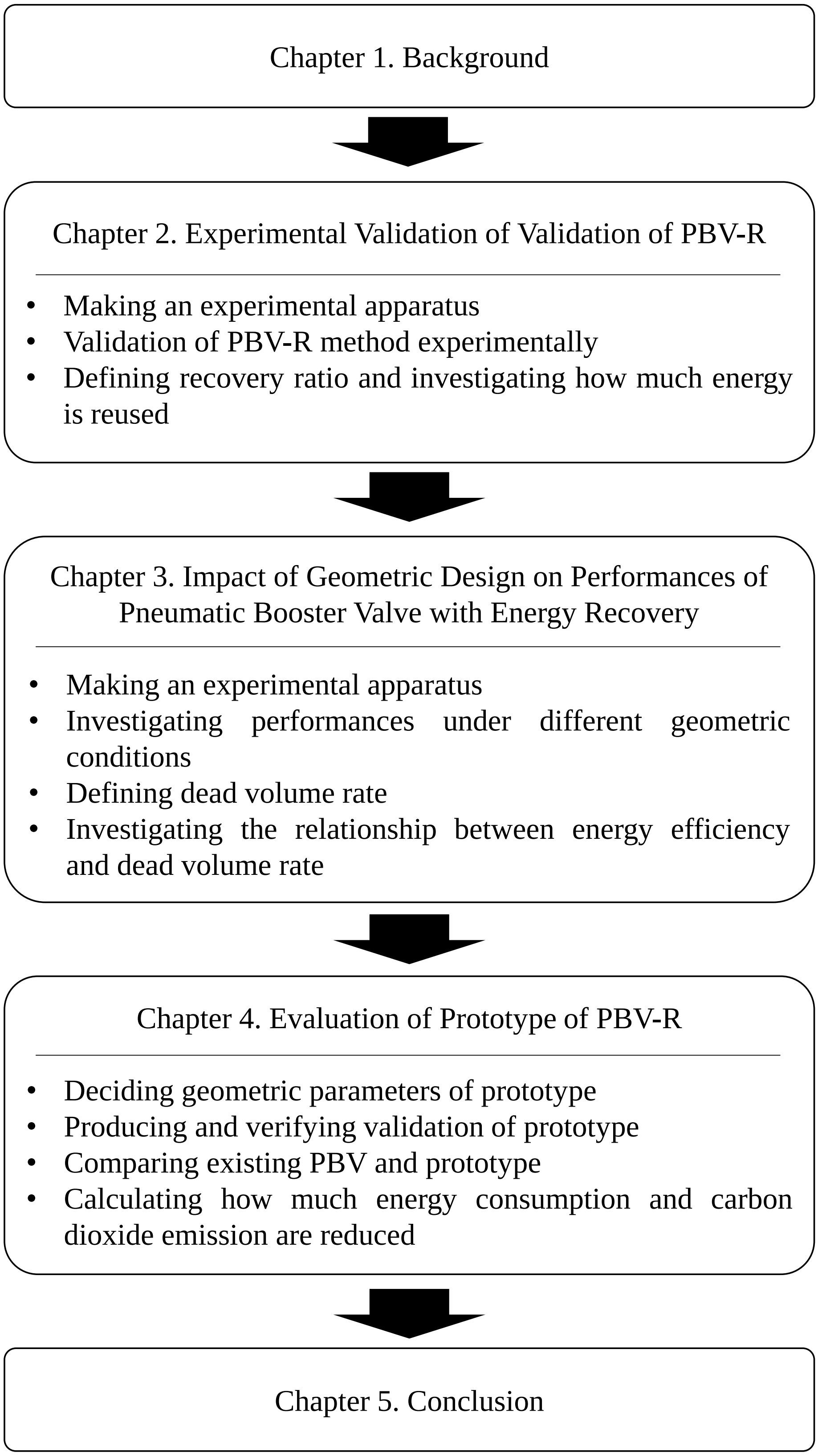

Fig.1-11. Structure of thesis

Chapter 2

Experimental Validation of Pneumatic Booster Valve with Energy Recovery

2.1 Principle of Pneumatic Booster Valves

2.1.1 Principle of Pneumatic Booster Valve (PBV)

PBV is based on the principle of a resultant force acting on pistons and a piston rod. As it is shown in Fig.2-1, it is composed of two driver chambers, two boost chambers, two pistons, a piston rod, four check valves and a 4-way/2-position mechanical valve. Especially in terms of chambers, we call "Drive Chamber 1", "Boost Chamber 1", "Boost Chamber 2" and "Drive Chamber 2" from left to right. The piston moves by the force of air pressure in each chamber, and it pushes a button and changes the direction of pneumatic circuit by switching the mechanical valve when it reaches the end of each boost chamber. There are two modes for the PBV; the movement of the piston either to the left or right. Basically, the two modes do the same process because PBV is symmetric, but we call the movement to the right as "Mode 1" and the movement to the left as "Mode 2" for the convenience of explanation.

In Mode 1, the piston moves to the right. Fig.2-2(a) and Fig.2-2(b) present Mode 1. First, as shown in Fig.2-2(a), supply air flows into Drive Chamber 1, Boost Chamber 1 and Boost Chamber 2. Second, because the air in Drive Chamber 1 and Boost Chamber 2 presses pistons to the right, the air in Boost Chamber 1 is compressed. Finally, as shown in Fig.2-2(b), Boost Chamber 1 exhausts air at higher than supply pressure. In this case, Drive Chamber 2 is open to the atmosphere. When the left piston reaches the end of Boost Chamber 1, it pushes the button that changes position of the mechanical valve and Mode 2 starts.

In Mode 2, as it is presented in Fig.2-2(c) and Fig.2-2(d), the principle is the same as

Mode 1. First, as shown in Fig.2-2(c), supply air flows into Drive Chamber 2, Boost Chambers 1 and 2, then the piston moves to the left. Second, because the air in Drive Chamber 2 and Boost Chamber 1 presses pistons to the left, the air in Boost Chamber 2 is compressed. As shown in Fig.2-2(d), finally, Boost Chamber 2 exhausts air at higher than supply pressure. In this case, Drive Chamber 1 is open to the atmosphere. When the right piston reaches the end of Boost Chamber 2, it pushes the button that changes position of the mechanical valve and Mode 1 restarts.

2.1.2 Principle of Pneumatic Booster Valve with Energy Recovery (PBV-R)

PBV-R, which was first proposed in a Japanese patent, has a similar principle to PBV but has one additional cylinder, the expansion cylinder, which includes two expansion chambers and recover energy. As we described in section 2.1.1, the air in Drive Chamber 2 in Mode 1 or in Drive Chamber 1 in Mode 2, is exhausted to the atmosphere. This means that energy is partly wasted in the process of PBV. To address this waste, PBV-R recovers and reuses the air exhausted to the atmosphere in case of PBV. Fig.2-3 shows the inside of PBV-R that includes two drive chambers, two boost chambers, two expansion chambers, three pistons, a piston rod and two 5-way/2-position directional control valves. One of the pistons pushes a button and changes the direction of pneumatic circuit by switching the directional control valves when it reaches the end of each boost chamber. There are also two modes in PBV-R; the movement of the piston either to the left or right. Basically, the two modes do the same process because PBV-R is symmetric, but we call the movement to the right as "Mode 1" and the movement to the left as "Mode 2" for the convenience of explanation.

In Mode 1, the piston moves to the right. Fig.2-4(a) and Fig.2-4(b) present Mode 1. First, as shown in Fig.2-4(a), supply air flows into Drive Chamber 1, Boost Chamber 1 and Boost Chamber 2. Second, because the air in Drive Chamber 1 and Boost Chamber 2 presses pistons to the right, the air in Boost Chamber 1 is compressed. Third, in this process, the supply air that remains from previous Mode 2 in Drive Chamber 2, unlike PBV, moves to Expansion Chamber 1, where it adds force to the middle piston. Finally, as shown in Fig.2-4(b), Boost Chamber 1 emits air at higher than supply pressure. In this case, Expansion Chamber 2 is open to the atmosphere. When the left piston reaches the end of Boost Chamber 1, it pushes the button that changes position of the directional control valves and Mode 2 starts.

In Mode 2, as it is presented in Fig.2-4(c) and Fig.2-4(d), the principle is the same as mode 1. First, as shown in Fig.2-4(c), supply air flows into Drive Chamber 2, Boost Chamber 1 and Boost Chamber 2. Second, because the air in Drive Chamber 2 and Boost Chamber 1 presses pistons to the left, the air in Boost Chamber 2 is compressed. Third, in this process, the supply air that remains from previous Mode 1 in Drive Chamber 1 moves to Expansion Chamber 2, where it adds force to the middle piston. Finally, as shown in Fig.2-4(d), Boost Chamber 2 emits air at higher than supply pressure. In this case, Expansion Chamber 1 is open to the atmosphere. When the left piston reaches the end of Boost Chamber 2, it pushes the button that changes position of the valves and Mode 1 restarts.

2.1.3 Differences between PBV and PBV-R

One of the biggest differences between PBV and PBV-R is an expansion cylinder; PBV has no expansion cylinder, while PBV-R has an expansion cylinder that can recover and reuse high-pressure air. Because the number of chambers of PBV-R is greater than that of PBV, two 5-way/2-position directional control valves or a 7-way/2-position directional control valve are/is necessary for PBV-R, while PBV needs only one 4-way/2-position directional control valve. In terms of high-pressure air in drive chambers, in the case of PBV, the high-pressure air starts being exhausted from Drive Chamber 1/2 immediately after Mode 2/1 begins, respectively. However, in the case of PBV-R, part of the high-pressure air in Drive Chamber 1/2 moves into Expansion Chamber 2/1 immediately after Mode 2/1 begins, respectively. In this case, because the high-pressure air that moved into expansion chambers does positive work, it is expected that energy efficiency or boost ratio of PBV-R is better than that of PBV.

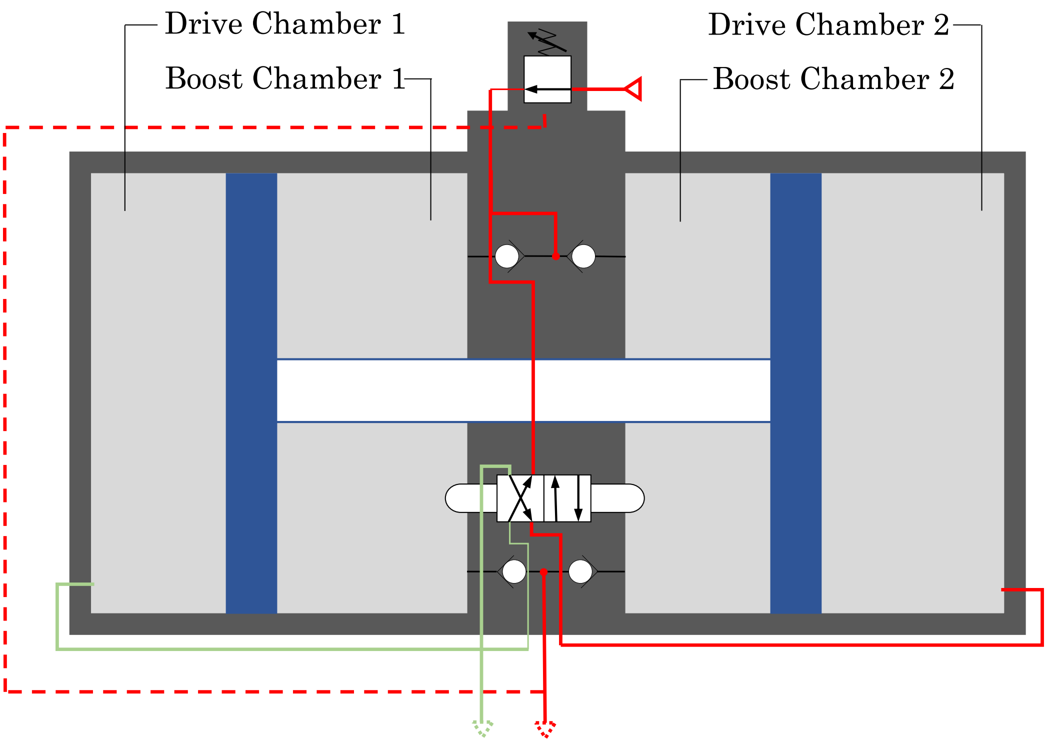

Fig.2-1. Schematic of pneumatic booster valve

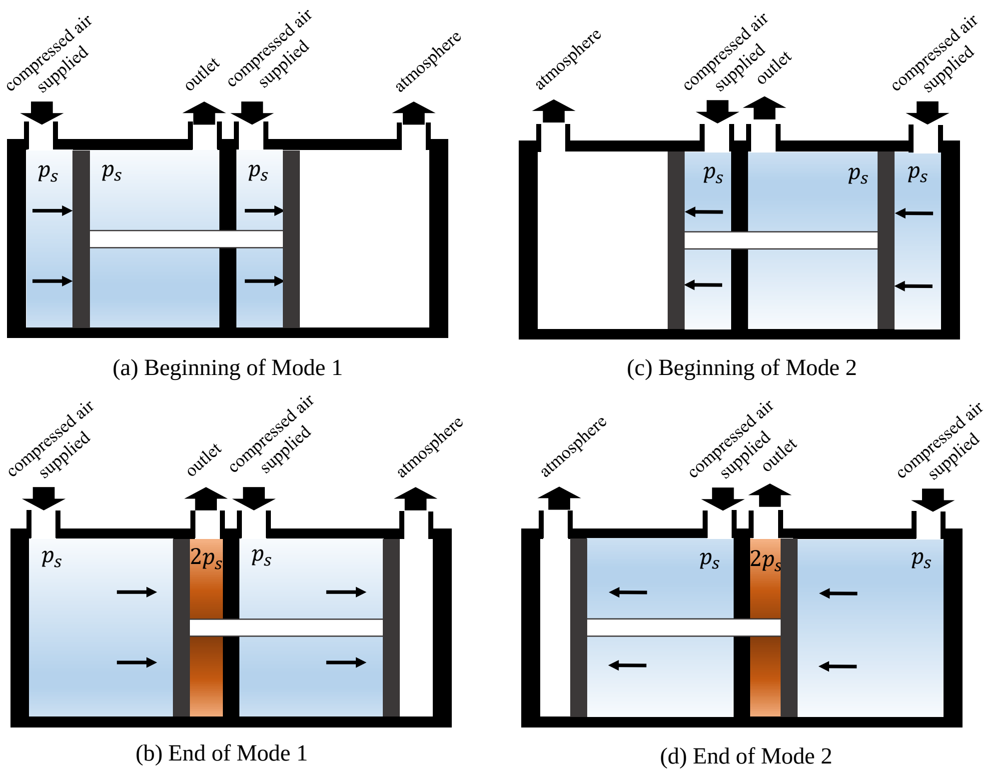

Fig.2-2. Principle of pneumatic booster valve

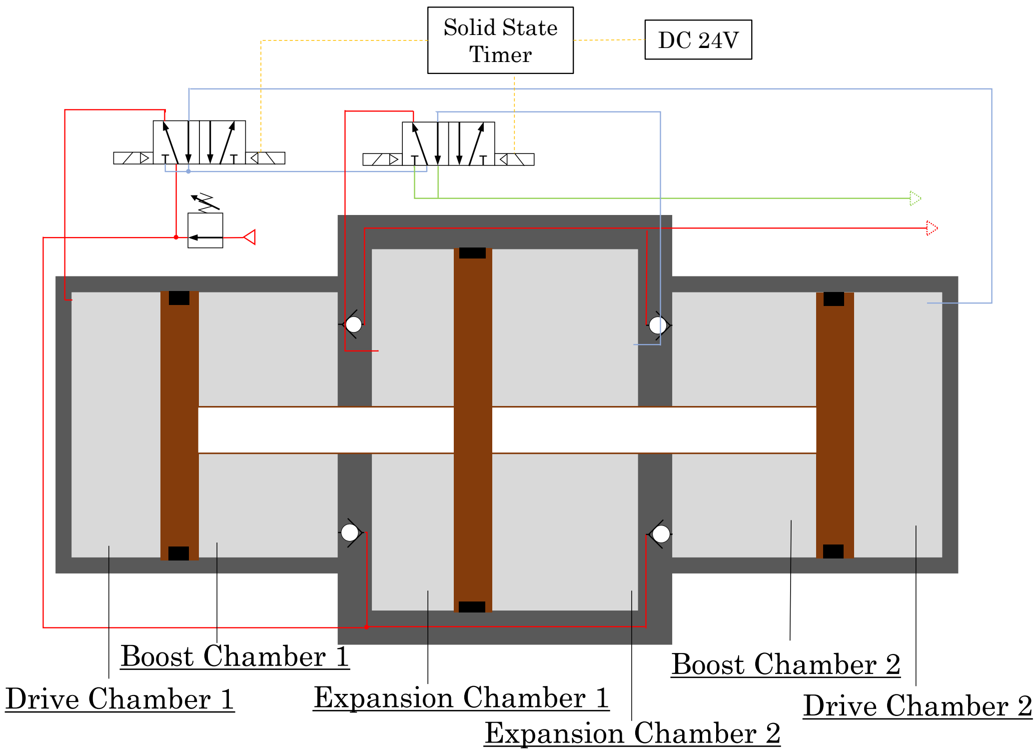

Fig.2-3. Schematic of pneumatic booster valve with energy recovery

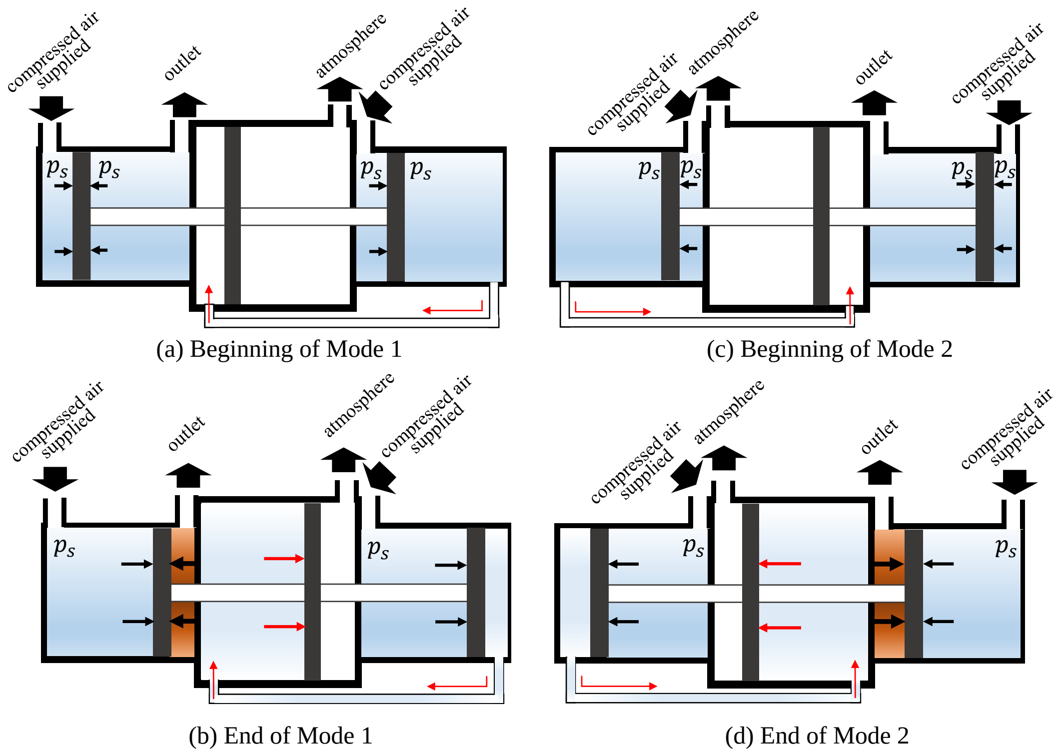

Fig.2-4. Principle of pneumatic booster valve with energy recovery

2.2 Experimental Validation of PBV-R

2.2.1 Purpose of the Experiment

In this chapter, we carry out experiment for verifying and validating PBV-R. In the previous studies, performances such as energy efficiency and boost ratio of PBV-R have been improved compared with that of PBV on certain conditions. However, these have not been studied by actual experiment. As indicated in Fig.2-1 and Fig.2-3, PBV-R has one more cylinder called “Expansion Cylinder” than PBV, which includes additional components such as one more piston, a longer piston rod and several additional pneumatic seals. Those components cause more friction and dead volume, which are the determinants that lead energy loss increases and have not been considered in the previous studies. However, since Expansion Chamber has proper function that it recovers and reuses high-pressure air, we cannot be sure whether Expansion Chamber actually do a positive function or negative function. Thus, the purpose of the experiment is to compare the results of PBV-R method with that of PBV method and verify that the performances of PBV-R method are better than those of PBV method.

2.2.2 Experimental Apparatus

Fig.2-5 presents the pneumatic circuit of the experimental apparatus in this study. The experimental apparatus consists of a filter-regulator-lubricator (FRL), two air power meters (APM) that can measure air power in real time, as well as pressure, temperature, and flow rate; six pressure sensors for each chamber; two single-rod air cylinders with a 63 mm diameter and a 100 mm stroke length; one large double-rod air cylinder with an 80 mm diameter and a 100 mm stroke length; two 5-way/2-position solenoid valves; four check valves; and a 0.01 m^3 air tank. Since, according to the previous study [51,52,53], energy efficiency gets the maximum where the area ratio of drive chamber to expansion cylinder is around 1.55, we use the two air cylinders with a 63 mm diameter as drive cylinders, the air cylinder with an 80 mm diameter as an expansion chamber. Pressure gauges are attached at each chamber of the cylinders. We acquire data with a sampling rate of 1000 Hz. A solid-state timer controls the two solenoid valves. Table.2-I shows a list of components included in the apparatus and their main specifications. By the components mentioned above, we make an experimental apparatus as Fig.2-7 including an air tank shown in Fig.2-6. In this experiment, the pressures of inflow, outflow, and each chamber; the flow rates of inflow and outflow; and the air power of inflow and outflow are measured during operation.

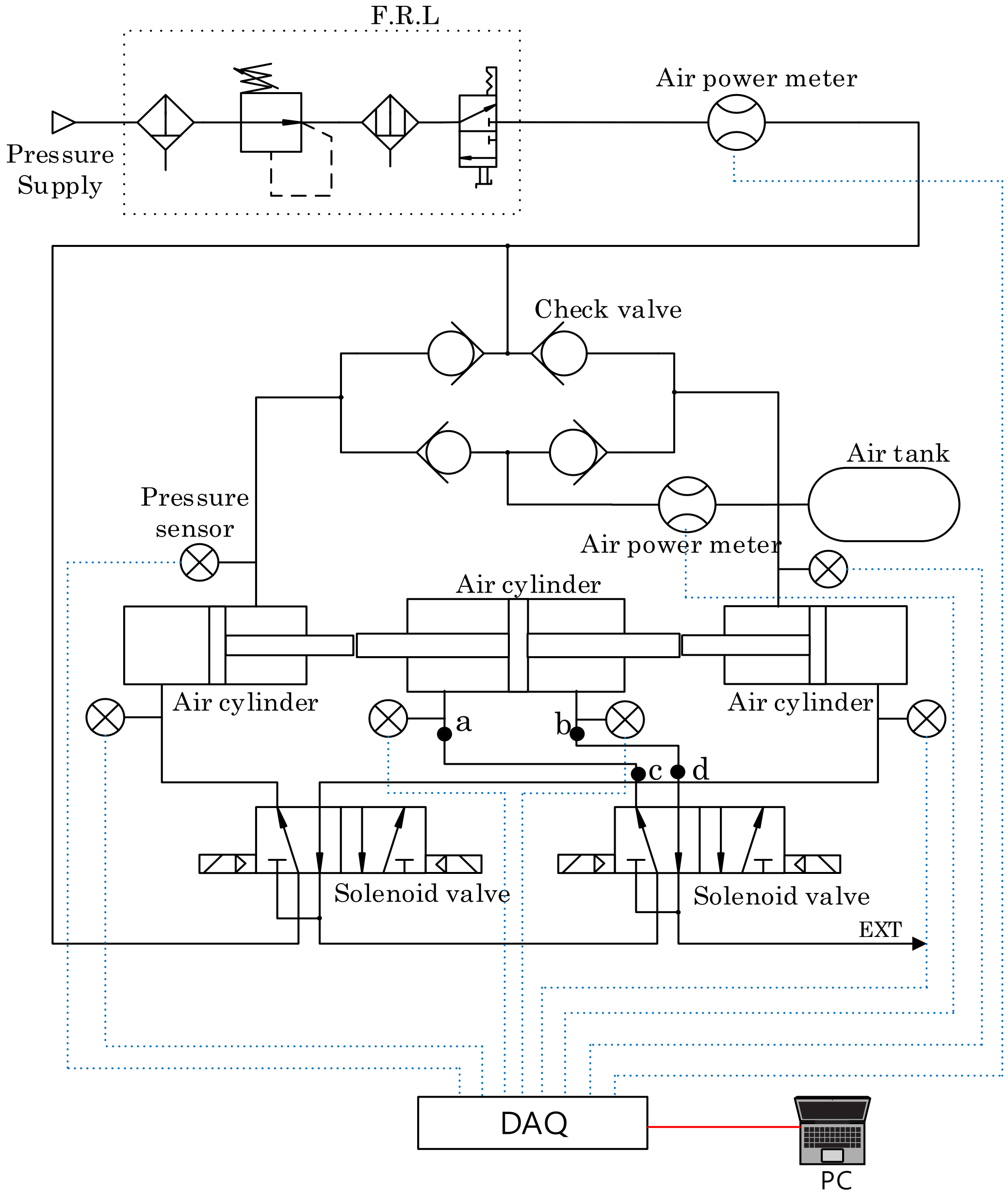

Fig.2-5. Pneumatic circuit of experimental apparatus

Table 2-I. Dead volume rate at each stroke length

Component			
No.	Parts	Article	Technical Date
1	Drive cylinder 1	SMC corporation, CDG1YL63-100FZ-M93BWN	Diameter : 63 [mm] Stroke : 100 [mm]
2	Expansion cylinder	SMC corporation, CG1WLN80-100FZ	Diameter : 80 [mm] Stroke : 100 [mm]
3	Drive cylinder	SMC corporation, CDG1YL63-100FZ-M93BWN	Diameter : 63 [mm] Stroke : 100 [mm]
4	Air power meter for inlet	Tokyo Meter Co., Ltd, APM-L-1600S	Air power range : 0~4.8 [kW] Flow rate range : 16~1600 [L/min(ANR)] Pressure range : 0~0.98 [MPa]
5	Air power meter for outltet	Tokyo Meter Co., Ltd, APM-L-1600S	Air power range : 0~4.8 [kW] Flow rate range : 16~1600 [L/min(ANR)] Pressure range : 0~0.98 [MPa]
6	Pressure sensors	SMC corporation, ISE8H-02-R-MD	Pressure range : -0.08~2.0 [MPa]
7	Air tank	SMC corporation, VBAT10A1-X15	Volume : 10 [dm^3]
8	Solenoid valves	SMC corporation, SV3200R-5W3LD-03	Effective area: 4.5~4.9 [$dm^3/s \cdot bar$] Critical pressure ratio : 0.27~0.29
9	Check valves	SMC corporation, AKH10-00	Effective area : 4.8 [$dm^3/s \cdot bar$] Critical pressure ratio : 0.5
10	Solid-state timer	OMRON, H3CA-FA	Available time range : 0.1 sec~9990 hours
11	F.R.L	SMC corporation, AC40D-03DG-V-A	

Fig.2-6 An air tank with 10 dm^3 volume

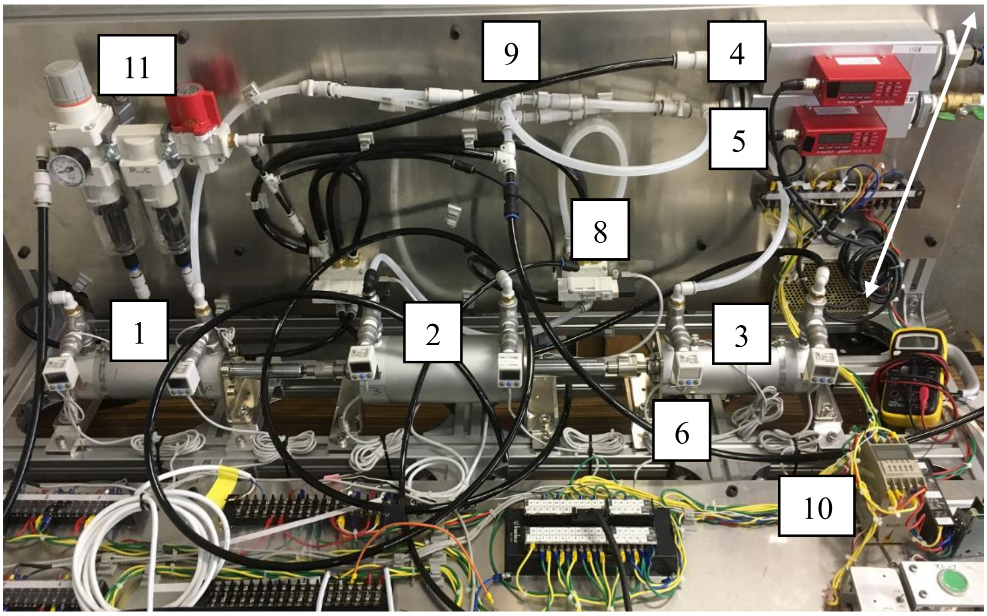

Fig.2-7 Experimental apparatus

2.2.3 Experimental Procedure

First, we investigate the performances of both PBV and PBV-R. In this thesis, there are mainly three evaluation methods that indicate the performances of PBV and PBV-R as follows:

- Energy efficiency
- Boost Ratio
- Effective Consumption Rate

Firstly, we investigate energy efficiency of both PBV and PBV-R. To do that, we need to set an evaluation method for measuring the energy of compressible air. For compressible air, air power is usually employed for evaluating the energy of air. Air power is a concept that, according to Cai and Kagawa, quantifies the energy of flowing compressed air [61,62]. Air power can be presented as follows:

$$P = GRT_a[\ln\frac{p}{p_a} + \frac{\kappa}{\kappa-1}\left(\frac{T}{T_a} - 1 - \ln\frac{T}{T_a}\right)] \tag{2.1}$$

Based on Equation (2.1), we investigate the energy efficiency of both PBV and PBV-R. If input air power, P_{in}, and output air power, P_{out}, are already known, the energy efficiency, η, during the operating time [0,∞] can be calculated with a ratio of output energy to input energy as follow:

$$\eta = \frac{E_{\text{out}}}{E_{\text{in}}} = \frac{\int_0^\infty P_{\text{out}}\,dt}{\int_0^\infty P_{\text{in}}dt} \tag{2.2}$$

In Equation (2.2), both input energy E_{in} and output energy E_{out} can be calculated by integrating each air power from $t = 0$ to $t = \infty$.

Secondly, we also investigate boost ratio, which is one of the significant characteristics of PBV and PBV-R. Because the expansion chamber recovers and reuses high-pressure air, it is expected that the boost ratio of PBV-R is higher than that of PBV. Generally, while PBV or PBV-R is working, inlet pressure, p_{in}, and tank pressure, p_{out}, are fluctuant. However, if PBV or PBV-R are on condition that there is no air consumption at downstream, the pistons stop their movement when p_{out} reaches the maximum pressure, then both p_{in} and p_{out} gradually become constant after sufficient time has elapsed. Thus in this thesis, we define the boost ratio, k_p, with the p_{in} and the p_{out} on the condition that there is no use of the air at downstream: in other words, the boost ratio means the maximum boost ratio. The definition of the boost ratio is as follow:

$$k_p = \frac{p_{\text{out}}(\infty)}{p_{\text{in}}(\infty)} \tag{2.3}$$

In Equation (2.3), ∞ is the time when p_{in} and p_{out} converge to certain values and do not fluctuate anymore.

Lastly, effective consumption rate, which indicates the ratio of input air to output air, is an index that can evaluate how much air is efficiently used. The effective consumption rate, k_v, during the time $[0, \infty]$ can be calculated as the ratio between volumes of input air and output air as follow:

$$k_v = \frac{V_{\text{out}}}{V_{\text{in}}} = \frac{\int_0^\infty Q_{\text{out}}dt}{\int_0^\infty Q_{\text{in}}dt} \tag{2.4}$$

In Equation (2.4), both input air V_{in} and output air V_{out} can be calculated by integrating each flow rate from $t = 0$ to $t = \infty$. In addition, both V_{in} and V_{out} are quantity of air at conditions 101325 Pa, $20℃$ and 65% relative humidity.

Next, we explain the method of the experiment. The purpose of the following experiments is to investigate the differences between PBV method and PBV-R method. Using the experimental apparatus presented in Fig.2-7, we test both PBV and PBV-R methods. Firstly, we carry out PBV method based on Fig.2-7 except pneumatic cylinders: we only make a use of two drive cylinders connecting with an extra rod, then we disconnect (a) and (b) and connect (c) and (d). Secondly, we carry out PBV-R method based on Fig.2-7 as it is without any change: we connect the three cylinders using double-ended bolts and we do not disconnect any pneumatic circuit.

In terms of supply pressure, because we need to investigate at various supply pressures, we change supply pressure from 200 kPa to 500 kPa at intervals of 100 kPa using a regulator. Also, the experiment is carried out 5 times at each supply pressure and each case of PBV and PBV-R. We set the solid-state timer for 0.5 second in order to change the position of the solenoid valves, i.e., two modes repeat every one second. As shown in Fig.2-6, we store compressed air in a 10 dm³ air tank at downstream.

Through the equations and methods above, we investigate and compare performance of PBV and PBV-R in terms of efficiency, boost ratio, air consumption and pressure response. If the pistons and the piston rod stop the movement, we determine that the operation of PBV or PBV-R ends and stop measurement.

2.2.4 Experimental Results

First, Fig.2-8 illustrates the energy efficiency at each supply pressure. The dashed line indicates the energy efficiency of PBV method, and the solid line indicates that of PBV-R method. The Energy efficiency of PBV-R is from 5 % to 8 % greater than that of PBV, i.e., the energy efficiencies of PBV-R method are improved at the entire supply pressures, compared with that of PBV method. Also, the energy efficiencies of both PBV method and PBV-R method tend to decrease as the supply pressure increases, except at p_s=200 kPa.

Secondly, boost ratios at each supply pressure are shown in Fig.2-9. The boost ratio of PBV-R method is from 5% to 17% higher than that of PBV method, which means the boost ratios of PBV-R method are improved at the entire supply pressures, compared with that of PBV method. The boost ratios of both PBV method and PBV-

R method tend to increase as the supply pressure increases, and the differences of the boost ratios between PBV method and PBV-R method also tends to be greater as the supply pressure increases.

Thirdly, effective consumption rates at each supply pressure is shown in Fig.2-10. The effective consumption rates for PBV-R method is around 4 % higher than that of PBV method at p_s=200 kPa, 300 kPa, 400 kPa and 5 % at p_s=500 kPa, i.e., the PBV-R method uses the air more efficiently than the PBV method during the operation. Also, both tend to decrease as the supply pressure increases.

Fourthly, the pressure response is shown in Fig.2-11. The pressure responses of both PBV method and PBV-R method do not differ until t=13 s or an outlet pressure of 600 kPa; the pressure increases linearly for the first 13 seconds. Then, these two lines separate: the speed of PBV-R method becomes faster than that of PBV method after t=13 s. As a result, both converge according to the boost ratios that are shown in Fig.2-11.

Finally, the pressure responses of each chamber at p_s=400 kPa for PBV-R method are shown in Fig.2-12. For lack of space, we only deal with pressure behaviors of Drive Chamber 1, Boost Chamber 1 and Expansion Chamber 1. The dashed line indicates the pressure of Expansion Chamber 1, the dotted line indicates that of Drive Chamber 1 and the solid line indicates that of Boost Chamber 1. Because the lines overlap when the time range is large, Fig.2-12 shows the time range of $[0,7]$ seconds. The pressure of each chamber fluctuates with the cycle set by the solid-state timer. We can see that the lines of the Boost Chamber 1 increase incrementally, which in turn increases the tank pressure. We also see that the Expansion Chamber 1 always has an air pressure of approximately 250 kPa recovered from the Drive Chamber 1. From this result, hence, it is obvious that the high-pressure air that was supposed to be exhausted in case of PBV method is partly reused in PBV-R method, which means that the expansion cylinder performs a role of recovering energy.

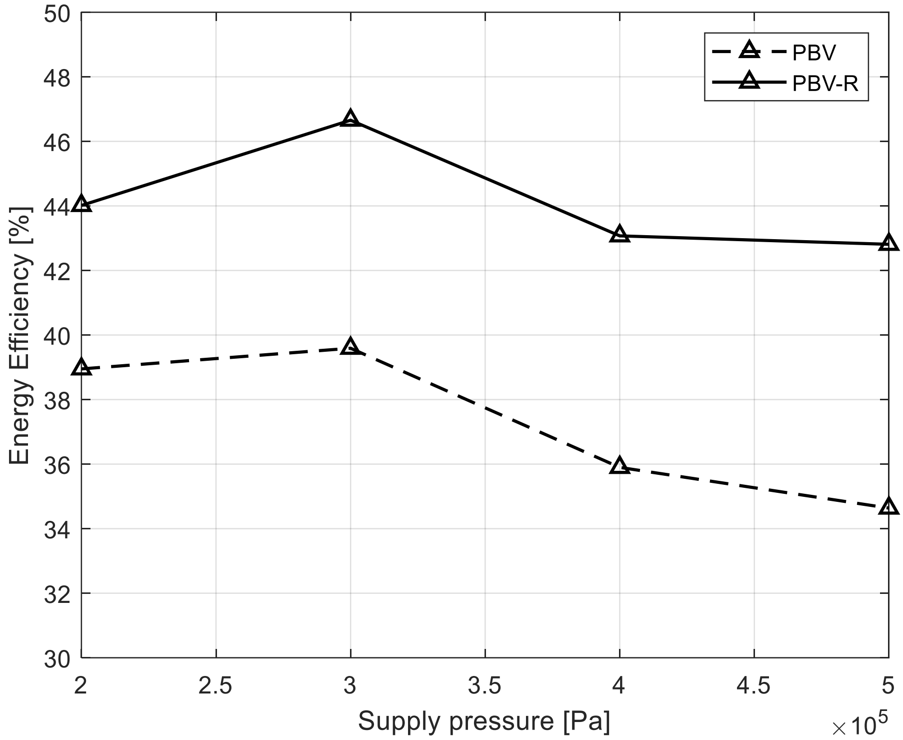

Fig.2-8 Energy efficiency of PBV and PBV-R methods

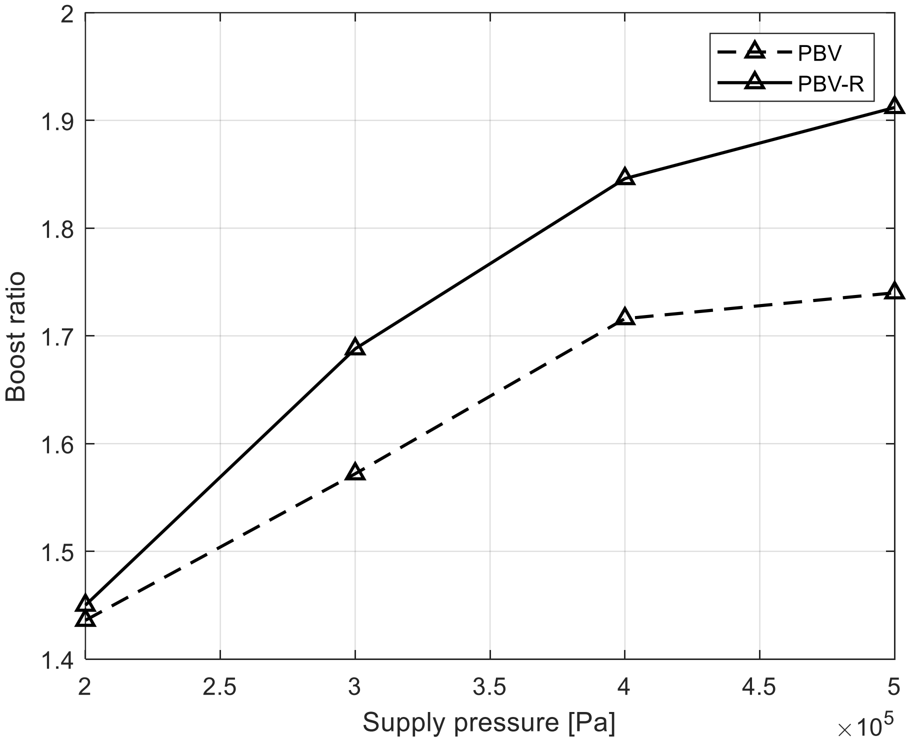

Fig.2-9 Boost ratio of PBV and PBV-R methods

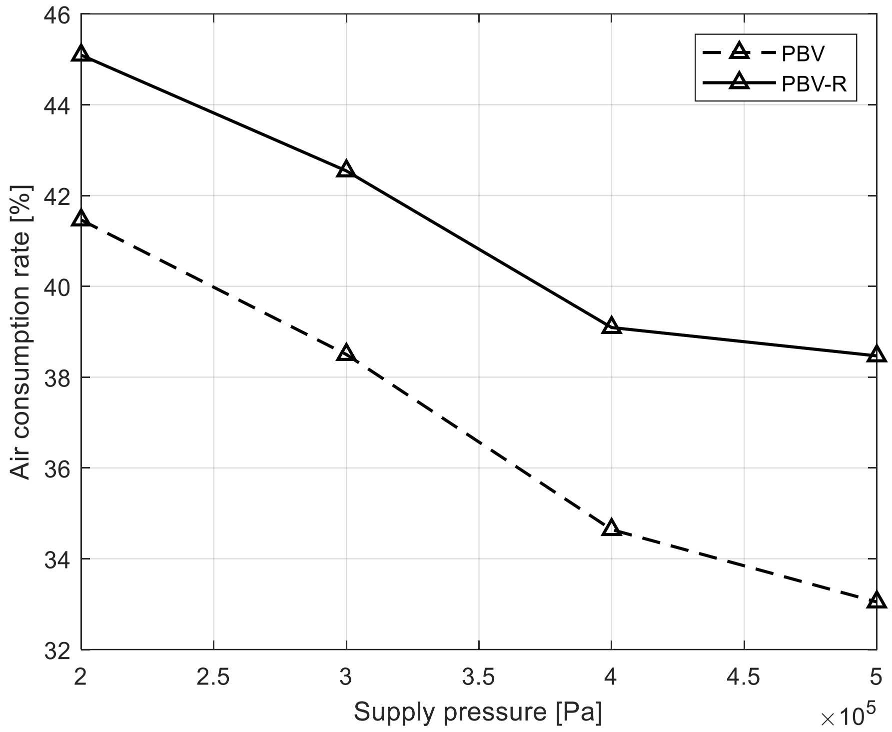

Fig.2-10 Effective consumption rate of PBV and PBV-R methods

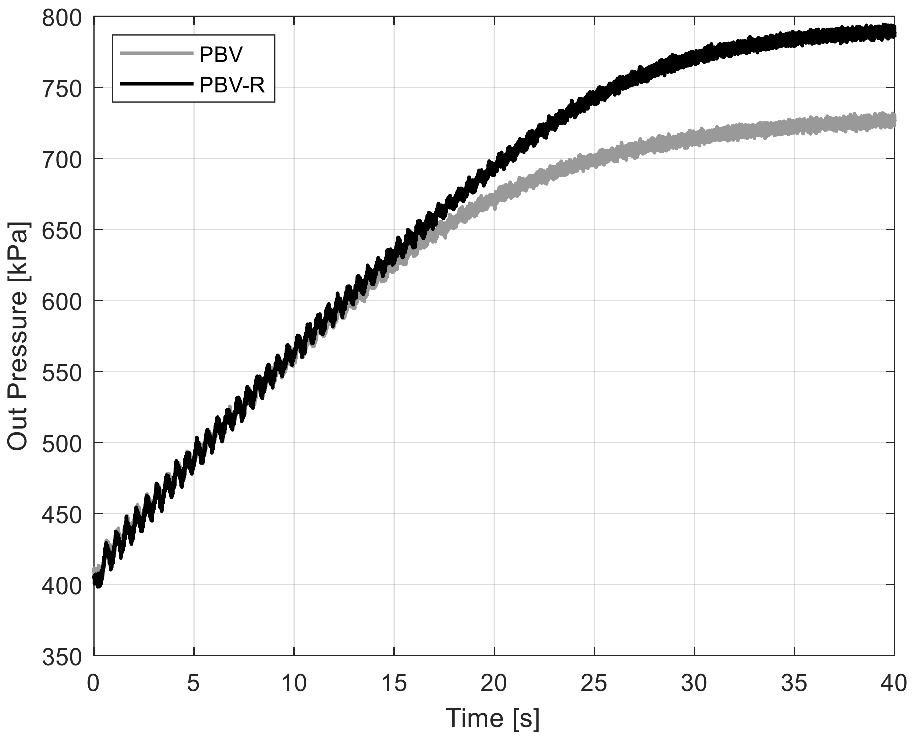

Fig.2-11 Filling-up characteristics of PBV and PBV methods

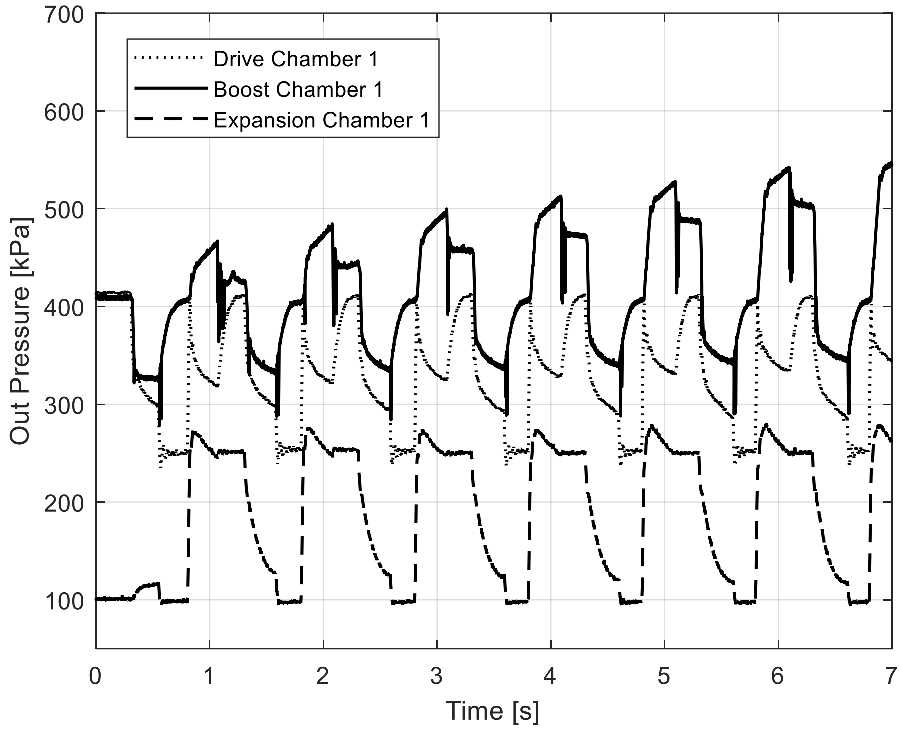

Fig.2-12. Pressure behavior of PBV and PBV-R methods

2.3 Evaluating Method of Energy Recovery

2.3.1 Definition of Recovery Ratio for PBV-R

Because PBV-R has one more cylinder called expansion cylinder than PBV, it affects several characteristics e.g. boost ratio, energy efficiency and effective consumption rate. However, we cannot ensure that every form of the additional cylinder will contribute to the improvement of PBV. Thus, we investigate how much energy is recovered and reused by an expansion chamber with various parameters. In this chapter, because area ratio, k_r, is one of the influential parameters, we discuss the energy efficiency focusing on the area ratio.

As mentioned previously, the method how PBV-R recovers energy is to let high-pressure air of the previous mode in the drive chamber move to the expansion chamber by connecting both chambers, which occurs by changing the position of solenoid valves. Then, the high-pressure air is shared by both drive chamber and expansion chamber. Because the area of the piston in the expansion chamber is greater than the area of the piston in the drive chamber, the high-pressure air works toward the motion direction of the piston. However, although recovered high-pressure air consequently works in the positive direction, the air in the drive chamber causes the force to reverse direction, i.e., we can see that some of the energy is used for negative work. Therefore, to investigate how much recovered air is actually used for positive work, we make a calculation as follows: First, valid energy of the high-pressure air in the drive chamber can be written as Equation (2.5) [61,62].

$$E = pV \ln \frac{p}{p_a} - (p - p_a)V \tag{2.5}$$

Next, the high-pressure air is divided into two forces; a force acting in the forward direction and a force acting against the forward direction. The air in each chamber does work, so we first calculate pressure in both chambers. To simplify calculation, we assume as follows:

(a) The air in the system is considered to be an ideal gas: the states of the air satisfy

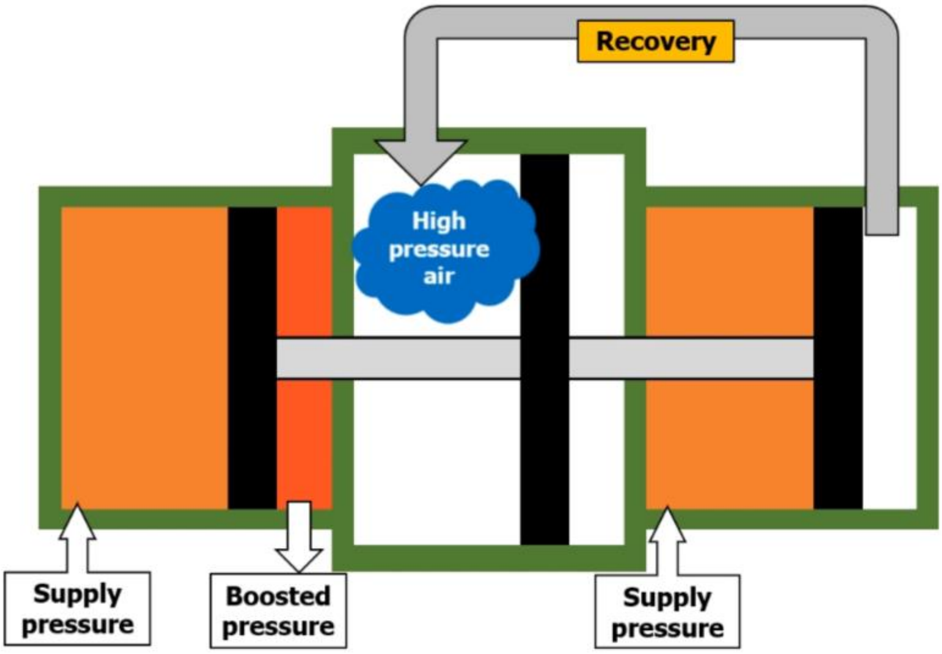

Fig.2-13. Energy recovery process in PBV-R

ideal gas state equation

(b) There is no air leakage in the system

(c) There is no temperature change of the air: no heat transfer through the wall of the air cylinders occurs and all processes of state changes are isothermally.

(d) All volumes except the volume of pneumatic cylinders can be neglected; pipe, end of pneumatic cylinders, etc.

(e) If air supplied to a chamber, the pressure of the chamber reaches the pressure of the air immediately without any delay.

Also, from now on, we only consider the case of Mode 1. As shown in Fig.2-13, When PBV-R starts operating and pistons moving to the right, the air in Drive Chamber 2 starts moving into Expansion Chamber 1. According to the general gas equation, because Drive Chamber 2 and Expansion Chamber 1 are considered as a closed system, we can write the gas equation in terms of displacement of pistons x as follow:

$$p_{e1}k_rA_{d2}x + p_{d2}A_{d2}(l - x) = C \tag{2.6}$$

where

$$C = p_s A_{d2} l \tag{2.7}$$

In Equation (2.6) and (2.7), p_s represents supply pressure, p_{e1} represents pressure of Expansion Chamber 1, p_{d2} represents pressure of Drive Chamber 2, A_{d2} represents area of the piston in Drive Chamber 2, k_r represents area ratio and l represents stroke length. Assuming there is no friction or resistance between the drive chamber and the expansion chamber, then p_{e1} and p_{d2} can be considered equal, according to the assumption above, and Equation (2.6) can be simplified in terms of p_{e1} as follow:

$$p_{e1} = \frac{C}{k_r A_{d2} x + A_{d2}(l - x)} \tag{2.8}$$

Then, we need to consider all additional forces that occurred by adding the expansion cylinder. As indicated in Fig.2-14, in comparison with PBV, PBV-R has four more forces; a force from Expansion Chamber 1, $p_{e1}A_{e1}$, a force from Expansion Chamber 2, $p_a A_{e2}$, a force from Drive Chamber 2 $(p_{d2} - p_a)A_{d2}$ and friction force caused by expansion cylinder, f_e. Because the force of Drive Chamber 2 is $p_a A_{d2}$ in the case of PBV, we need to subtract this from the force of Drive Chamber 2 in the case of

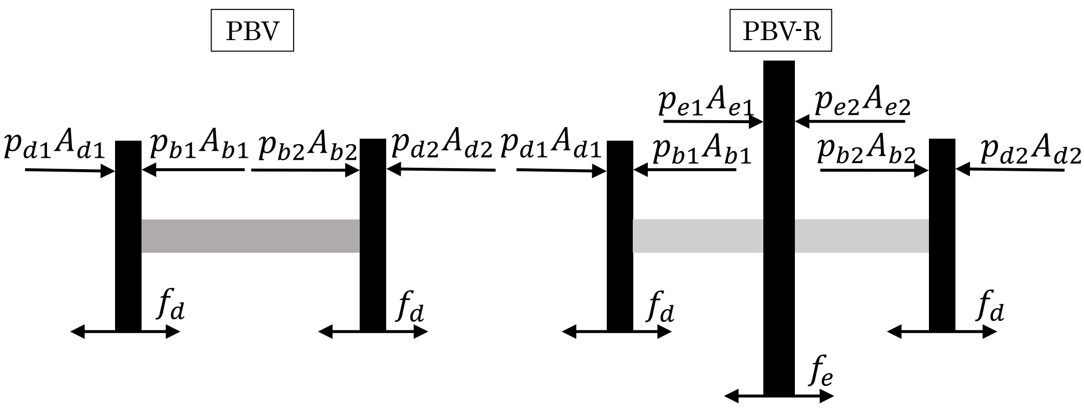

Fig.2-14 Schematic of forces acting on pistons at PBV-R

PBV-R, $p_{d2}A_{d2}$. Thus, the work that these four new forces do can be written as follow:

$$W = \int_0^l [(p_{e1} - p_a)(k_r - 1)A_{d2} - f_e]dx \tag{2.9}$$

There exist many friction models for pneumatic cylinders generally based on Coulomb model, viscous model and Striberk model in a pneumatic cylinder [63], but in this discussion, we only consider the Coulomb model and viscous model as follow [64]:

$$f_e = f_s + cu \tag{2.10}$$

In Equation (2.10), since a piston of a pneumatic cylinder moves with almost the same velocity, we assume that u is constant. We refer to the previous study for values under various conditions [65].

Next, we define the recovery ratio, k_e, which indicates how much energy from the drive chamber is actually reused. By using the ratio of the work that these four new forces do to valid air energy of the high-pressure air in the drive chamber, the equation of the recovery ratio can be written as follow:

$$k_e = \frac{\int_0^l [(p_{e1} - p_a)(k_r - 1)A_{d2} - f_e]dx}{p_s A_{d2} l \ln(p_s/p_a) - (p_s - p_a)A_{d2} l} \tag{2.11}$$

p_{e1} is described by Equation (2.8), thus we can find out that the recovery ratio is determined by k_r and p_s. In this study, k_r of the cylinders of the apparatus is 1.5 and the recovery ratio is around 10~20 % at every supply pressure. This means that around 10~20 % of the energy, which was supposed to be exhausted in case of PBV, is reused by adding the expansion cylinder.

2.3.2 Relationship between Recovery Ratio and Energy Efficiency

Next, we investigate the recovery ratio at various k_r. Let p_s from 200 kPa to 500 kPa and k_r from 1 to 6. Fig.2-15 indicates the relationship between k_r and recovery ratio. As shown on the graph, the recovery ratio is less than 0 % when k_r=1 because, according to Equation (2.11), all forces do the same work in different directions except friction acting as a backward force, which causes a negative work and a negative term in the numerator of Equation (2.11). Also, the recovery ratio gets the maximum with k_r=1.9 by 3.6%, k_r=2.6 by 30% and k_r=3.6 by 45.4%. In comparison to the recovery ratio at k_r=1.46 which is real value for this experimental apparatus, the maximum value is up to 23 % greater, although the previous study has shown that energy efficiency has the maximum at k_r=1.46. One of the reasons is considered that the recovery ratio is calculated under assumption that both p_{e1} and p_{d2} are the same. In fact, as shown in Fig.2-13, p_{e1} is not consistent with p_{d2} due to impedance of the experimental circuit or pressure loss. The difference of the pressure has an effect on the recovery ratio, which needs accurate calculation of fluid dynamics. Therefore,

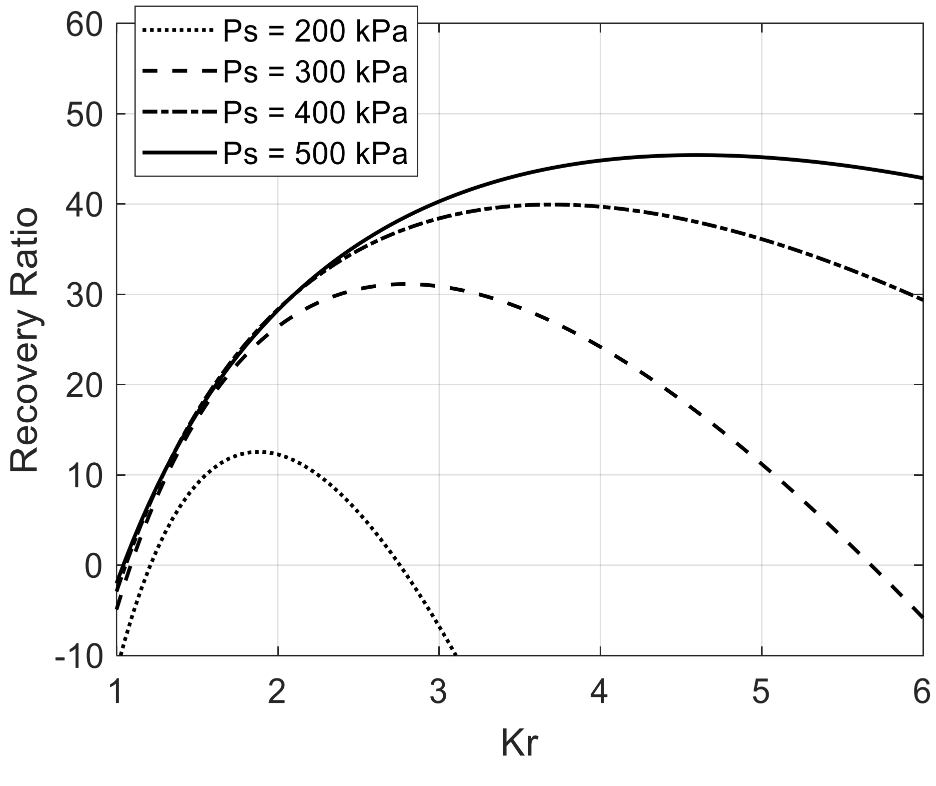

Fig.2-15. Relationship between area ratio and recovery ratio

further research about the recovery ratio by numerical analysis of air flow including pipe is necessary.

Next, we apply this recovery ratio to the result of the experiment. Because recovery ratio indicates how much energy is recovered from PBV, energy efficiency of PBV-R can be calculated as the sum of energy efficiency of PBV and recovery ratio as follows:

$$\bar{\eta}_{\mathrm{PBVR}} = \eta_{PBV} + \frac{E_d}{E_d + E_b} k_e \tag{2.12}$$

To verify whether the discussion of recovery ratio is correct or not, we compare the result at section 2.2.4, η_{PBVR}, with the value calculated by Eq.2.3, $\bar{\eta}_{\mathrm{PBVR}}$. Recovery ratios at k_e=1.5 are 8% at 200 kPa, 15% at 300 kPa, 400 kPa and 500 kPa. Fig.2-16 shows the relationship between η_{PBVR} and $\bar{\eta}_{\mathrm{PBVR}}$: the black solid line indicates η_{PBVR} and the red solid line indicates $\bar{\eta}_{\mathrm{PBVR}}$. The difference between the two results is in error by less than 0.5%, therefore, the discussion with recovery ratio is considered appropriate.

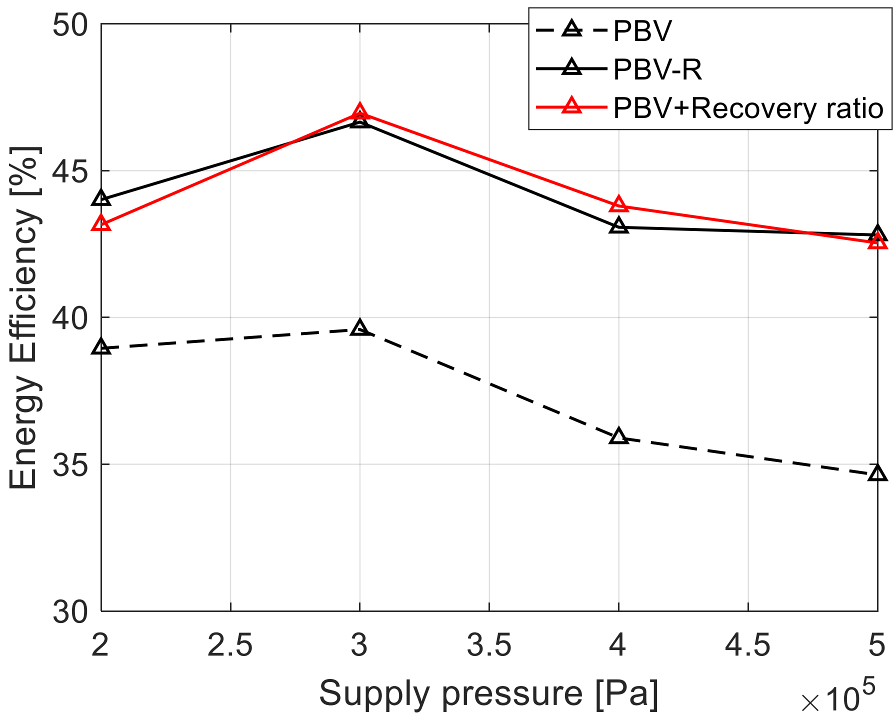

Fig.2-16 Energy efficiency with recovery ratio

2.4 Summary

We list the following conclusion from the experiment and discussion in this chapter:

1. We designed a pneumatic circuit and set up an experimental apparatus with mainly two single-rod air cylinders with a 63 mm diameter and a 100 mm stroke length as drive cylinder; one large double-rod air cylinder with an 80 mm diameter and a 100 mm stroke length as expansion cylinder; two 5-way/2-position solenoid valves; and four check valves. Also, we investigated the energy efficiency, boost ratio, effective consumption rate and pressure responses by measuring inlet and outlet air powers; inlet and outlet pressures; inlet and outlet flow rate; and pressures in each chambers on the condition that there is a 10 dm^3 air tank and no use of the air at downstream. With the apparatus, we operated by both PBV method and PBV-R method and compared the performances of both methods.

2. According to the results of the experiment, firstly, the energy efficiencies of PBV-R method were up to 8% greater than PBV method. Secondly, the boost ratios of PBV-R method were up to 17% greater than that of PBV method. Thirdly, effective consumption rates of PBV-R method are up to 5% greater than those of PBV method. Fourthly, the pressure response of both PBV and PBV-R method do not differ until certain time, but after that, the speed of PBV-R method became faster than that of PBV method. Finally, we confirmed that the high-pressure air that was supposed to be exhausted in case of PBV method was partly reused in PBV-R method.

3. To investigate how much energy is recovered and reused by an expansion cylinder, we defined "recovery ratio". According to Equation (2.11), the recovery ratio varies by supply pressure, p_s, and area ratio, k_r. By calculation, we found that the area ratio that maximizes recovery ratio is 1.9 at p_s=200 kPa, 2.6 at p_s=300 kPa, 3.6 at p_s=400 kPa and 4.6 at p_s=500 kPa, respectively. Also, since the experimental energy efficiency of PBV-R is almost the same as the sum of the experimental energy efficiency of PBV and recovery ratio, the discussion with recovery ratio is considered appropriate.

Conclusionally, PBV-R incorporating an additional expansion cylinder offers not only energy efficiency but also higher pressure gains than PBV.

Chapter 3

The Impact of Geometric Design on Performance of Pneumatic Booster Valve with Energy Recovery

3.1 Experimental Validation of Impact of Area Ratio and Stroke Length

3.1.1 Impact of Geometric Design

For designing PBV-R, stroke length and area ratio are two of the most important parameters. In terms of area ratio, firstly, we found that area ratio is a main determinant of energy efficiency of PBV-R. As shown in Fig.2-15, PBV-R has greater energy efficiency than PBV at only certain area ratio. In other words, not every area ratio makes the energy efficiency of PBV-R higher than that of PBV. Also, according to Fig.2-15, PBV-R has maximum energy efficiency at different area ratio under different supply pressure. In terms of stroke length, secondly, it has been proved that stroke length has no influence on the performances of PBV-R, according to the previous studies [51,52,53]. In the previous studies, however, several factors such as dead volume and pressure drop are neglected, which are considered to change the performances of PBV-R. Furthermore, the previous studies have carried out misguided analysis on energy efficiency.

Both stroke length and area ratio have not been experimentally verified yet. As explained in Chapter 1, experiment is different from calculation. In this chapter, therefore, we experimentally investigate performances of PBV-R under various geometric parameters e.g. area ratio and stroke length, then confirm relationship between the performances and area ratio of PBV-R and between the performances and stroke length of PBV-R.

3.1.2 Experimental Apparatus

Fig.3-1 presents the pneumatic circuit of the experimental apparatus in this study. The experimental apparatus includes a filter-regulator-lubricator (F.R.L); two air power meters (APM); six pressure sensors for each chamber; two single-rod air cylinders with a 40 mm diameter for drive cylinders; three double-rod air cylinders with a 50 mm, 63 mm, 80 mm diameter each for an expansion cylinder; two 5-way/2-position solenoid valves; four check valves; a solid-state timer; two button switches for switching position of the solenoid valves; and a 10 dm^3 tank. Each diameter has

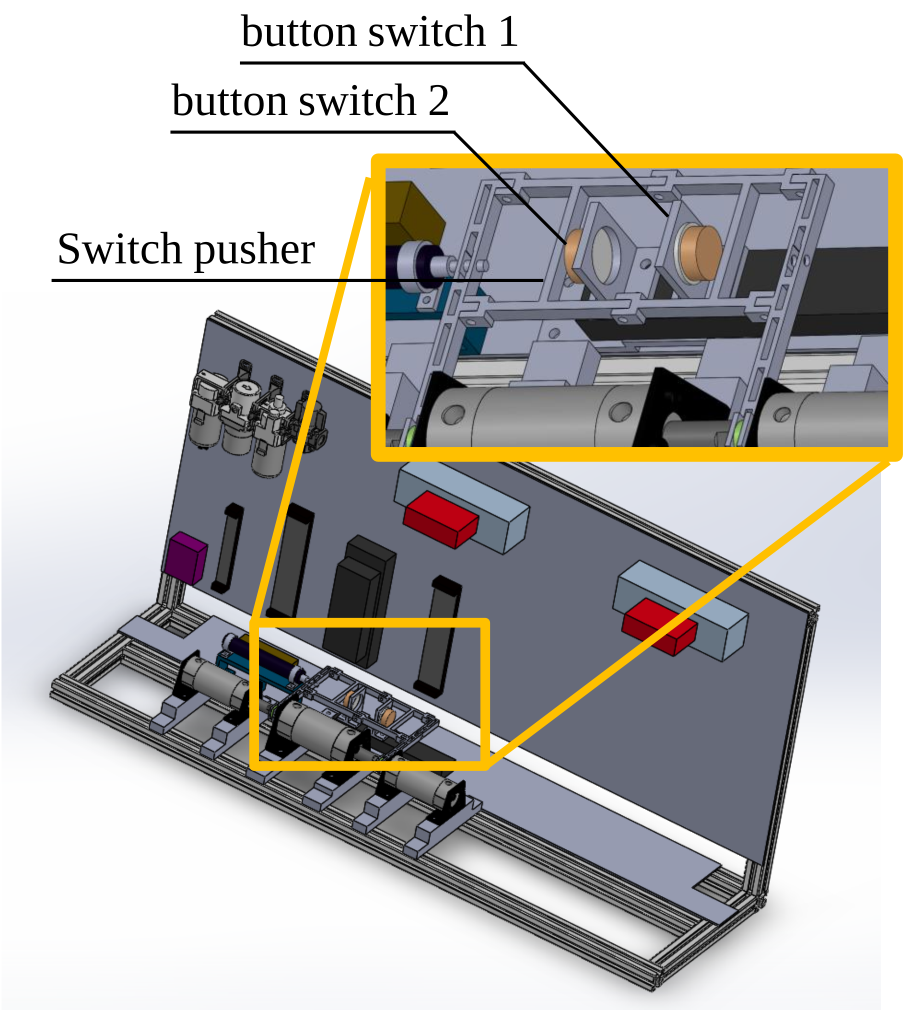

Fig.3-1 3D design of experimental apparatus

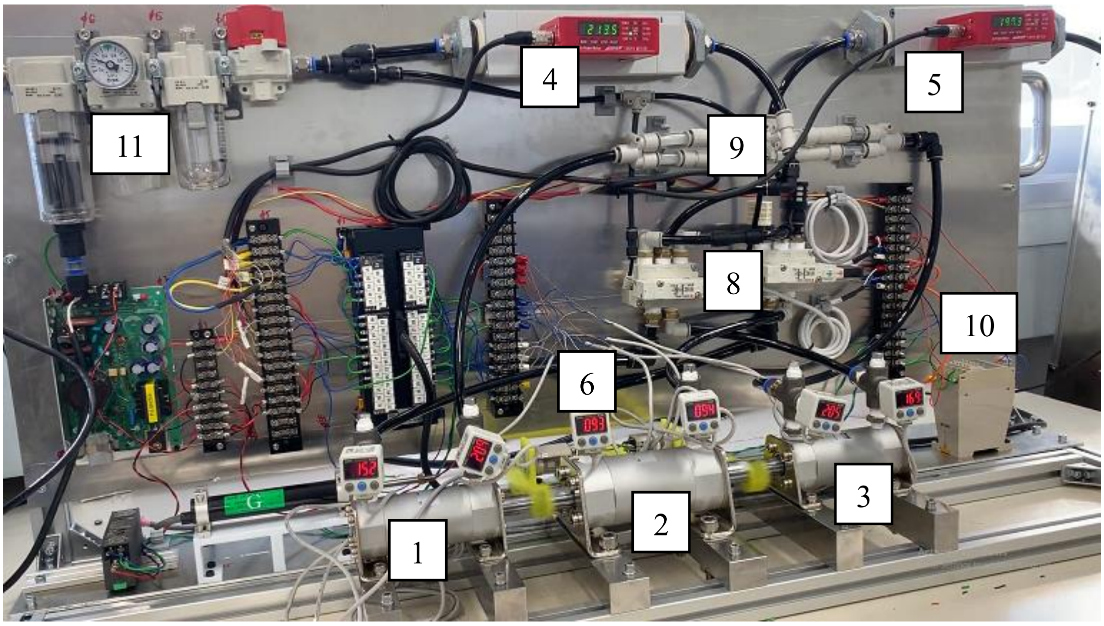

Fig.3-2 Experimental apparatus

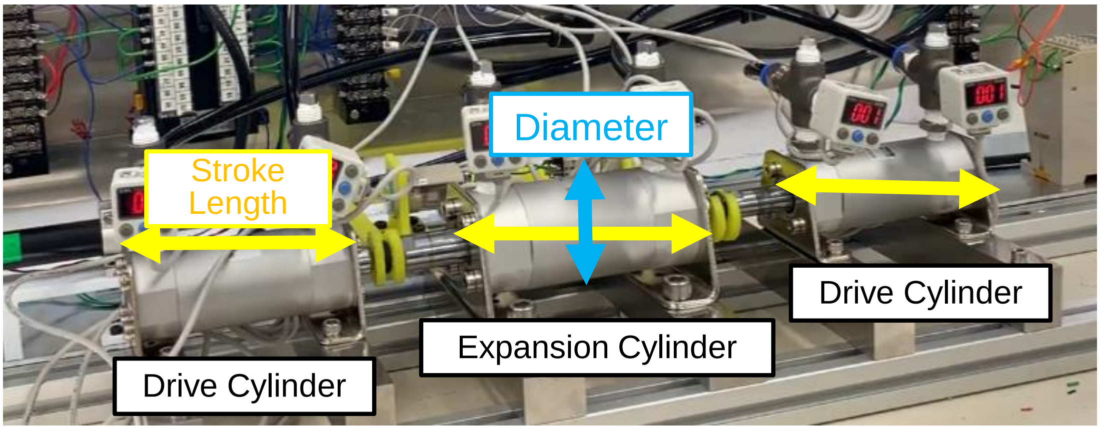

Fig.3-3 Changeable geometric parameters in experimental apparatus

four different strokes; 25 mm, 50 mm, 75 mm and 100 mm, so total number of air cylinders we prepare is twenty. Direction control of pneumatic circuit is operated by two 5-way/2-position solenoid control valves and a solid-state timer that has a function of a relay. The pressures of inflow, outflow and each chamber; the air power of inflow and outflow; and the flow rate of inflow and outflow are measured during operation. All data is acquired by converting analog signals to digital signals with a sampling rate of 1000 Hz. Table.3-I shows a list of air cylinders and the other components included in the experimental apparatus are the same as Table.2-I. Fig.3-2 is the actual

Table.3-I. List of components

Component				
No.	Parts	Article	Technical Date	
1 & 3	Drive cylinder 1	SMC corporation,	diameter	stroke length
		(1) CDG1YL40-25FZ	40 mm	25 mm
		(2) CDG1YL40-50FZ	40 mm	50 mm
		(3) CDG1YL40-75FZ	40 mm	75 mm
		(4) CDG1YL40-100FZ	40 mm	100 mm
2	Expansion cylinder	SMC corporation,	diameter	stroke length
		(5) CG1WLN50-25FZ	50 mm	25 mm
		(6) CG1WLN50-50FZ	50 mm	50 mm
		(7) CG1WLN50-75FZ	50 mm	75 mm
		(8) CG1WLN50-100FZ	50 mm	100 mm
		(9) CG1WLN63-25FZ	63 mm	25 mm
		(10) CG1WLN63-50FZ	63 mm	50 mm
		(11) CG1WLN63-75FZ	63 mm	75 mm
		(12) CG1WLN63-100FZ	63 mm	100 mm
		(13) CG1WLN80-25FZ	80 mm	25 mm
		(14) CG1WLN80-50FZ	80 mm	50 mm
		(15) CG1WLN80-75FZ	80 mm	75 mm
		(16) CG1WLN80-100FZ	80 mm	100 mm

experimental apparatus made with the components described above: Two drive cylinders and one expansion cylinder are included for the apparatus. Because every end of piston rod of air cylinder has a female screw, we connect the rods by double-ended bolts on both ends. Also, a U-shaped button pusher is fixed on the bolts and pushes button switches when the pistons reach to the end of the stroke.

3.1.3 Experimental Procedure

First, we investigate the performances of each case, e.g. energy efficiency, boost ratio and effective consumption rate, which are also defined and applied in Chapter 2. Firstly, we define energy by air power and the energy efficiency, η, during the operating time $[0, \infty]$ can be calculated by Equation (2.2) with input air power, P_{in}, and output air power, P_{out}. Secondly, by using the definition as Equation (2.3), we calculate boost ratio, k_p, with inlet pressure, p_{in}, and output pressure, p_{out}. Thirdly, we also calculate effective consumption rate, k_v, during the operating time $[0, \infty]$ by

Equation (2.4) with inlet flow rate, Q_{in}, and outlet flow rate, Q_{out}.

Next, we explain the method of the experiment. The purpose of this chapter is to investigate the performances of PBV-R under different area ratios and stroke lengths. Accordingly, using the part of experimental apparatus presented in Fig.3-3, we firstly test how the performances of PBV-R change under the area ratios of 1.56, 2.66, 4.30 and no expansion chamber: k_r is 1.56, 2.66 and 4.30 when diameter of an expansion chamber is 50 mm, 63 mm and 80 mm, respectively; and carrying out with no expansion chamber is PBV method for comparing the results of both PBV and PBV-R method. To do that, we fix the stroke length of 25 mm and carry out the experiment for each area ratio cylinder. Then, we carry out the same experiment on the other stroke lengths: 50 mm, 75 mm and 100 mm. Secondly, we set supply pressure of 300 kPa, 400 kPa and 500 kPa using a regulator. Also, the experiment is carried out 5 times at each supply pressure. We use the solid-state timer for changing a position of the solenoid valves by pushing a button switch.

3.1.4 Results of Experiment with Constant Stroke Length

In this section, we show the results of experiment when the stroke length is constant. Firstly, we explain the results of energy efficiency. From Fig.3-4 to Fig.3-7 illustrate the energy efficiencies of each area ratio. The dotted line indicates the energy efficiency at p_s=300 kPa, the dashed line indicates the energy efficiency at p_s=400 kPa and the solid line indicates the energy efficiency at p_s=500 kPa. Also, the dots at around k_r=0 are the results with no expansion cylinder, i.e., the results of PBV method. First, regardless of the stroke length, the energy efficiency is the greatest where k_r=1.56. Also, the energy efficiency tends to be higher as supply pressure becomes higher, but the energy efficiency tends to be lower as the area ratio becomes larger. When the stroke length and the supply pressure are fixed, the energy efficiency is up to 10% different between k_r =1.56 and k_r =4.30. In some cases, the energy efficiencies are lower than those of PBV method although the expansion cylinder recovers energy at k_r=2.66 and k_r=4.30, while the energy efficiencies are all greater than those of PBV at k_r=1.56.

Secondly, we explain the results of boost ratio. From Fig.3-8 to Fig.3-11 illustrate the boost ratios of each area ratio. All boost ratio shows a similar tendency that has the highest boost ratio at k_r=2.66: The boost ratio of k_r=2.66 is up to 0.4 higher than that of k_r=4.30, up to 0.2 higher than that of k_r=1.56. Also, the boost ratio tends to increase as supply pressure becomes higher.

Thirdly, we explain the results of effective consumption rate. From Fig.3-12 to Fig.3-15 illustrate the effective consumption rates of each area ratio. Regardless of the stroke length, effective consumption rate is the greatest where k_r=1.56 at all supply pressures. Also, the effective consumption rate tends to be lower as the area ratio becomes larger: the effective consumption rates at k_r=1.56 are up to 5% greater than those at k_r=2.66, up to 10% greater than those at k_r=4.30.

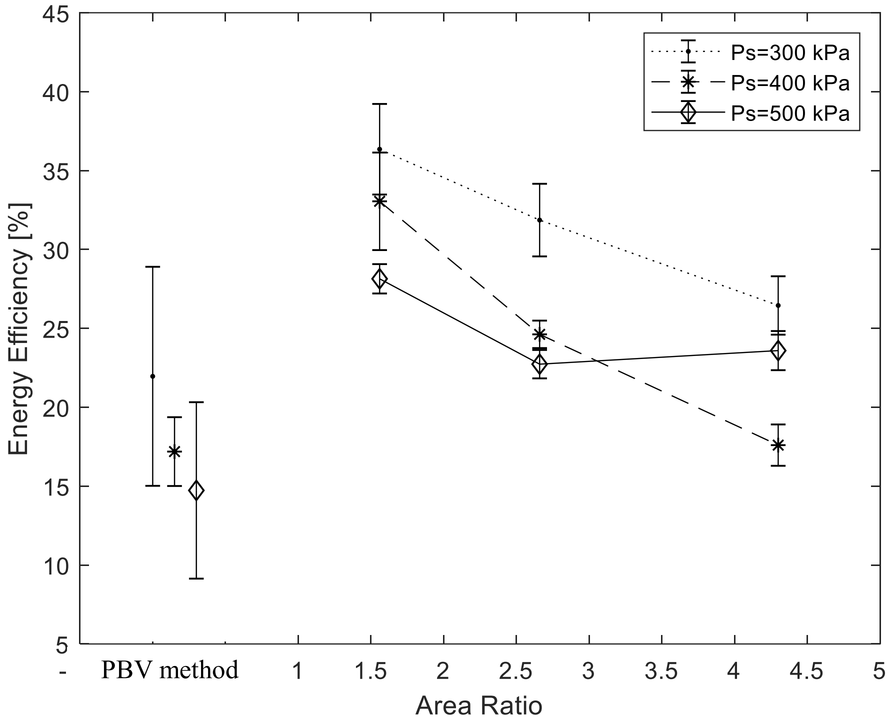

Fig.3-4. Energy efficiency at *L*=25 mm

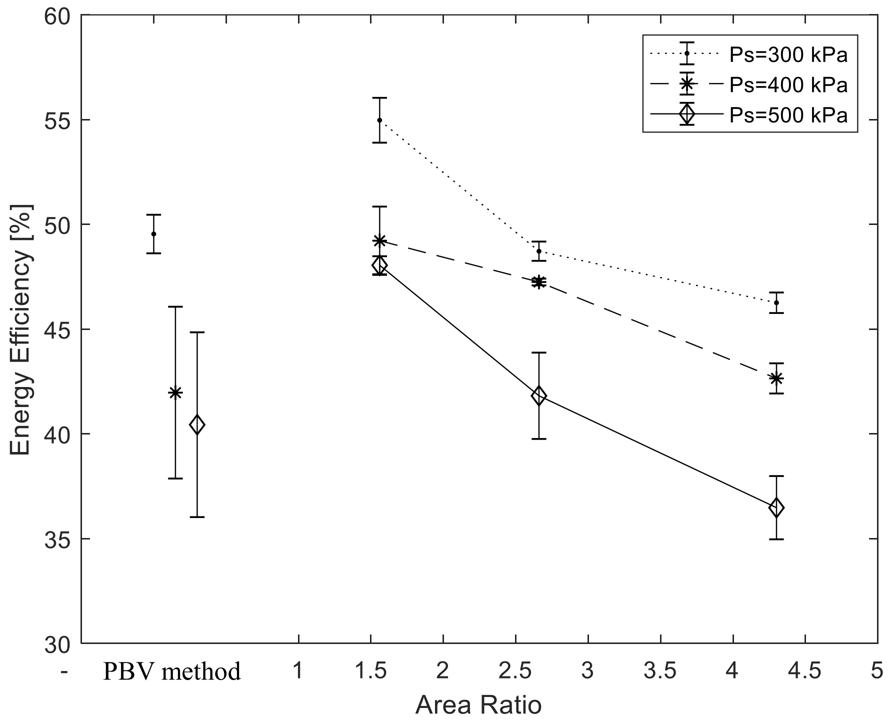

Fig.3-5. Energy efficiency at *L*=50 mm

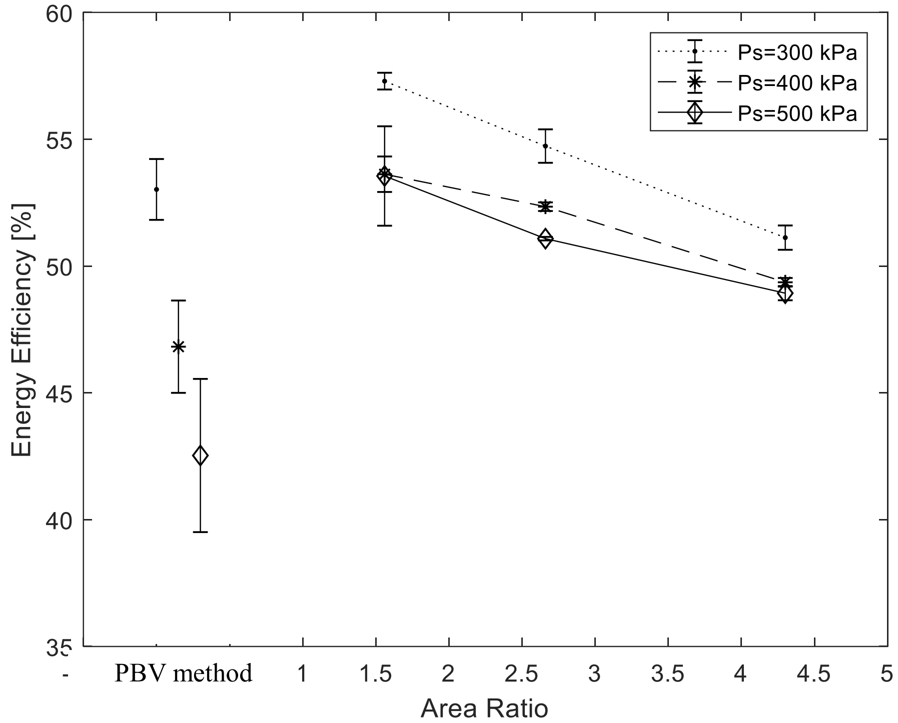

Fig.3-6. Energy efficiency at L=75 mm

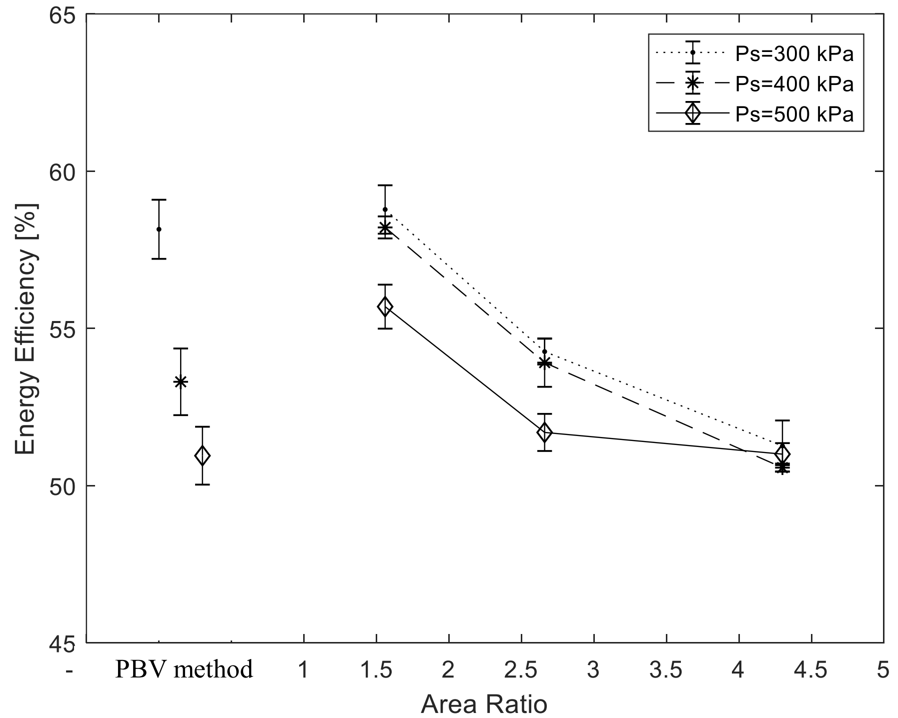

Fig.3-7. Energy efficiency at L=100 mm

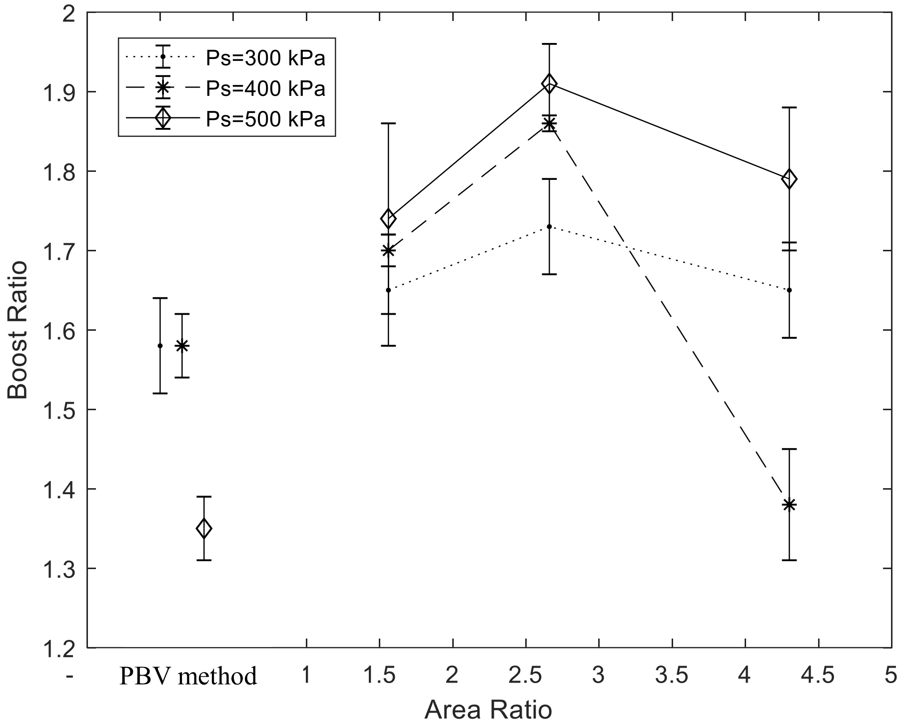

Fig.3-8. Boost ratio at L=25 mm

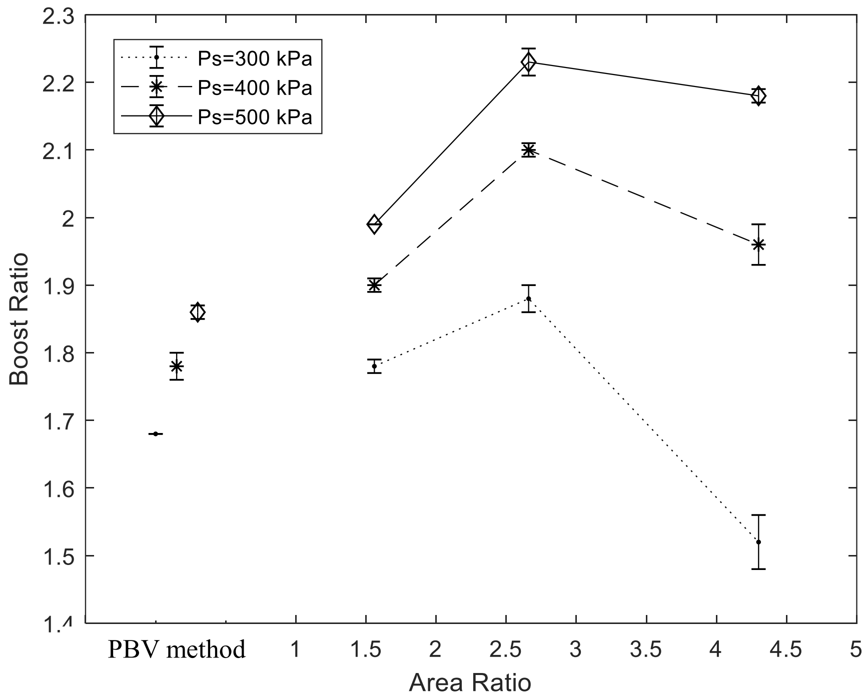

Fig.3-9. Boost ratio at L=50 mm

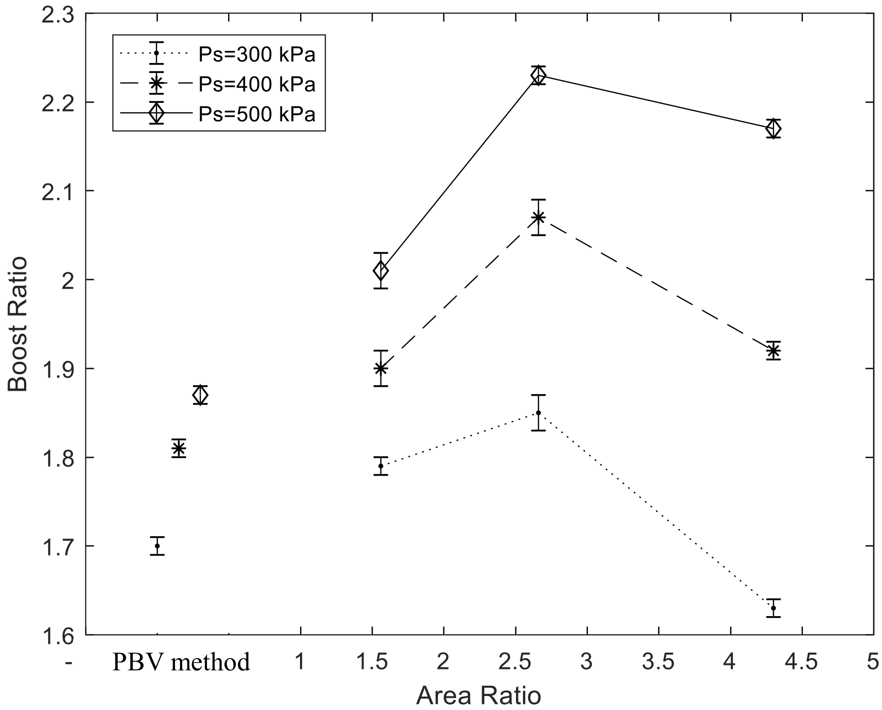

Fig.3-10. Boost ratio at *L*=75 mm

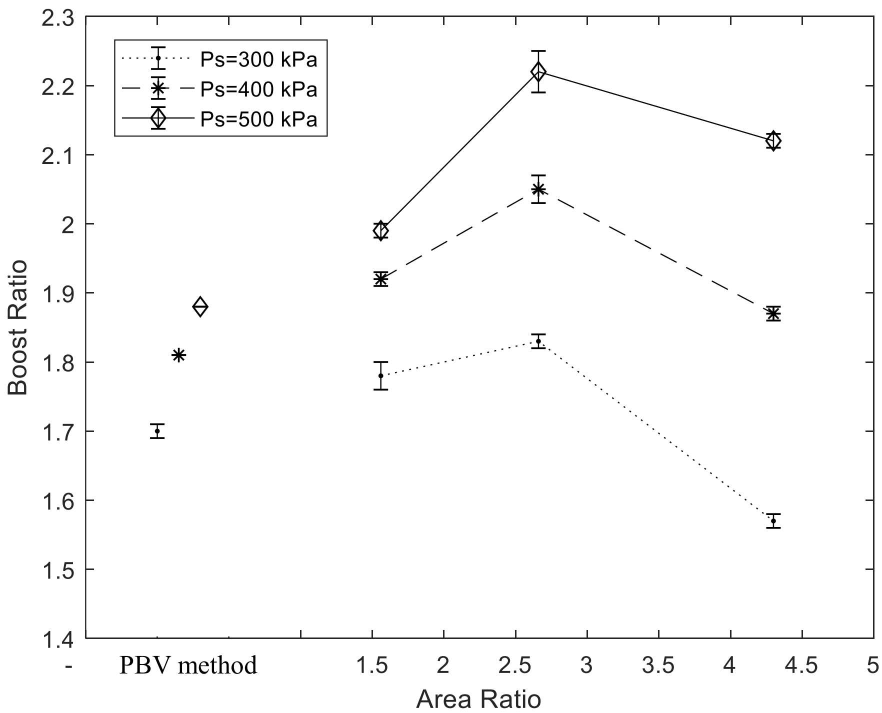

Fig.3-11. Boost ratio at *L*=100 mm

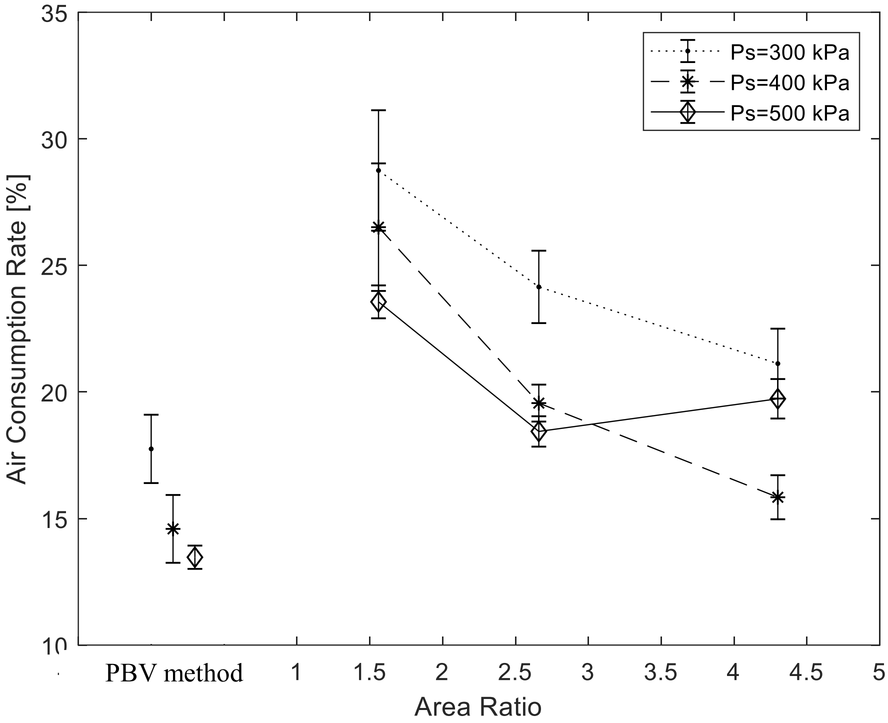

Fig.3-12. Effective consumption rate at *L*=25 mm

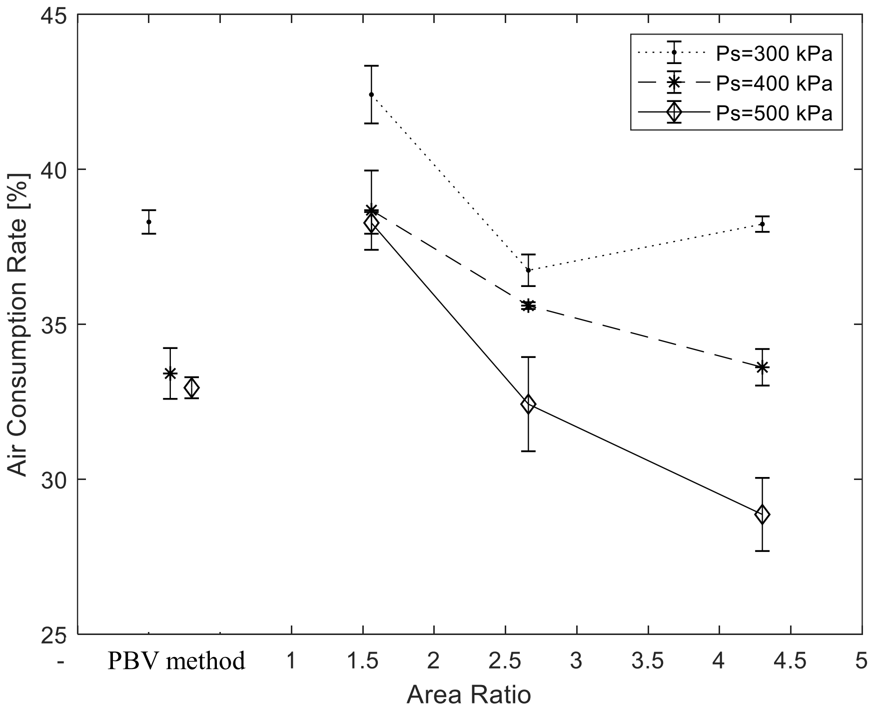

Fig.3-13. Effective consumption rate at *L*=50 mm

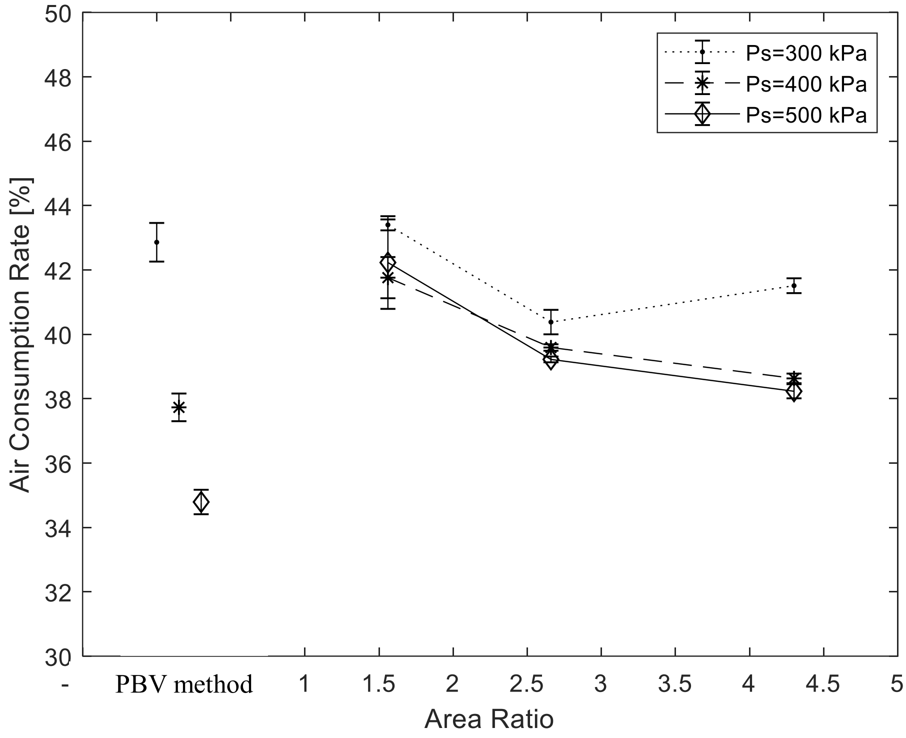

Fig.3-14. Effective consumption rate at *L*=75 mm

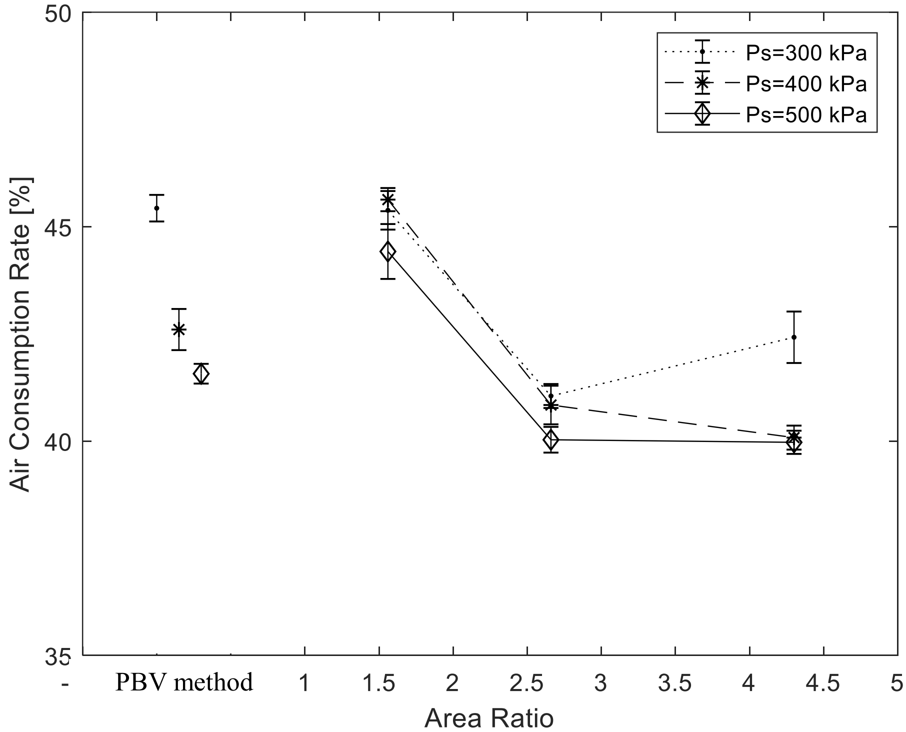

Fig.3-15. Effective consumption rate at *L*=100 mm

3.1.5 Results of Experiment with Constant Area Ratio

In this section, we show the results of experiment when the area ratio is constant. Firstly, we explain the result of energy efficiency. From Fig.3-16 to Fig.3-18 illustrate the energy efficiency of each stroke length. The energy efficiency tends to increase as the stroke length becomes higher for all area ratio. Especially, the energy efficiency at L =100 mm is from 50 % to 55 %, while the efficiency at L = 25 mm is around 20 % for all area ratios. The energy efficiency also becomes higher when supply pressure increases.

Secondly, we explain the result of boost ratio. From Fig.3-19 to Fig.3-21 illustrates the boost ratio of each stroke length. For all area ratio, the boost ratio is almost constant at all stroke length, exclusive of L=25 mm: the boost ratio has difference of less than 0.1 at L=50 mm, L=75 mm, L=100 mm, although these are around 0.6 different from the boost ratio at L=25 mm. Also, the boost ratio becomes greater when supply pressure increases.

Thirdly, we explain the result of effective consumption rate. From Fig.3-22 to Fig.3-24 illustrate the effective consumption rate of each stroke length. For all area ratio, the effective consumption rate tends to increase as the stroke length increases: the effective consumption rate is averagely from 40 to 45% at L=100 mm, whereas it is from 20 to 25 % at L=25 mm. the effective consumption rate also indicates tendency that becomes greater when supply pressure increases.

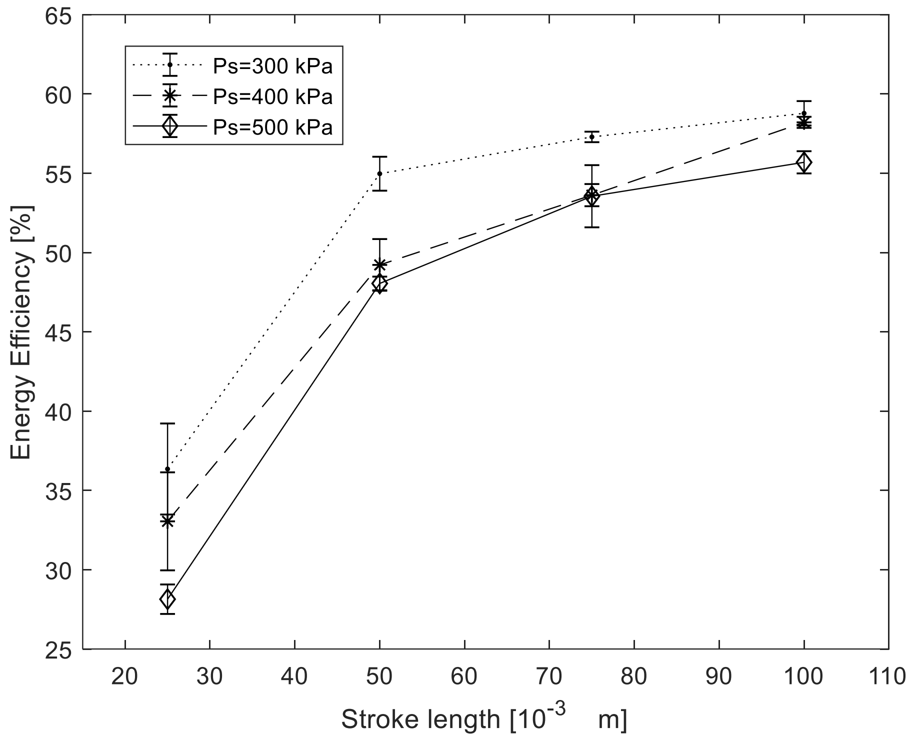

Fig.3-16. Energy Efficiency at k_r=1.55

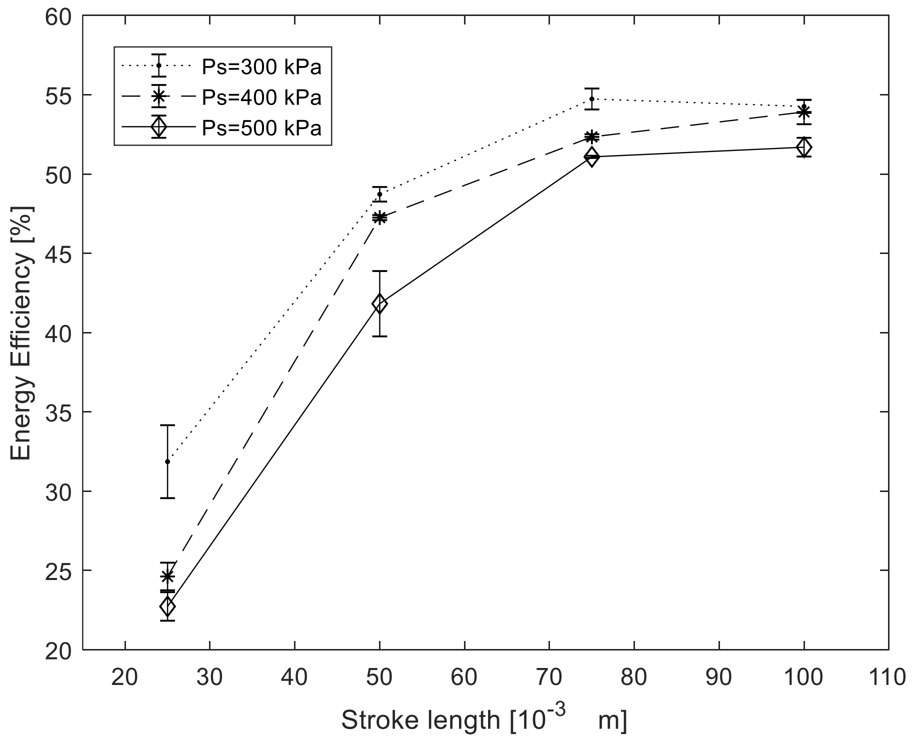

Fig.3-17. Energy Efficiency at k_r=2.55

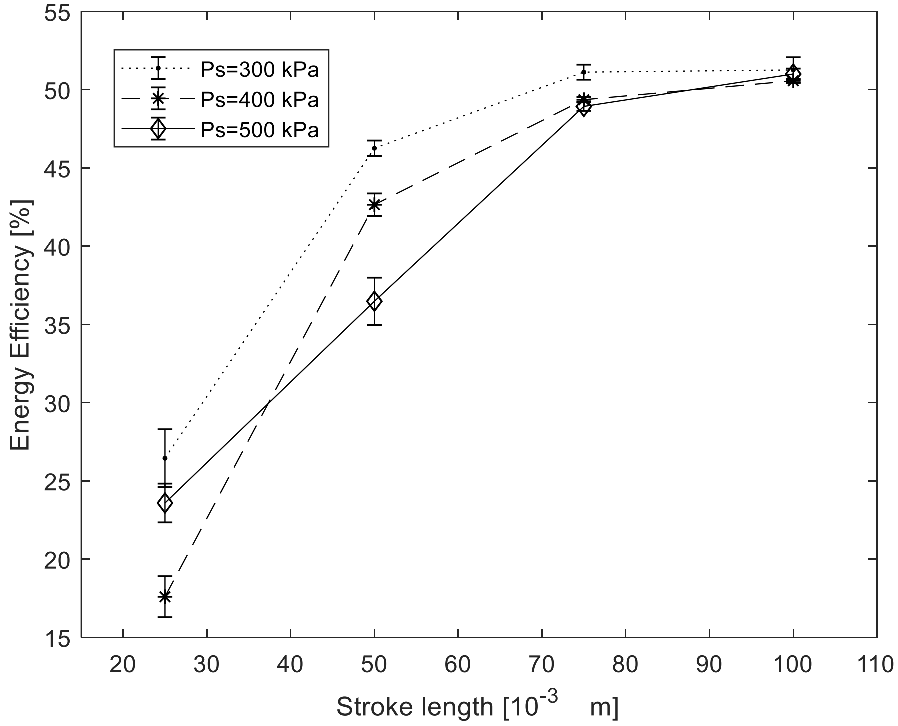

Fig.3-18. Energy Efficiency at k_r=4.30

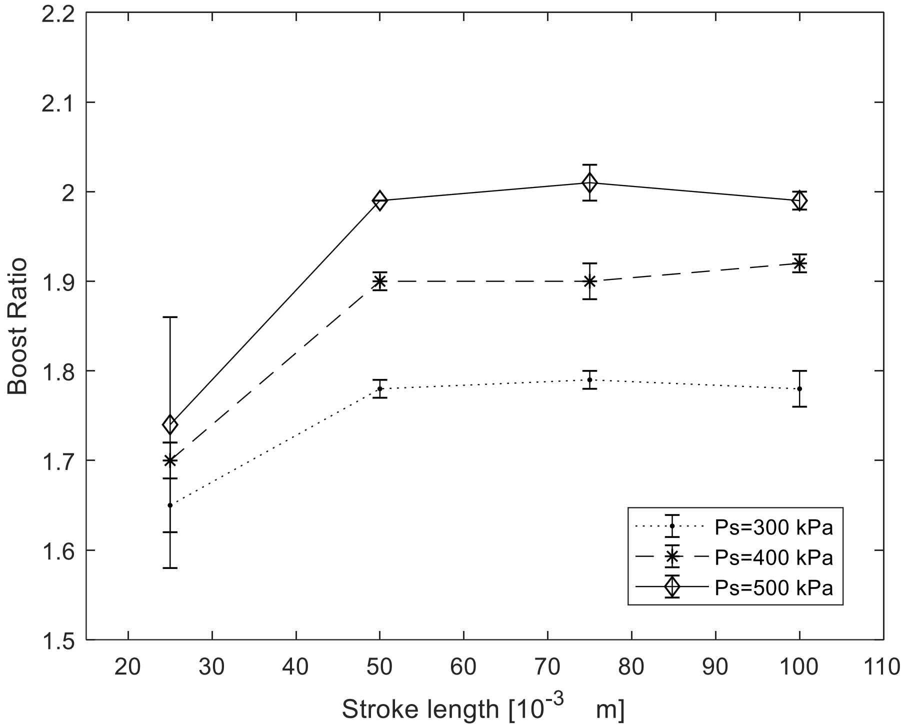

Fig.3-19. Boost ratio at k_r=1.55

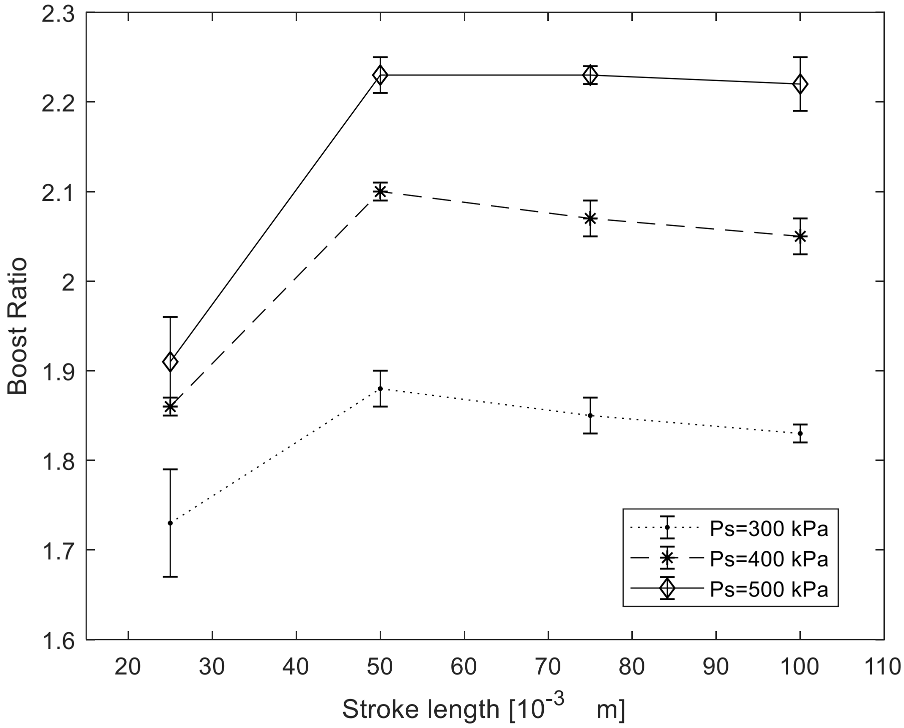

Fig.3-20. Boost ratio at k_r=2.55

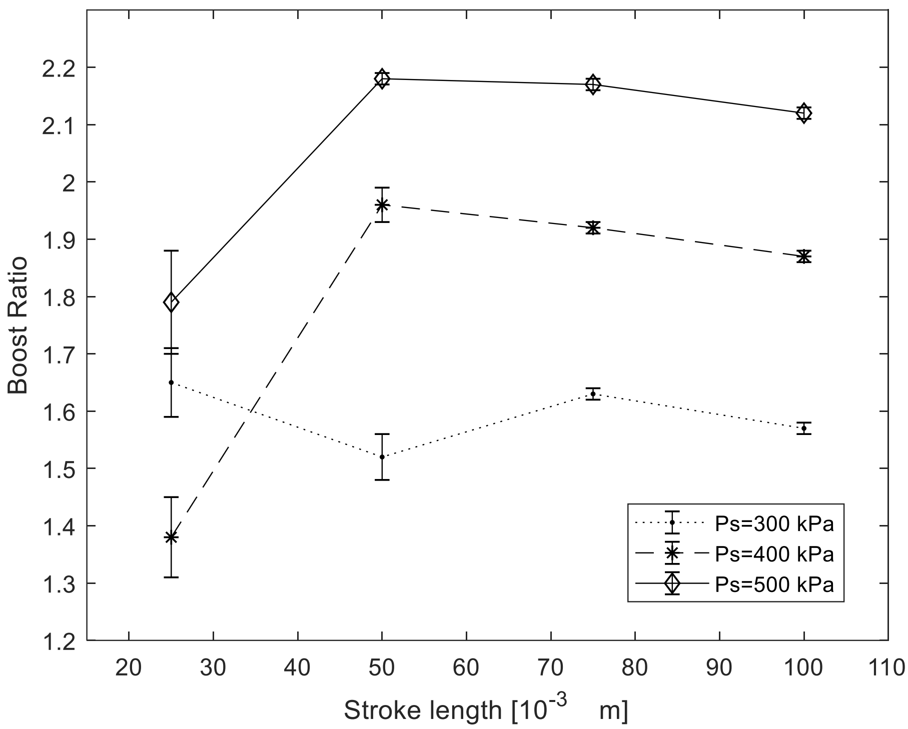

Fig.3-21. Boost ratio at k_r=4.30

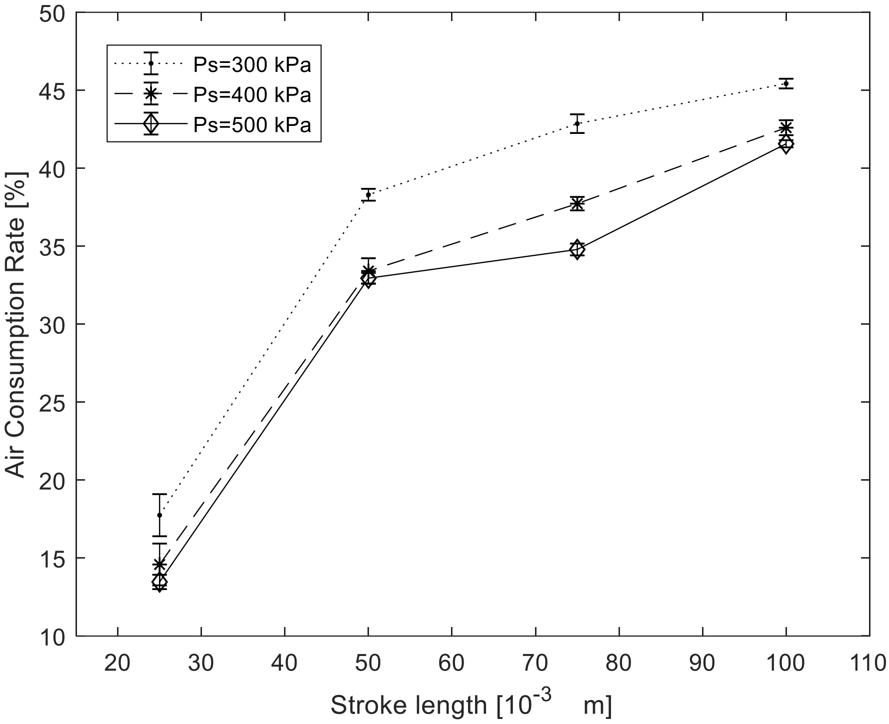

Fig.3-22. Effective consumption rate at k_r=1.55

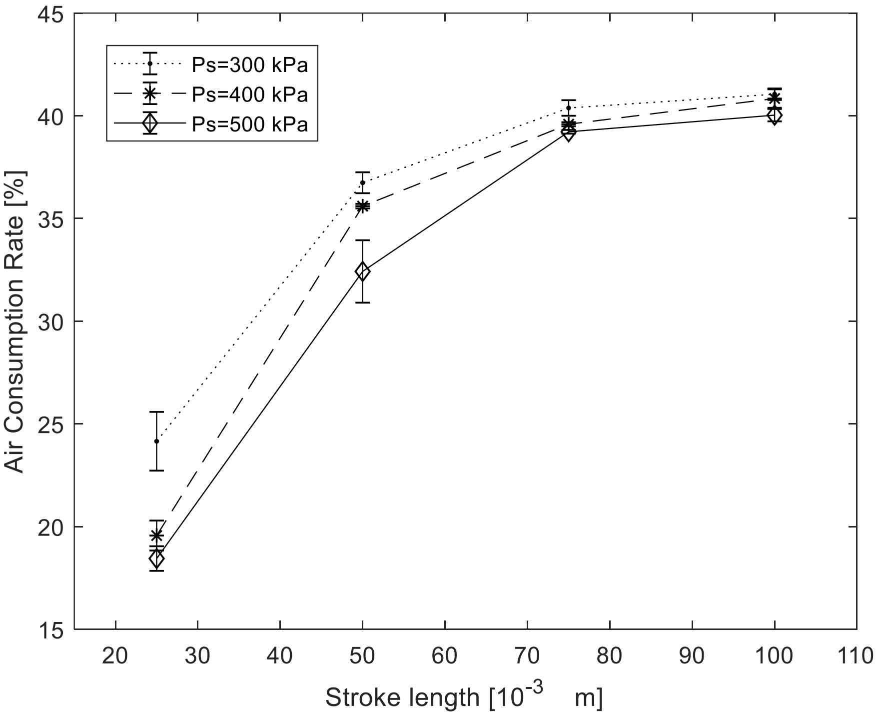

Fig.3-23. Effective consumption rate at k_r=2.55

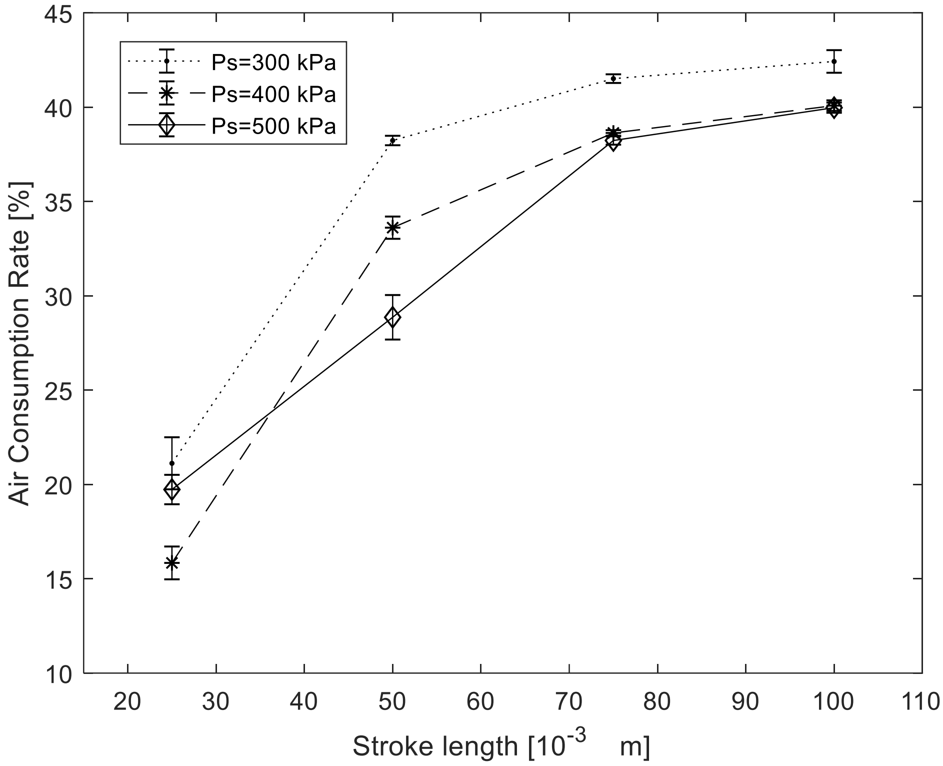

Fig.3-24. Effective consumption rate at k_r=4.30

3.2 Impact of Area Ratio and Stroke Length

3.2.1 Discussion

In this section, we mainly deal with the two things: energy efficiency and boost ratio. First, we discuss the results of boost ratio. Basically, the boost ratio, k_p, can be presented according to the resultant force as follow:

$$k_p = \frac{p_s(A_d + A_b) + p_s k_r (A_e - A_d) - p_a A_e - 2f_d - f_e}{p_s A_b} \tag{3.1}$$

Firstly, we discuss the boost ratio where stroke length is constant. According to from Fig.3-8 to Fig.3-11, the boost ratio has properties that it becomes maximum where k_r=2.66 if stroke length is constant. However, in Equation (3.1), we can find that the boost ratio increases as the area ratio, k_r, becomes greater, if friction forces f_d and f_e does not change. The reason that the boost ratio decreases at greater than k_r=2.66 is considered as increase of the friction forces. Since the air cylinders used in the experiment are manufactured devices, the mass of the pistons and the piston rod becomes greater as diameter of the air cylinder increases, according to the catalog [66]. Moreover, size of pneumatic seals in the air cylinders in proportion to the diameter, although the information about pneumatic seals is not on the catalog. Thus, it is obvious that the friction forces increase as the area ratio increases. Secondly, we discuss the boost ratio where area ratio is constant. According to Fig.3-19, Fig.3-20 and Fig.3-21, the boost ratio has a certain value at all stroke lengths, except stroke length of 25 mm, i.e., the stroke length affect boost ratio. As it is indicated in Equation (3.1), however, we can find that stroke length has generally no effect on boost ratio.

Table 3-II. Dead volume rate at each stroke length

25 mm	15.8 %
50 mm	7.9 %
75 mm	5.3 %
100 mm	3.9 %

The reason is considered that dead volume disturbs boosted air from flowing into air tank.

Next, we discuss the results of energy efficiency. As shown in from Fig.3-4 to Fig.3-7, we can found that stroke length affects the energy efficiency of PBV-R. However, it was numerically proved that there is no relationship between them. It is considered that the determinant of energy efficiency drop is dead volume. According to Equation (2.1), air power is in proportion to mass flow *G* and the dead volume can reduce the mass flow. Also, as represented in Table.3-II, dead volume tends to increase if stroke length becomes shorter. Furthermore, from the results, energy efficiency decreases as stroke length becomes shorter. Thus, we can suppose that there is a positive correlation between dead volume and stroke length.

3.2.2 Definition of Dead Volume Rate

In Section 3.2.1, we supposed that dead volume affects both energy efficiency and boost ratio of PBV-R. thus, in this section, we discuss how large an influence of the dead volume is on PBV-R. More precisely, we now calculate energy efficiency of PBV-R including dead volume.

First, in this paper, we define the dead volume as the whole volume except a chamber of an air cylinder, i.e., the dead volume includes tube, pipes, measurement devices, etc. Then, we also define and use 'dead volume rate' that indicates a ratio of the dead volume to the whole volume. The whole volume, V_{all}, can be presented by using an ideal volume of a chamber which is considered that no dead volume exists, V_{ideal}, and the dead volume rate, α, as follow:

$$V_{\mathrm{all}} = V_{\mathrm{ideal}}(1+\alpha) \tag{3.2}$$

Using the dead volume rate, we calculate the energy efficiency of PBV-R including dead volume. To simplify the calculation, we assume as follows:

(A) The air in the system is considered to be an ideal gas: the states of the air satisfy ideal gas state equation

(B) There is no air leakage in the system

(C) Temperature change of the air can be neglected: no heat transfer through the wall of the air cylinders occurs and all processes of state changes are isothermally. Also, all temperatures are considered as 293 K.
(D) All volumes except the volume of pneumatic cylinders can be neglected; pipe, end of pneumatic cylinders, etc.
(E) The pressure in a chamber is constant as supply pressure while air flows in and out: if air supplied to a chamber, the pressure of the chamber reaches the pressure of the air immediately without any delay, and if compressed air is exhausted, it does not fluctuate.

In order to calculate energy efficiency, it is necessary to define an equation of energy of compressed air. According to the definition of air power as Equation (2.1), because we assume that temperature change of the air can be neglected, energy of compressed air can be simplified with pressure, p, volume, V, mass, m, temperature, T, and gas constant, R, as follow:

$$E = pV \ln \frac{p}{p_a} = mRT \ln \frac{p}{p_a} \tag{3.2}$$

In Equation (3.2), we can find that only pressure and mass are necessary for calculating energy of compressed air. However, the outlet pressure and the outflow mass is not constant but changeable according to the number of stroke, n. Therefore, we need to generalize the pressure and the mass equation in terms of n: the pressure indicates average pressure of boosted air during the *n*th stroke and the mass indicates the entire mass of boosted air flowing into the air tank during the *n*th stroke.

A. The general equation of pressure

In the case of pressure of air tank, it is necessary to consider the case with no dead volume in different light from the case with dead volume calculation.
First, we find the general equation of pressure of air tank without dead volume. In this case, inlet pressure is the same as supply pressure, p_s, regardless of the number of stroke, n, whereas outlet pressure changes by the number of stroke. as shown in Fig.

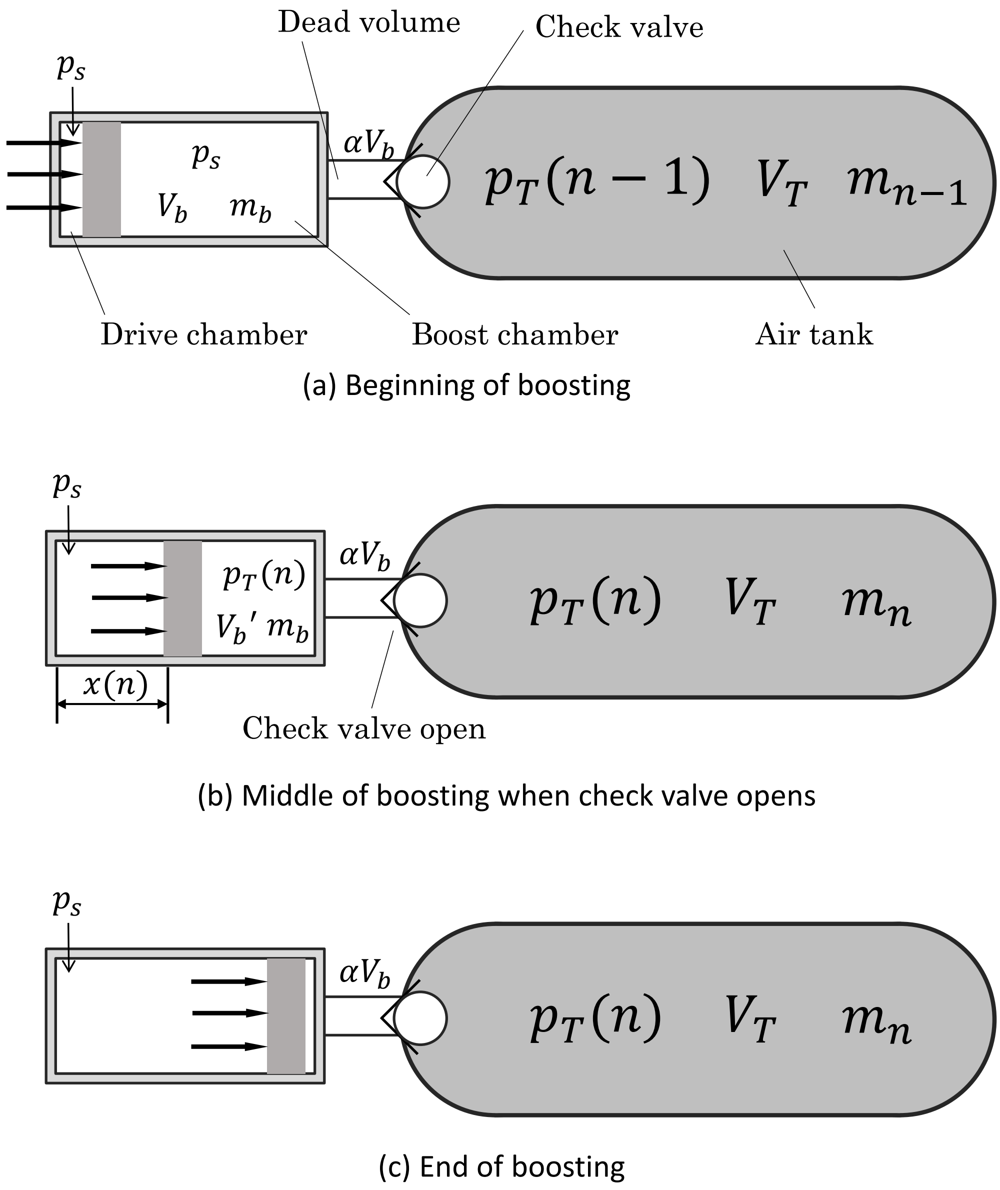

Fig.3-25. Schematic of boost chamber and air tank

3-25, the boost chamber and the air tank can be considered as a closed system and the initial pressures in the boost chamber and the air tank are p_s. Therefore, according to the general gas equation, state equation is established as follow:

$$p_s V_b + p_T(n-1)V_T = p_T(n)V_T \tag{3.3}$$

In Equation (3.3), $p_T(\mathrm{n})$ is the pressure of the air tank when the *n*th stroke ends and $p_T(0)$ is p_s. From Equation (3.3), the general equation of $p_\mathrm{T}(n)$ can be presented as follow:

$$p_T(n) = p_s(1 + \frac{V_b}{V_T}n) \tag{3.4}$$

In addition, by using Equation (3.4), it is also possible to calculate the number of strokes of PBV, N, that occur until the piston stops if final outlet pressure, p_{PBVR}, is already known. Let $p_T = p_{\mathrm{PBVR}}$ and $n = N$, then N can be presented as follow:

$$N = \frac{(p_{\mathrm{PBVR}} - p_s)V_T}{p_s V_b} \tag{3.5}$$

p_s, V_T, V_b are given in Equation (3.5) and p_{PBVR} can be calculated in Equation (3.1), then we can find the number of stroke N.

Next, we find a general equation of pressure of air tank with dead volume. Similarly, inlet pressure is the same as supply pressure, p_s, regardless of n, whereas outlet pressure changes by the number of stroke n. As shown in Fig.3-25, the boost chamber, the dead volume and the air tank can be considered as a closed system, then the initial pressures in the boost chamber, the dead volume and the air tank are all p_s. Thus, following equation is established, according to the general gas equation:

$$p_s V_b(1 + \alpha) + \hat{p}_T(n - 1)V_T = \hat{p}_T(n)(V_T + \alpha V_b) \tag{3.6}$$

From Equation (3.6), the general equation of $\hat{p}_T(n)$ can be presented as follow:

$$\hat{p}_T(n) = \frac{p_s}{\alpha}\left[\alpha + 1 - \left(\frac{V_T}{V_T + \alpha V_b}\right)^n\right] \tag{3.7}$$

Like above, by using Equation (3.7), it is also possible to calculate the number of strokes of PBV-R, $\widehat{N}$, that occur until the piston stops if final outlet pressure, p_{PBVR}, is already known. Let $\hat{p}_T = p_{\mathrm{PBVR}}$ and $n = \widehat{N}$, then $\widehat{N}$ can be presented as follows:

$$\widehat{N} = \frac{\ln(\alpha + 1 - \frac{\alpha p_{\mathrm{PBVR}}}{p_s})}{\ln V_T - \ln(V_T + \alpha V_b)} \tag{3.8}$$

p_s, V_T, V_b, α are given in Equation (3.7) and p_{PBVR} can be calculated in Equation (3.1), then we can find the number of stroke $\widehat{N}$.

B. The general equation of mass

Before calculating, we need to make clear that the general equation of mass means mass of boosted air that flows into air tank during *n*th stroke. In Fig.3-25, the piston of the air cylinder moves to the right side and boost the pressure in the boost chamber, while the check valve is closed. When the pressure in the boost chamber reaches to the tank pressure, the air in the boost chamber starts to flow into the tank. Therefore, first, we find a distance, x, that the piston moves until the check valve opens. The dead volume and the boost chamber can be considered as a closed system until the check valve opens. Therefore, because initial pressure is p_s and the pressure when the check valve opens is $\hat{p}_T(n)$, following equation is established according to the general gas equation:

$$p_s V_b (1 + \alpha) = \hat{p}_T(n) V_b \frac{L - x(n)}{L} \tag{3.9}$$

In Equation (3.9), L is the length of a stroke and $x(n)$ is the distance that piston moves until the check valve opens during the *n*th stroke. From Equation (3.9), the general equation of $x(n)$ can be written as follow:

$$x(n) = L(\alpha + 1)(1 - \frac{p_s}{\hat{p}_T(n)}) \tag{3.10}$$

Next, it is necessary to find how much mass of boosted air actually flows into the tank. Fig.3-25(b) represents the moment that the check valve opens, while Fig.3-25(c) shows that the piston reaches at the end of the boost chamber. Because we assume that the pressure is constant, the ratio of the mass that actually flows into the tank is $1 - x/L$

out of $1-x/L+\alpha$. Therefore, by using Equation (3.10), nth mass that actually flows into the air tank, m_n, can be presented as follow:

$$m_n = \frac{1 - x/L}{1 - x/L + \alpha} m_b = \left[1 - \frac{\alpha \hat{p}_T(n)}{(\alpha + 1)p_s}\right] m_b \tag{3.11}$$

In Equation (3.11), m_b is the initial mass in the boost chamber. By Equation (3.11), both the case with dead volume and the case without dead volume can be calculated: $m_n = m_b$ if $\alpha = 0$, i.e. m_n is always equal to m_b if there is no dead volume.

C. The general equation of energy efficiency

First, we calculate inlet energy of air. Because supply pressure flows into both drive chamber and boost chamber, and we assume that pressure is constant, the entire inlet energy during the operation of PBV-R, E_{in}, is established as follow, based on Equation (3.2):

$$E_{\text{in}} = n p_s (V_b + V_d) \ln \frac{p_s}{p_a} \tag{3.12}$$

In Equation (3.12), n is N if there is no dead volume and n is $\hat{N}$ if there is dead volume. Next, we calculate outlet energy of air. During the nth stroke, the pressure changes from p_{n-1} to p_{n}. However, because it is much smaller than the supply pressure, we assume that the pressure during the nth stroke is constant as $(p_{n-1} + p_n)/2$. Then, the entire outlet energy during the operation of PBV-R, E_{out}, can be calculated as follow:

$$E_{\text{out}} = \sum_{n=1}^{k} \bar{p}_n (V_b + V_d) \ln \frac{\bar{p}_n}{p_a} \tag{3.13}$$

In Equation (3.13), k is N if dead volume exists and k is $\hat{N}$ if dead volume does not exist. Also, $\bar{p}_{\text{n}} = (p_{\text{n}-1} + p_{\text{n}})/2$ where $p_{\text{n}} = p_T(n)$ if dead volume exists and $p_{\text{n}} = \hat{p}_T(n)$ if dead volume does not exist. Thus, the energy efficiency with and without dead volume can be calculated by using Equation (2.2), (3.12) and (3.13).

3.2.3 Relationship between Dead Volume Rate and Energy Efficiency

Fig.3.26 indicates the relationship between dead volume rate and the energy efficiency. The dotted lines indicate the area ratio of 1.55, the dashed lines indicate the area ratio of 2.55, and the solid lines indicate the area ratio of 4.30. Also, the blue lines indicate the supply pressure of 300 kPa, the green lines indicate the supply pressure of 400 kPa, and the red lines indicate the supply pressure of 500 kPa. Overall, we can find that the energy efficiency diminishes as the dead volume rate increases. The energy efficiency has the maximum value as 62.1 % where k_r =1.55 and p_s=300 kPa. However, the energy efficiency decreases until 14.0 % under the same condition. In addition, Energy efficiency shows almost the same tendency under different conditions.

In this chapter, because we did not change the pipe or tube in the experimental apparatus and the dead volume accounts for the most part of the apparatus, the dead volume rate in the experiment is inversely proportional to the stroke length. In other words, PBV-R with 25 mm stroke length has 4 times greater dead volume rate than PBV-R with 100 mm stroke length. Thus, the differences between the energy efficiency

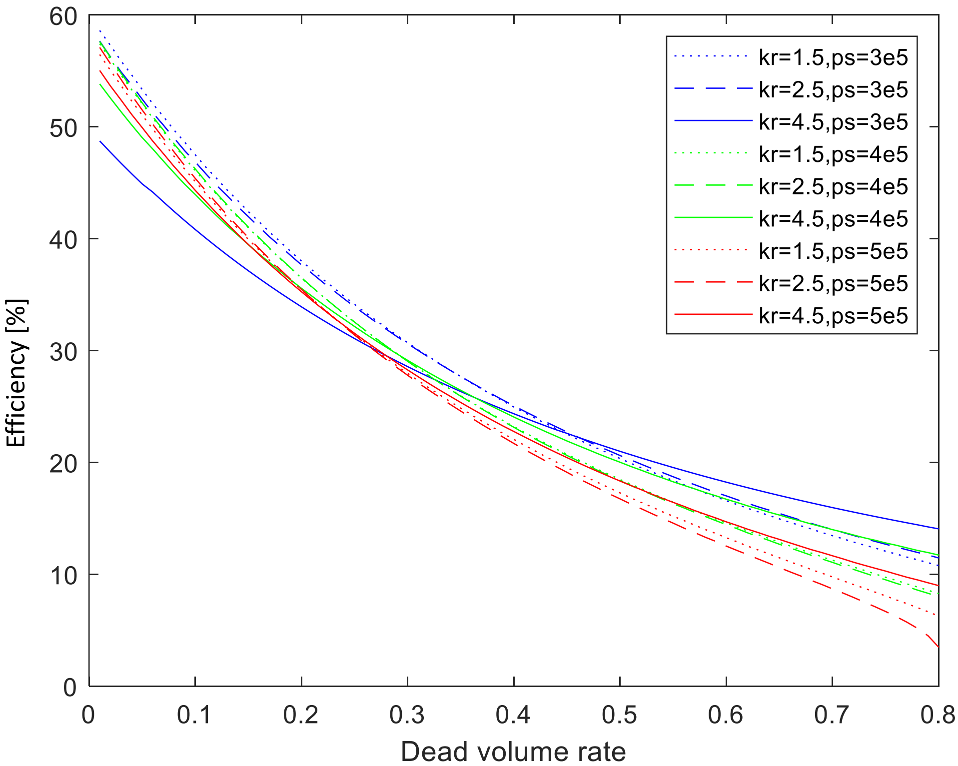

Fig.3-26. Relationship between dead volume rate and energy

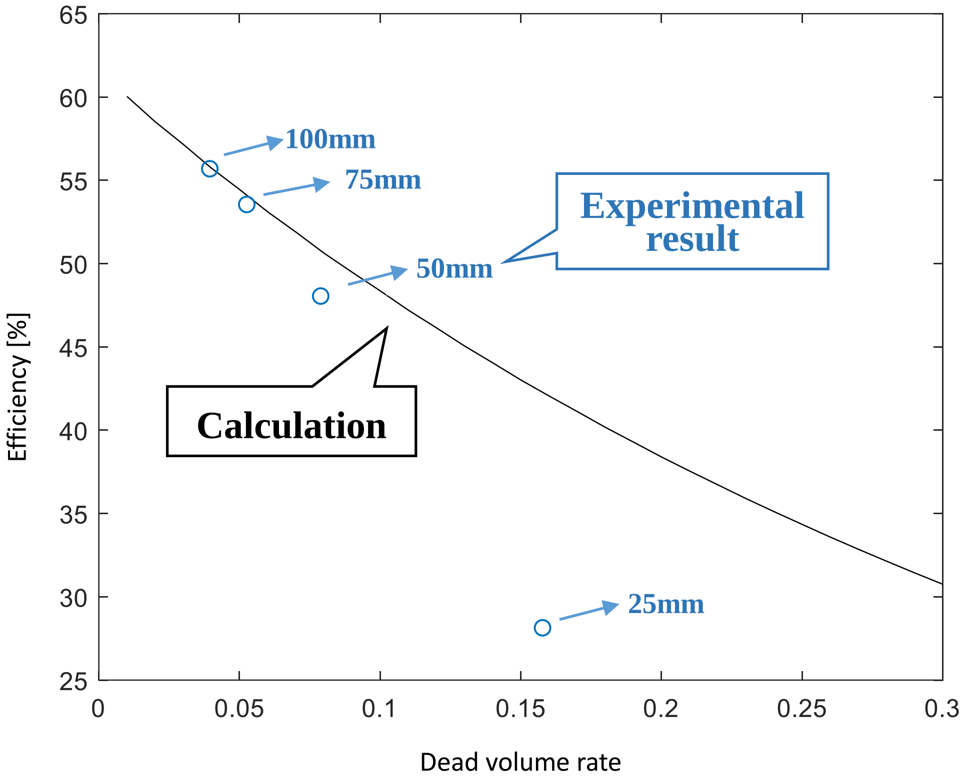

Fig.3-27. Comparison between calculation and experimental result at p_s=300 kPa and k_r=1.55

of several stroke lengths can be explained by Fig.3-26.

Next, we compare the experimental results with the calculational results. As shown in Fig.3-26, because the all cases have the same tendency and there are small differences between them, we only deal with the case where supply pressure of 300 kPa and area ratio of 1.55. According to Table.3-II, the experimental results and calculational results, we can indicate the relationship as Fig.3-27. Except at stroke length of 25 mm, the calculational results agree well with the experimental results at all stroke length. The reason that the results does not coincide at stroke length of 25 mm is considered as depth of button switches. The button switches of experimental apparatus are designed that position of solenoid valves is changed when the button switches are fully pushed. However, if the position of the solenoid valves is changed before the button switches are fully pushed, boosted air cannot fully flow into an air tank and is exhausted on the next mode of PBV-R, which is considered as the reason that the difference between calculation result and experimental result become greater as stroke length decreases. Hence, we can say the discussion with dead volume is reasonable.

3.3 Summary

We list the following conclusion from the experiment and discussion in this chapter:

1. We designed a pneumatic circuit and set up a new experimental apparatus that can, unlike the experimental apparatus in Chapter 2, change all air cylinders. The experimental apparatus mainly consists of two single-rod air cylinders as drive cylinder, one double-rod air cylinder as expansion cylinder, two 5-way/2-position solenoid valves, and four check valves. A diameter of the drive cylinder is 40 mm, while a diameter of the expansion cylinder is 50 mm, 63 mm or 80 mm. Also, the whole air cylinder has four different stroke lengths: 25 mm, 50 mm, 75 mm and 100 mm. By using the experimental apparatus, we investigate energy efficiency, boost ratio and effective consumption rate under two conditions: stroke length is constant, and area ratio is constant.

2. If the stroke length is constant, firstly, the energy efficiency is the greatest where an area ratio is 1.56. Also, the energy efficiency tends to be higher as supply pressure becomes higher, but the energy efficiency tends to be lower as the area ratio becomes larger. Secondly, the boost ratio is the greatest where an area ratio is 2.66. The boost ratio at k_r=2.66 is up to 0.4 higher than that of k_r=4.30, up to 0.2 higher than the boost ratio at k_r=1.56. Thirdly, the effective consumption rate is the greatest where a stroke length is 100 mm and an area ratio is 1.56. Also, the effective consumption rate tends to be lower as the area ratio becomes larger.

3. If the area ratio is constant, firstly, the energy efficiency is the greatest where a stroke length is 100 mm. The energy efficiency tends to increase as the stroke length becomes higher for all area ratio. Secondly, the boost ratio is the greatest where a stroke length is 50 mm or more: the boost ratio is almost constant at all stroke length for all area ratio, exclusive at L=25 mm. Thirdly, the effective consumption rate is the greatest where a stroke length is 100 mm. Also, for all area ratio, the effective consumption rate tends to increase as the stroke length increases.

4. The results show that the energy efficiency of PBV-R increases as stroke length

becomes longer, whereas numerical results indicates stroke length does not have any effect on energy efficiency of PBV-R. The reason is considered that dead volume rate decreases as stroke length becomes longer. Therefore, we carry out calculation of energy efficiency of PBV-R with consideration of dead volume. According to the experimental results and the calculation, we can conclude that dead volume rate has a large effect on energy efficiency of PBV-R and this conclusion can explain the reason that PBV-R with shorter stroke length shows smaller energy efficiency.

Chapter 4

Proposal of Design Policy and Evaluation of Prototype of Pneumatic Booster Valve with Energy Recovery

4.1 Determination of Geometric Parameters

4.1.1 Determination of Stroke Length of PBV-R

In this chapter, we produce a prototype of PBV-R. Before making, we determine parameters of the prototype e.g. stroke length and area ratio, and the results in Chapters 2 and 3 can be very important clues for the parameters of the prototype. We produce the prototype of PBV-R by manufactured products and reflect all the results in Chapters 2 and 3.

First, we explain area ratio of the prototype. According the experimental results, energy efficiency of PBV-R was the greatest at area ratio of 1.6. Also, as shown in Table.4-I, there is a limit to change area ratio. Therefore, we utilize two air cylinders

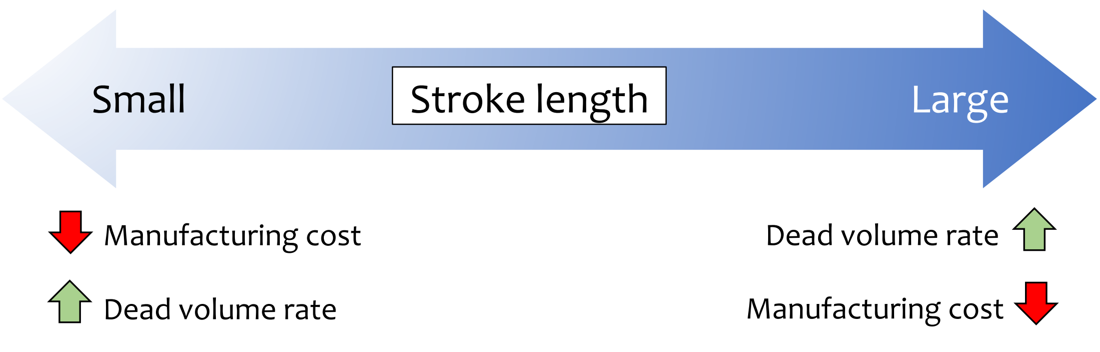

Fig.4-1. Diagram of the relationship between stroke length and manufacturing cost

with 40 mm diameter as drive cylinders and one air cylinder with 50 mm diameter as an expansion cylinder.

Next, we consider stroke length of the prototype. We confirmed that energy efficiency of PBV-R increases as dead volume rate decreases, which is inversely proportional to stroke length. Thus, we need to make the dead volume rate as small as possible in order for energy efficiency to be higher. However, if the dead volume rate is near zero, stroke length has to diverge to infinity, which makes production cost of PBV-R higher. If the dead volume rate increases, operating time of air compressors is lengthened as much as energy efficiency decreases, i.e., energy consumption increases if dead volume rate increases.

Fig.4-1 shows the relationship between stroke length and production cost of PBV-R. dead volume is inversely proportional to stroke length, so if stroke length converges to zero or diverges to infinity, the production cost of PBV-R diverges to infinity as well. Thus, it is assumed that the function of the production cost has the maximum value between zero and infinity. In this section, we find the stroke length that makes the production cost minimum. Since it is very difficult to compare electricity energy with cost directly, we evaluate the electricity energy by converting into monetary unit, Yen, in this section.

Firstly, we calculate cost loss by dead volume. Because electricity energy loss that is correspond to dead volume occurs each stroke, we need to find how many strokes occur in lifespan of an air cylinder, which is one of characteristics of an air cylinder and usually indicated by the entire distance of a piston. Therefore, the number of strokes can be calculated by dividing lifespan of an air cylinder by stroke length. Then, we can find cost loss, w_d, by multiplying the number of strokes by electricity charge per unit volume as follow:

$$w_d = \frac{svE_v}{L} \tag{4.1}$$

where s represents lifespan of an air cylinder, v represents dead volume, E_v represents electricity charge per unit volume and L represents stroke length. Secondly, we calculate cost of an air cylinder. the cost of an air cylinder is linearly related to stroke length as follow:

$$w_c = b_1 L + b_2 \tag{4.2}$$

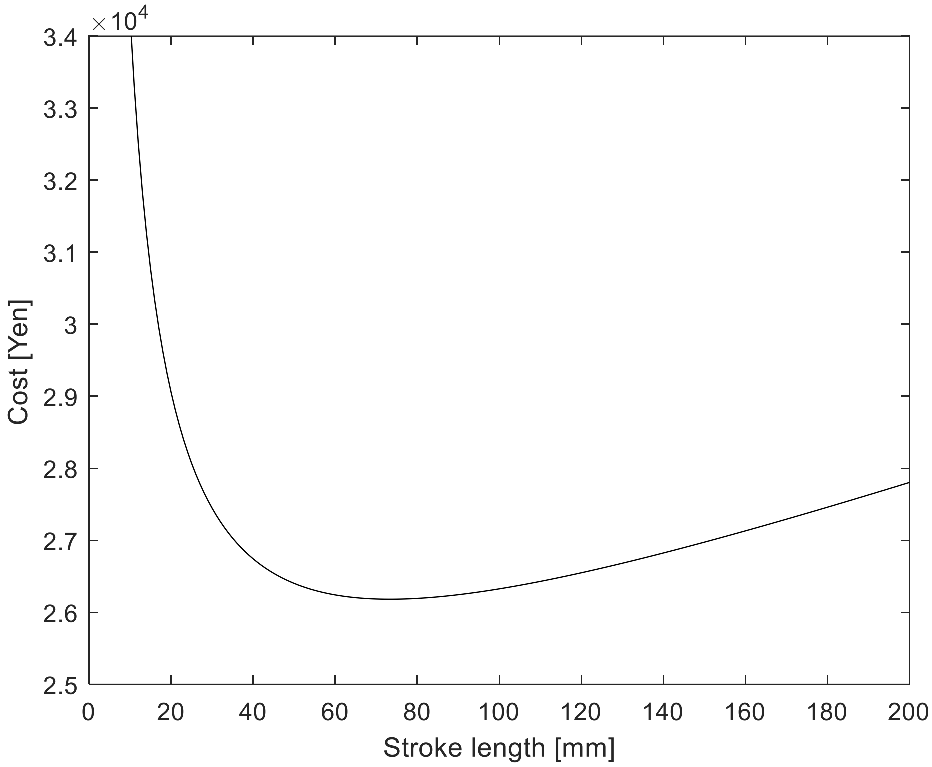

Fig.4-2. Relationship between stroke length and production cost

where b_1 represents price per unit length and b_2 represents basic price. Lastly, we find the minimum cost of production PBV-R. By adding Equation (4.1) and (4.2), we can calculate the entire cost. Each parameter is given in Table.4-I. Fig.4-2 shows the relationship between the entire cost and stroke length of an air cylinder. The entire cost tends to diverge to infinity where stroke length converges to zero and infinity. Also, the cost has the minimum value as 2.62×10^4 Yen at stroke length of 73 mm. For those reason, we choose stroke length of 75 mm for producing the prototype of PBV-R because 75 mm is the closest stroke length from 73 mm among manufactured air cylinders.

4.1.2 Suggestion for Higher Energy Efficiency of PBV-R

We propose the optimal design of PBV-R. Firstly, in terms of area ratio, it can be determined according to recovery ratio, Equation (2.11), in Section 2.3, i.e., the area

Table.4-I Value of each parameter

s[69]	8.0×10^{6} [m]
v	7.54×10^{-6} [m^3]
E_v[72]	1.8 [Yen/m^3]
b_1	4.02×10^{4} [Yen/m]
b_2	2.32×10^{4} [Yen]

ratio that maximizes recovery ratio also maximize energy efficiency of PBV-R. Secondly, in terms of stroke length, for a plant who wants high energy efficiency regardless of production cost, longer stroke length performs higher energy efficiency. For a plant who wants less production cost, it is necessary to find the stroke length that minimizes a sum of Equation (4.1) and (4.2). In addition, because it is obvious that both production expense and energy efficiency decrease if stroke length is shorter than optimal stroke length, shorter length than optimal value is not necessary for optimal design.

4.2 Production and Validation of Prototype of PBV-R

4.2.1 Production of Prototype of PBV-R

In Section 4.1, we found that the most suitable stroke length of the air cylinder is 75 mm for a prototype of PBV-R. Furthermore, because producing PBV-R from A to Z costs much expense, we utilize manufactured components for the prototype. Prototype consists of two single-rod air cylinders with a 40 mm diameter and a 75 mm stroke length, one double-rod air cylinders with a 50 mm diameter and a 75 mm stroke length, four check valves, two 5-way/2-position solenoid valve, aluminum frame for fixing three air cylinders, two double-ended bolts for connecting rods of the cylinders, two button switch for switching position of the solenoid valves, and polyurethane tube with 5 mm diameter. Since one of the aims of the prototype is 250 L/min(ANR) flow rate and an existing PBV manufactured by SMC has flow rate of 250 L/min(ANR) with diameter of 40 mm, we choose 40 mm as a diameter of the prototype [69]. Table.4-II indicates all components of the prototype.

Next, by using the components above, we produce the prototype of PBV-R. Fig.4-3 represents 3D design of the prototype. To minimize dead volume, we make length

Table 4-II. Components of prototype of PBV-R

Component			
No.	Parts	Article	Technical Date
1	Drive cylinder 1	SMC corporation, CDG1YL40-75FZ	Diameter : 40 [mm] Stroke : 75 [mm]
2	Expansion cylinder	SMC corporation, CG1WLN50-75FZ	Diameter : 40 [mm] Stroke : 75 [mm]
3	Drive cylinder 2	SMC corporation, CDG1YL40-75FZ	Diameter : 50 [mm] Stroke : 75 [mm]
4	Solenoid valves	SMC corporation, SV3200R-5W3LD-03	Effective area: 4.5~4.9 [dm³/s・bar] Critical pressure ratio : 0.27~0.29
5	Check valves	SMC corporation, AKH10-00	Effective area : 4.8 [dm³/s・bar] Critical pressure ratio : 0.5
6	Button switches	NKK switch, LP01-15CCKNS1R	changeover contact

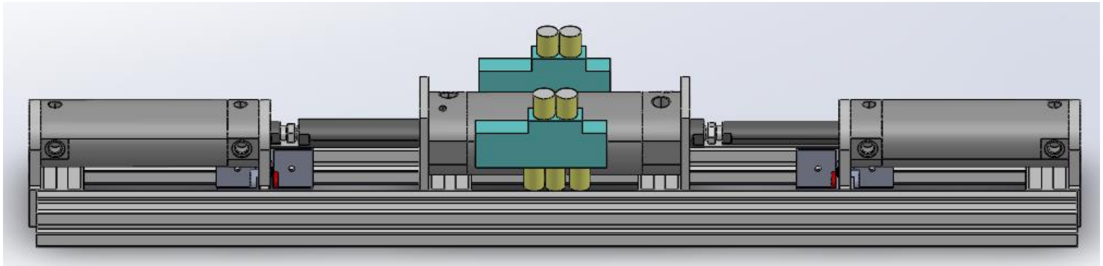

Fig.4-3. 3D design of prototype of PBV-R

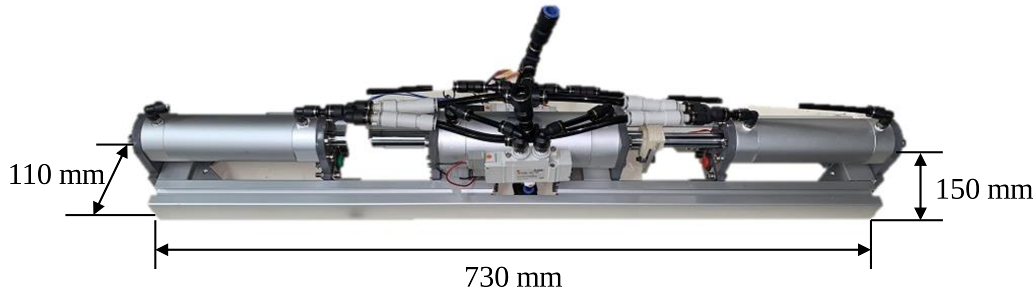

Fig.4-4. Actual prototype of PBV-R

of pipe as short as possible. To do that, we attach the solenoid valves parallel to a direction of piston rod and vertical to the ground on both sides of the expansion cylinder. Also, we add the button switches under the air cylinders. A button switch pusher for the button switches is also included. The two button switch pushers are fixed on each double-ended bolts and pushes button switches for changing position of the solenoid valves when the pistons reach to the end of the stroke. Based on the design and explanation above, we made the prototype of PBV-R as Fig.4-4.

4.2.2 Experimental Procedure

We investigate energy efficiency, boost ratio, effective consumption rate and pressure characteristic. In order to investigate the performances of the prototype of PBV-R, we carry out an experiment. First, we design a pneumatic circuit for the experiment as indicated in Fig.4-5. Compressed air from an air compressor is supplied, then it flows through a filter-regulator-lubricator (F.R.L) and PBV-R. if the compressed air is boosted by the PBV-R, it is exhausted and flows into an air tank of 10 dm^3. The states of the compressed air, e.g. pressure, flow rate and air power, are measured at both inlet

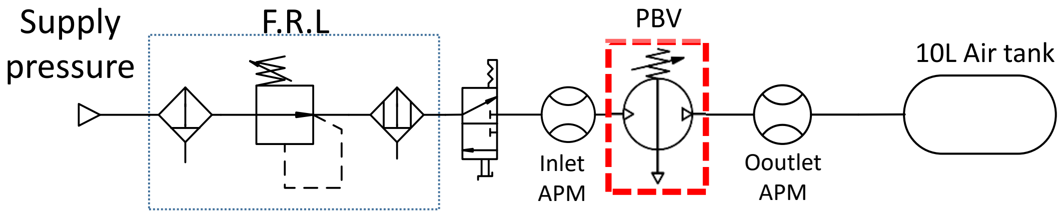

Fig.4-5. Pneumatic circuit of testing prototype

and outlet by the APMs.

Next, we explain the method of the experiment. We carry out the experiment by setting supply pressure as 300 kPa, 400 kPa and 500 kPa, respectively. Furthermore, we start measuring and supplying the compressed air at the same time. When the pistons and the piston rod do not move anymore, we stop the measurement.

4.2.3 Result of Experiment

Fig.4-6 indicates the energy efficiency of the prototype of PBV-R. The energy efficiency is around 63.9 percent at 300 kPa, 58.2 percent at 400 kPa and 58.0 percent at 500 kPa. In comparison to the results in Chapter 2, the energy efficiency of the prototype is 17.2 percent, 15.1 percent and 15.2 percent improved than that of the experimental apparatus at 300 kPa, 400 kPa and 500 kPa, respectively. It is considered that the reason is, as we found in Chapter 3, that dead volume rate of the experimental apparatus is higher than that of the prototype.

Fig.4-7 represents the boost ratio of the prototype of PBV-R. The boost ratio is around 1.69, 1.81 and 1.90 at 300 kPa, 400 kPa and 500 kPa, respectively. In comparison to the results in Chapter 2, the boost ratio decreases around 10 percent because the area ratio of the prototype is smaller than that of the experimental apparatus.

Fig.4-8 shows the effective consumption rate of the prototype of PBV-R. The effective consumption rate is around 46.8 percent, 45.6 percent and 45.9 percent at 300 kPa, 400 kPa and 500 kPa, respectively. Compared to the result in Chapter 2, these results are 3.3 percent, 6.4 percent and 7.4 percent greater than those of the apparatus. The main reason is considered as dead volume rate, like the energy efficiency.

Fig.4-9 indicates the pressure characteristic of the prototype of PBV-R at p_s=400 kPa. The pressure reaches the maximum at t=42 s.

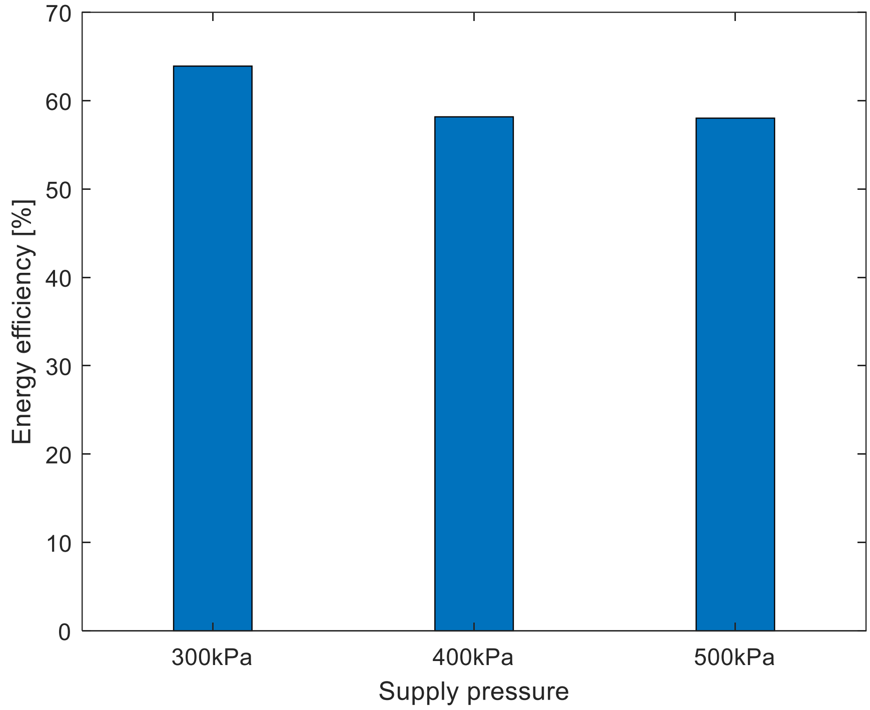

Fig.4-6. Energy efficiency of the prototype of PBV-R

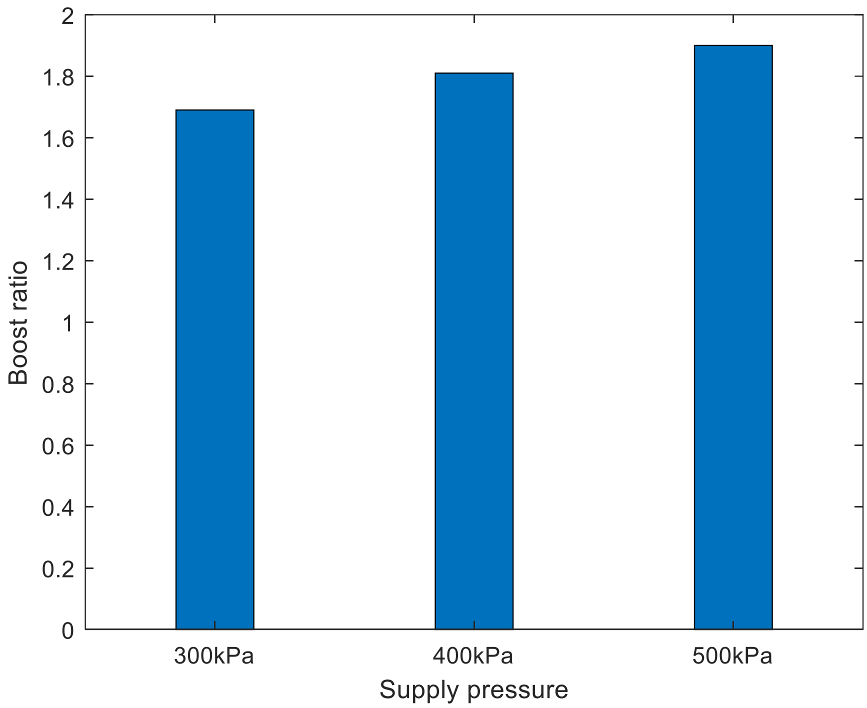

Fig.4-7. Boost ratio of the prototype of PBV-R

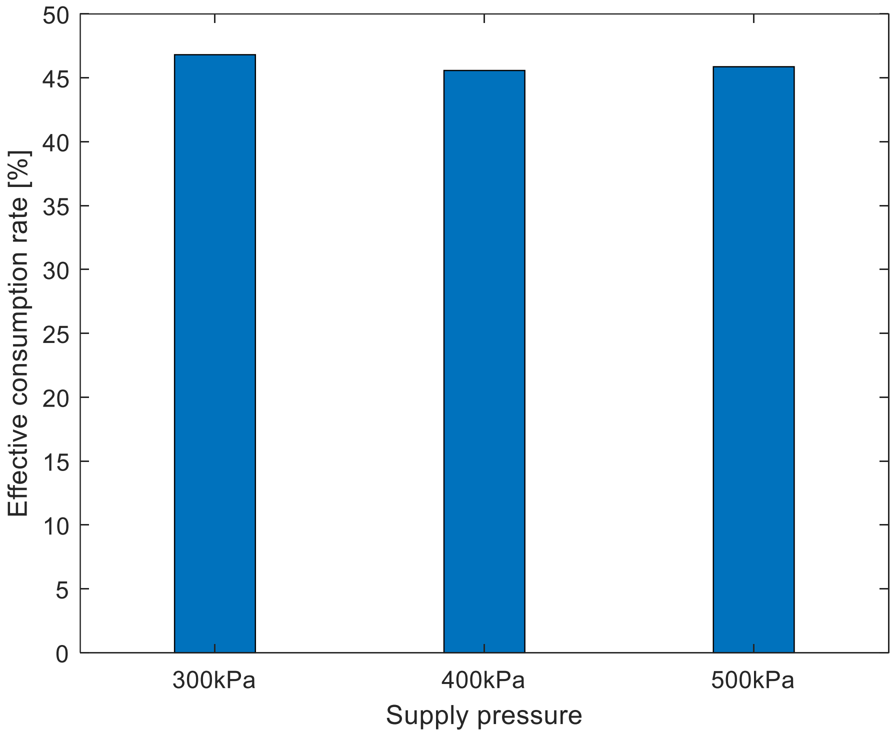

Fig.4-8. Effective consumption rate of the prototype of PBV-R

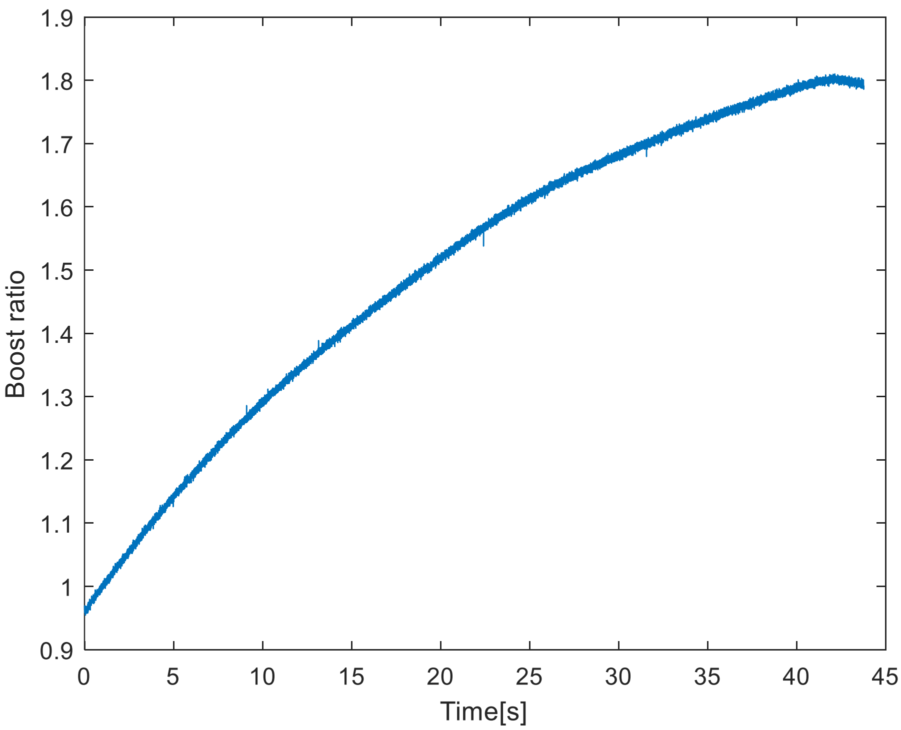

Fig.4-9. Pressure characteristic of the prototype of PBV-R

4.2.4 Comparison between PBV and PBV-R

First, in order to investigate the performances of the PBV on the market, VBA20A, manufactured by SMC, we carry out the same experiment in Section 4.2.2 and make use of PBV instead of the prototype of PBV-R.

Next, we compare the performance of the prototype with that of the VBA20A. Fig.4-10 indicates the comparison of energy efficiency of both prototype of PBV-R and VBA20A. the energy efficiency of the prototype is 10.5 percent, 6.3 percent and 6.9 percent higher than that of VBA20A at 300 kPa, 400 kPa and 500 kPa, respectively.

Fig.4-11 shows the comparison of boost ratio of both prototype of PBV-R and VBA20A. The boost ratio of the prototype is 6.1 percent, 8.1 percent and 31.9 percent higher than that of VBA20A at 300 kPa, 400 kPa and 500 kPa, respectively.

Fig.4-12 represents the comparison effective consumption rate of both prototype of PBV-R and VBA20A. The effective consumption rate of the prototype is 1.5 percent, 2.4 percent and 2.1 percent lower than that of VBA20A at 300 kPa, 400 kPa and 500 kPa, respectively, i.e., the results indicates that the effective consumption rate of the prototype of PBV is not improved. One of the reason is considered that dead volume of VBA20A is smaller than that of the prototype of PBV-R. In the case of VBA20A, because the whole pipes are built inside, the length of pipes are structurally shorter than that of the prototype of PBV-R whose pipes are built on the outside. Also, in the case of the prototype, because we produced this with manufactured air cylinders, there exist spaces between the air cylinders, which causes longer pipes. In the case of VBA20A, however, it has no space between air cylinders and has less dead volume than the prototype of PBV-R.

Table.4-III shows the comparison between VBA20A and the prototype of PBV-R. The prototype of PBV-R has structurally more disadvantages: the prototype is heavier, larger than VBA20A. Also, the prototype use electricity, while VBA20A does not. Furthermore, in terms of pneumatic circuit, the prototype has longer pipes than VBA20A. Those disadvantages occur because the prototype is made with existing manufactured components e.g. air cylinders, solenoid valves, check valves, etc., which cause more air leak and dead volume. However, in spite of the structural disadvantages, the prototype has better functional performances than VBA20A; energy efficiency and boost ratio of the prototype are greater than those of VBA20A. Hence, from these results, it is obvious that PBV-R can save a lot of energy consumption by mass production and application to industries.

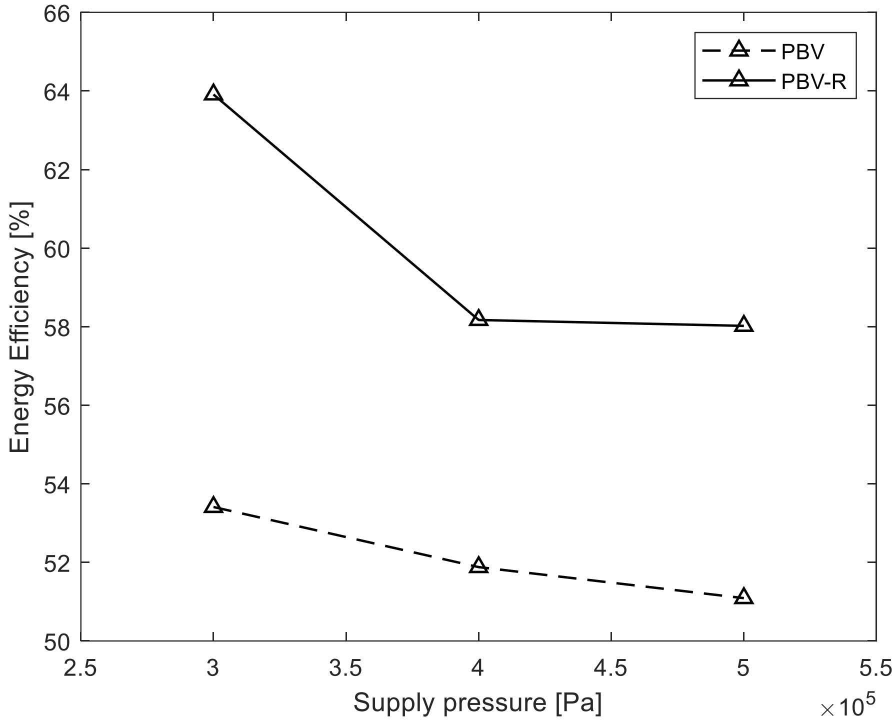

Fig.4-10. Comparison of energy efficiency between the prototype of PBV-R and PBV

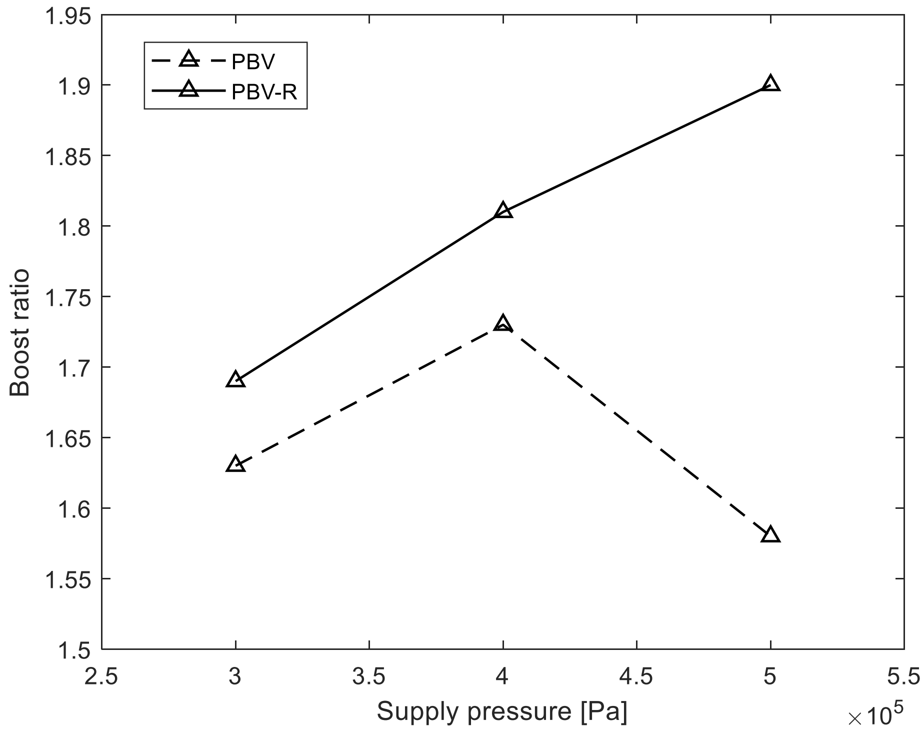

Fig.4-11. Comparison of boost ratio between the prototype of PBV-R and PBV

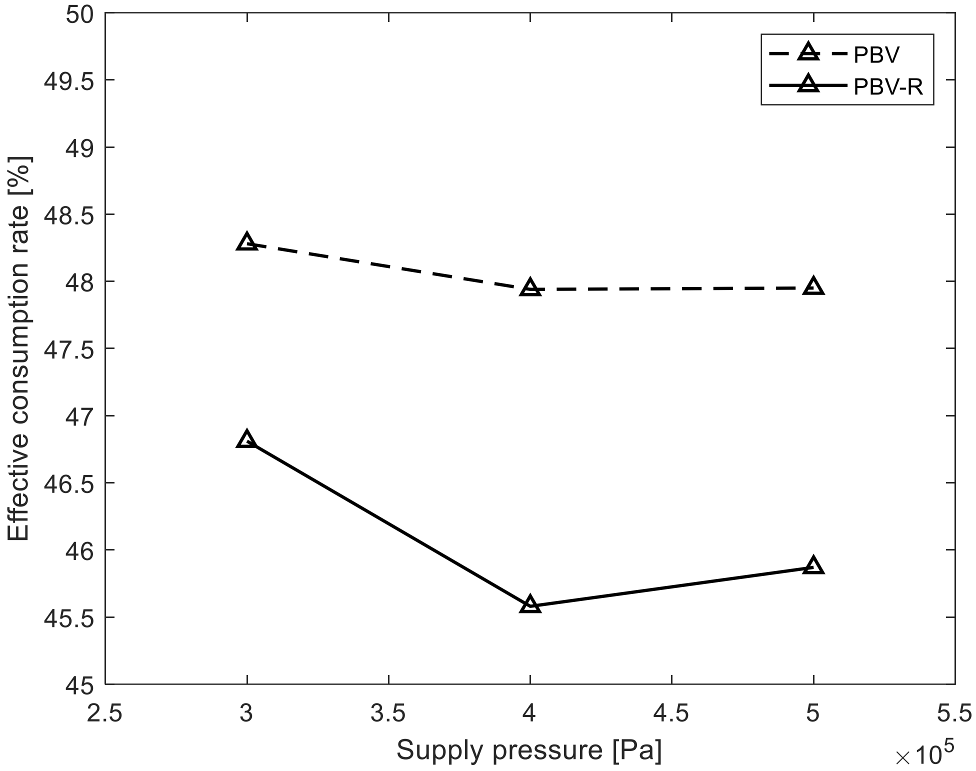

Fig.4-12. Comparison of effective consumption rate between the prototype of PBV-R and PBV

Table 4-III. Comparison of spec between VBA20A and prototype of PBV-R

Spec	VBA20A	Prototype of PBV-R
Size (mm)	L300×W98×H176	L730×W110×H150
Weight (kg)	3.9	6.2
Electric power	unnecessary	Necessary
Energy efficiency	53 %	60 %
Boost ratio	1.7	1.8

4.3 Effect of PBV-R on Energy Consumption of Whole Industry

The purpose of this thesis is to maximize the performances of PBV-R, e.g. energy efficiency, boost ratio and effective consumption rate. By using the results of this thesis, decrease of electricity energy consumption is expected if PBV-R is applied to the whole industries, as well as greenhouse gas emissions reduction which is encouraged by Kyoto protocol and Paris agreement. In this section, we calculate how much the electricity energy consumption and the greenhouse gas emissions can be reduced by applying PBV-R.

First, we carry out the calculation in case of a plant. The electricity energy consumption, E_e, can be obtained from the following equation:

$$E_e = P_{comp}Mt(1-e)[q+\frac{1}{\eta}(1-q)] \tag{4.5}$$

where P_{comp} represents electric power consumption, M represents motor load factor, t represents operation time, e represents energy-saving ratio which is a ratio of reduced power rate to existing power rate, q represents a ratio of the process that PBV or PBV-R is necessary in a plant, η represents energy efficiency of PBV or PBV-R.
Suppose there is a plant that operates air compressor under conditions shown in Table.4-IV [70]. Also, we assume q=1/3 and supply pressure is reduced from 0.6 MPa to 0.35 MPa, i.e., e is 0.2 according to Fig.1-3. We compare electricity energy consumption and carbon dioxide emission under three different conditions; (a) to operate the plant with supply pressure of 0.6 MPa without any PBV or PBV-R; (b) to operate the plant with supply pressure of 0.35 MPa and apply PBV to one-third of processes; and (c) to operate the plant with supply pressure of 0.35 MPa and apply PBV-R to one-third of processes. In the case of (a), due to e=0 and q=1, we can obtain the electricity energy consumption rate with only P_{comp}, M and t. In the case of (b) and (c), according to the results in Section 4.2, η is 51% in the case of PBV, while η is 64% in the case of PBV-R. In terms of CO_2, carbon dioxide emission factor is 0.455kg-CO_2/kWh in metropolitan area in Japan [71]. Table.4-V indicates the electricity energy consumption and the carbon dioxide emission of each case for a year.

Table 4-IV. Value of each parameter

parameter	value		
P_{comp}	320 [kW]		
t	500 [h/year]		
M	0.8		
q	(a) 0	(b) 1/3	(c) 1/3
e	-	(b) 0.2	(c) 0.2
η	-	(b) 0.51	(c) 0.60

Table 4-V. Energy efficiency, gas emission and electric charge in a plant

	(a) without PBV	(b) applying PBV	(c) applying PBV-R
Energy(MWh)	1280	1234	1140
Gas(t-CO_2)	582	561	518
Electric Charge(10^6Yen)	24.6	23.7	21.9

The difference of annual electricity energy consumption between (a) and (c) is 220 MWh, in other words, around 10.9 percent of the energy consumption is reduced. In Comparison to (b), 3.6 percent of the energy consumption is more reduced. In terms of the carbon dioxide emission, the difference between (a) and (c) is 64 t-CO_2, while the difference between (a) and (b) is only 21 t-CO_2. From the result, it is obvious that PBV-R can reduce both electricity energy consumption and carbon dioxide emission, and applying PBV-R to a plant brings improved results than applying PBV. In terms of the electric charge, applying PBV-R can save 2.7 million Yen a year, while applying PBV can save only 0.9 million Yen a year [72]. Because net profit of this company in 2017 was 8.2 billion Yen, the saved electric charge accounts for 0.3 percent of the net profit [73]. Hence, it is considered that applying PBV-R is meaningful for this company.

Next, we expand the calculation in case of the whole industries in Japan. According to statistics [74], electricity consumption of the whole industry accounts for 42.8 percent of the entire electricity consumption in Japan. Also, electricity consumption by machines using motors accounts for 62 percent of the electricity consumption of the whole industries, 23 percent of which is caused by air compressor. Then, as we carried out above, we compare electricity energy consumption and carbon dioxide emission under three different conditions. (a) to operate the entire plants in Japan with supply pressure of 0.6 MPa without any PBV or PBV-R; (b) to operate the entire plants in Japan with supply pressure of 0.35 MPa and apply PBV to one-third of processes; and (c) to operate the entire plants in Japan with supply pressure of 0.35 MPa and apply PBV-R to one-third of processes. From the calculation above, we already know that 7 percent or 16.2 percent of the electricity consumption by air compressors is reduced if PBV or PBV-R is applied, respectively. Also, according to the statistics, the entire electricity consumption in Japan is 1280 MWh [75]. Therefore, electricity energy consumption and the carbon dioxide emission of each case for a year can be calculated as Table.4-VI.

Table 4-VI. Energy efficiency, gas emission and electric charge in the entire industry in Japan

	(a) without PBV	(b) applying PBV	(c) applying PBV-R
Energy(TWh)	84.3	81.3	75.0
Gas(Mt-CO_2)	38.4	37.0	34.2
Electric Charge(10^{12}Yen)	1.62	1.51	1.35

The difference of annual electricity energy consumption between (a) and (c) is 9.3 TWh, which accounts for around 0.9 percent of the energy consumption of the whole industry, while the difference between (a) and (b) is 3.0 TWh, which accounts for only 0.4 percent of the energy consumption of the whole industry. In terms of the carbon dioxide emission, the difference between (a) and (c) is 4.2 Mt-CO_2, while the difference between (a) and (b) is only 1.4 Mt-CO_2.

4.4 Summary

We list the following conclusion from the experiment and discussion in this chapter:

1. We found that PBV-R with less dead volume rate can achieve higher energy efficiency from the result in Chapter 3. However, producing PBV-R with the dead volume rate of almost zero costs too much. Thus, it is considered that there exists optimal stroke length that makes energy efficiency of PBV-R higher and expense of manufacturing lower. By evaluating the production expense of PBV-R, we found that the expense has the minimum value at stroke length of 73 mm. Hence, it is desirable to utilize air cylinders with stroke length of 75 mm.

2. On the basis of the result in Chapter 3 and Section 4.1, we designed and produced a prototype of PBV-R, and carried out the experiment for investigate the performances of the prototype. The energy efficiency of the prototype is 63.9 percent, 58.2 percent and 58.0 percent at 300 kPa, 400 kPa and 500 kPa, respectively. The boost ratio of the prototype is 1.69, 1.81 and 1.90 at 300 kPa, 400 kPa and 500 kPa, respectively. Furthermore, the effective consumption rate of the prototype is 46.8 percent, 45.6 percent and 45.9 percent at 300 kPa, 400 kPa and 500 kPa, respectively. In comparison to the result in Chapter 2, the energy efficiency and the effective consumption rate were improved, whereas the boost ratio was not improved.

3. We compared the prototype with VBA20A, a product of PBV manufactured by SMC. The energy efficiency of the prototype of PBV-R is 10.5 percent, 6.3 percent and 6.9 percent higher than that of VBA201 at 300 kPa, 400 kPa and 500 kPa, respectively. Furthermore, the boost ratio of the prototype is 6.1 percent, 8.1 percent and 31.9 percent higher than that of VBA20A at 300 kPa, 400 kPa and 500 kPa, respectively. However, the effective consumption rate of the prototype is 1.5 percent, 2.5 percent and 2.1 percent lower than that of VBA20A at 300 kPa, 400 kPa and 500 kPa, respectively.

4. According to calculation under some assumptions, if PBV or PBV-R is applied to a plant, the plant that applied PBV can save 90 MWh, which is equivalent to 7.0

percent of the entire annual electricity energy, and reduce 41 ton of CO_2 emission annually. Furthermore, the plant that applied PBV-R can save 220 MWh annually, which is 130 MWh higher than the case of PBV and equivalent to 16.2 percent of the entire annual electricity energy, and also reduce 100 ton of CO_2 emission annually. Next, according to calculation like above, if PBV or PBV-R is applied to the whole industry in Japan, 5.7 TWh, which accounts for 0.6 percent of annual electricity energy consumption in the whole industry, can be saved if PBV is applied, while 14 TWh, which accounts for 1.4 percent, can be conserved if PBV-R is applied. Likewise, applying PBV-R to the entire industry can reduce 6.4 kiloton of carbon dioxide emission, whereas applying PBV can reduce only 2.6 kiloton of carbon dioxide emission.

Chapter 5
Conclusion

5.1 Summary

Previous version of pneumatic booster valve (PBV) has been used to boost compressed air for decades. In this research, a pneumatic booster valve with energy recovery (PBV-R), which is an improved version of PBV, is developed. The structure of PBV-R has one more air cylinder than PBV called 'Expansion Cylinder.' Since the Expansion Cylinder has an energy recovery function, PBV-R is improved in terms of energy efficiency than PBV.

In Chapter 1, we introduce background that too much energy consumption occurs in the industry in Japan, especially in pneumatic systems. Thus, the law of Japan, Kyoto Protocol and Paris Agreement encourage that mankind has to make effort to reduce energy consumption. Under the background, several researches have been carried out to develop technologies of energy saving in pneumatic systems. Among all, applying PBV to plants is considered as one of the simplest and most effective method that reduces the energy consumption. Furthermore, PBV-R has been proposed and the it has been numerically validated that the energy efficiency of PBV-R is greater than that of PBV. However, the performance of PBV-R has not been experimentally proved yet, although numerical simulation is usually inaccurate in fluid mechanics. Therefore, we set up the purpose of this thesis as experimental validation and development of PBV-R.

In Chapter 2, We designed a pneumatic circuit and set up an experimental apparatus for investigating the performances between PBV method and PBV-R method, e.g. energy efficiency, boost ratio and effective consumption rate. firstly, the energy efficiencies of PBV-R method were up to 8% greater than PBV method. Secondly, the boost ratios of PBV-R method were up to 17% greater than that of PBV method. Thirdly, effective consumption rates of PBV-R method are up to 5% greater than those of PBV method. Fourthly, we confirmed that the high-pressure air that was supposed to be exhausted in case of PBV method was partly reused in PBV-R method. Furthermore, we investigated how much energy is recovered and reused by an expansion cylinder. To do that, we defined "recovery ratio" and investigated at each area ratio. As a result, we found that the area ratio that maximizes recovery ratio is 1.9, 2.6, 3.6 and 4.6 at ps=200 kPa, 300 kPa, 400 kPa and 500 kPa, respectively.

In Chapter 3, unlike the experimental apparatus in Chapter 2, we designed a pneumatic circuit and set up a new experimental apparatus that can change all air cylinders in order to investigate the performances under different geometric parameters, e.g. area ratio and stroke length. If the stroke length is constant, firstly, the energy efficiency is the greatest where an area ratio is 1.56. Secondly, the boost ratio is the greatest where an area ratio is 2.66. Thirdly, the effective consumption rate is the greatest where a stroke length is 100 mm and an area ratio is 1.56. If the area ratio is constant, firstly, the energy efficiency is the greatest where a stroke length is 100 mm. Secondly, the boost ratio is the greatest where a stroke length is 50 mm or more. Thirdly, the effective consumption rate is the greatest where a stroke length is 100 mm. The results show that the energy efficiency of PBV-R increases as stroke length becomes longer, whereas numerical results indicates stroke length does not have any effect on energy efficiency of PBV-R. The reason is considered as dead volume, Therefore, we carried out calculation of energy efficiency of PBV-R with consideration of dead volume and the results indicates that dead volume rate has a large effect on energy efficiency of PBV-R and this conclusion can explain the reason that PBV-R with shorter stroke length shows smaller energy efficiency.

In Chapter 4, Since it is considered that there exists optimal stroke length that makes energy efficiency of PBV-R higher and expense of manufacturing lower, we investigated the optimal stroke length by evaluating cost and found that stroke length of 73 mm make the entire costs minimum. On the bases of the result, we designed and produced a prototype of PBV-R, and carried out the experiment for investigate the performances of the prototype. The energy efficiency of the prototype is 63.9 percent, 58.2 percent and 58.0 percent at 300 kPa, 400 kPa and 500 kPa, respectively. The boost ratio of the prototype is 1.69, 1.81 and 1.90 at 300 kPa, 400 kPa and 500 kPa, respectively. Furthermore, the effective consumption rate of the prototype is 46.8 percent, 45.6 percent and 45.9 percent at 300 kPa, 400 kPa and 500 kPa, respectively. In comparison to the result in Chapter 2, the energy efficiency and the effective consumption rate were improved, whereas the boost ratio was not improved. Also, in comparison to VBA20A, the energy efficiency and the boost ratio of the prototype of PBV-R are up to 10.5 percent and 31.9 percent improved, respectively, while the effective consumption rate of the prototype of PBV-R is up to 2.5 percent lower. According to a calculation, the plant that applied PBV-R can save 16.2 percent of the entire annual electricity energy and reduce 100 ton of CO_2 emission annually. Furthermore, if PBV-R is applied to the whole industry in Japan, 0.6 percent of annual electricity energy consumption in the entire industry can be saved and reduce 6.4 kiloton of carbon dioxide emission annually.

5.2 Future Work

In Chapter 3, we define dead volume as the entire volume except air cylinder and we confirm the effect of dead volume on energy efficiency of PBV-R. Since volume of pipe also belongs to the dead volume, it is necessary to reduce the volume of pipe as much as possible. There is a structural limit to shortening the pipe, thus we need to make cross section area of the pipe smaller. However, air cannot flow if the area is near zero. Moreover, according to flow-rate characteristics in ISO6358, because flow rate is proportional to effective cross-section area, the area needs to be not too small [76]. Therefore, it is assumed that the optimal area that makes the energy efficiency of PBV-R maximum exists between zero and positive infinity. It is considered that this can be calculated not by numerical analysis that uses ideal gas equation but by numerical analysis flow dynamics in air cylinders and pipes.

Reference

[1] Panasonic [Online], Available: https://web.archive.org/web/20081209114436/http://industrial.panasonic.com/ww/i_e/25000/fa_pro_acs_minas_a4_e/fa_pro_acs_minas_a4_e/a4_16.pdf/, Accessed Jan 2020.

[2] Platypus Power [Online], Available: https://web.archive.org/web/20091001190130/http://www.platypuspower.com.au/240specs.html, Accessed Jan 2020.

[3] Atlas Copco, [Online], Available: https://web.archive.org/web/20120401094336/http://www.atlascopco.co.uk/Images/AirMotor_catalogue.ENG_tcm795-1610751.pdf, Accessed Jan 2020.

[4] KYUSEI [Online], Available: https://www.kyusei.co.jp/factory/flow, Accessed Nov 2019.

[5] 東京都下水度局 [Online], Available: http://www.gesui.metro.tokyo.jp/business/technology-statistics/fukyu/kaisetsu/, Accessed Jan 2020.

[6] Daifuku [Online], Available: https://www.daifuku.com/en/solution/automotive/, Accessed Jan 2020.

[7] Healthy Enviro Solution ltd. [Online], Available: https://healthyenvirosolutions.com/sewage-treatment-plant-manufacturer-bhubaneswar-odisha-india/, Accessed Jan 2020.

[8] Tech4 [Online], Available: https://tech4gamers.com/intel-is-making-its-way-to-10nm-will-discuss-it-later-this-year/, Accessed Jan 2020.

[9] 日本経済新聞 [Online], Available: https://www.Nikkei.com/article/DGXMZO27203090R20C18A2L21000/, Accessed Jan 2020.

[10] EMARO Pneumatic Endoscope Manipulator Robot [Online], Available: https://www.riverf ieldinc.com/en/product/, Accessed Jan 2020.

[11] Nd, D.M.; Fischer, S.A.; Gauthier, P.W.; Luna, C.H.; Clancy, E.A.; Fischer, G.S. A soft robotic exomusculature glove with integrated sEMG sensing for hand rehabilitation. In Proceedings of the 2013 IEEE International Conference on Rehabilitation Robotics, Seattle, WA, USA, 24–26 June 2013; pp. 1–7.

[12] Nycz, C.J.; Delph, M.A.; Fischer, G.S. Modeling and design of a tendon actuated soft robotic exoskeleton for hemiparetic upper limb rehabilitation. In Proceedings of the 37th Annual International Conference of the IEEE Engineering in Medicine and Biology Society, Milan, Italy, 25–29 August 2015; pp. 3889–3892

[13] Xiloyannis, M.; Cappello, L.; Khanh, D.B.; Yen, S.C.; Masia, L. Modelling and design of a synergy-based actuator for a tendon-driven soft robotic glove. In Proceedings of the 2016

6th IEEE International Conference on Biomedical Robotics and Biomechatronics, Singapore, 26–29 June 2016; pp. 1213–1219
[14] Tsukagoshi, H., Sasaki, M., Kitagawa, A., & Tanaka, T. (2005, April). Design of a higher jumping rescue robot with the optimized pneumatic drive. In Proceedings of the 2005 IEEE International Conference on Robotics and Automation (pp. 1276-1283). IEEE.
[15] Kurumaya, S., Suzumori, K., Nabae, H., & Wakimoto, S. (2016). Musculoskeletal lower-limb robot driven by multifilament muscles. Robomech Journal, 3(1), 18.
[16] TOYOTA, [Online], Available: https://global.toyota/jp/company/profile/production-sales-figures/, Accessed Jan 2020.
[17] “Semiconductor Unit Shipments Exceeded 1 Trillion Devices in 2018”, [Online], Available: http://www.icinsights.com/news/bulletins/Semiconductor-Unit-Shipments-Exceeded-1-Trillion-Devices-In-2018/, Accessed Jan 2020.
[18] 日本フルードパワー工業会, [Online], Available: http://www.jfpa.biz/wp-content/uploa ds/39a601dd94d9a1374899ea1f112ca9d4.pdf, Accessed Jan 2020
[19] 経済産業省資源エネルギー庁 [Online], Available: https://www.enecho.meti.go.jp/about/whitepaper/2018html/2-1-4.html, Accessed Jan 2020.
[20] HITACHI [Online], Available: https://library.hitachi-ies.co.jp/assets/pdf/ZZ-172.pdf, Accessed Jan 2020.
[21] Government, S.V., Energy Efficiency Best Practice Guide Compressed Air Systems.
[22] Radgen, P. and E. Blaustein, Compressed Air System in the European Union: Energy, Emissions, Savings Potential and Policy Actions, 2001.
[23] Energy Tips: Compressed Air, U.D.o. Energy, Editor August 2004.
[24] Kyoto protocol, [Online], Available: https://treaties.un.org/pages/ViewDetails.aspx?src=TREATY&mtdsg_no=XXVII-7-a&chapter=27&lang=en, Accessed Jan 2020
[25] Paris Agreement , [Online], Available: https://treaties.un.org/pages/ViewDetails.aspx?src=TREATY&mtdsg_no=XXVII-7-d&chapter=27&clang=_en, Accessed Jan 2020.
[26] エネルギーの使用の合理化等に関する法律, [Online], Available: https://elaws.e-gov.go.jp/search/elawsSearch/elaws_search/lsg0500/detail?lawId=354AC0000000049, Accessed Jan 2020
[27] Rinoshika, A., & Suzuki, M. (2010). An experimental study of energy-saving pneumatic conveying system in a horizontal pipeline with dune model. Powder Technology, 198(1), 49-55.
[28] Yang, A., Pu, J., Wong, C. B., & Moore, P. (2009). By-pass valve control to improve energy efficiency of pneumatic drive system. Control Engineering Practice, 17(6), 623-628.
[29] Al-Dakkan, K. A., Goldfarb, M., & Barth, E. J. (2003, July). Energy saving control for

pneumatic servo systems. In Proceedings 2003 IEEE/ASME International Conference on Advanced Intelligent Mechatronics (AIM 2003) (Vol. 1, pp. 284-289). IEEE.
[30] Harris, P., Nolan, S., & O'Donnell, G. E. (2014). Energy optimisation of pneumatic actuator systems in manufacturing. Journal of cleaner production, 72, 35-45.
[31] Ke, J., Wang, J., Jia, N., Yang, L., & Wu, Q. H. (2005, August). Energy efficiency analysis and optimal control of servo pneumatic cylinders. In Proceedings of 2005 IEEE Conference on Control Applications, 2005. CCA 2005. (pp. 541-546). IEEE.
[32] 工場の省エネルギーガイドブック, [Online], Available: https://www.shindan-net.jp/pdf/factory.pdf, Accessed Jan 2020
[33] ANEST IWATA, [Online], Available: https://www.anest-iwata.co.jp/compressor/scroll/03_spec.html, Accessed Jan 2020.
[34] マックス株式会社, [Online], Available: https://wis.max-ltd.co.jp/kikouhin/catalog_search.html, Accessed Jan 2020.
[35] K. Nakasho, Pneumatic Booster Device, Japan Patent 昭 48-67303, Aug 27, 1973.
[36] R. S. Policonis, Pneumatic Booster Device, Japan Patent 昭 52-92104, Oct 3, 1977.
[37] A. Moriya, Pneumatic Booster Device, Japan Patent 昭 50-115603, Feb 5, 1975.
[38] R. Kawai, Pneumatic Booster Device, Japan Patent 昭 48-67303-01, Nov 27, 1973.
[39] S. Sugino, Pneumatic Booster Device, Japan Patent 昭 48-82267, Nov 2, 1973.
[40] K. Inoue, T. Yamane, S. Tokuda, Pneumatic Booster Device, Japan Patent 昭 61-6003, Jan 14, 1986.
[41] K. Kishimoto, Pneumatic Booster Device, Japan Patent 昭 63-243502, Oct 11, 1988.
[42] Hamaura, N., Fujita, T., Kagawa, T.: Characteristics Analysis of Pneumatic Booster, Proceedings of Autumn Symposium on Hydraulics and Pneumatics, p.77-80(1994)
[43] Wang, H., Xiong, W., Wang, X.: Research on the static characteristics of air driven gas booster, Proceedings of the JFPS International Symposium on Fluid Power, The Japan Fluid Power System Society, Vol. 2008, No. 7-3, p.715- 718 (2008)
[44] SMC corporation [Online], Available: http://ca01.smcworld.com/catalog/ja/frl/VBA/ 6-6-p1007-1038-vba/data/6-6-p1007-1038-vba.pdf, Accessed Jan 2020.
[45] Shi, Y., & Cai, M. (2013). Dimensionless study on output flow characteristics of expansion energy used pneumatic pressure booster. Journal of Dynamic Systems, Measurement, and Control, 135(2), 021007.
[46] M. Stephan, M. Murrenhoff, “Exergy based analysis of pneumatic air saving measures,” in ASME/BATH 2015 Symposium on Fluid Power and Motion Control, 2015, pp. V001T01A007.
[47] Y. Shi, M. Cai, “Working characteristics of two kinds of air-driven boosters,” Energy

Conversion and Management., vol. 52, no. 12, pp. 3399-3407, Accessed Jan 2020.
[48] Shi, Yan, et al. "Flow characteristics of expansion energy used pneumatic booster." Chinese Journal of Mechanical Engineering 25.5 (2012): 889-896.
[49] Shi, Yan, and Mao-lin Cai. "Study on efficiency and flow characteristics of two kinds of pneumatic booster valves." 2010 International Conference on Computer, Mechatronics, Control and Electronic Engineering. 2010.
[50] T. Kagawa, T. Takahashi, Pneumatic Booster Valve, Japan Patent 8-21404, 1996.
[51] Yang F, Li G, Tadano K, Kagawa T (2016) Characteristics Analysis of Pneumatic Booster Valve with Energy Recovery, BATH/ASME 2016 Symposium on Fluid Power and Motion Control, American Society of Mechanical Engineers, p. V001T01A016-V001T01A016
[52] Yang F, Tadano K, Li G, Kagawa T (2017) Analysis of the energy efficiency of a pneumatic booster regulator with energy recovery, Applied Sciences, Vol.7, Issue 8, 816
[53] Yang, F., Tadano, K., Li, G., & Kagawa, T. (2016). Dimensionless Analysis on the Characteristics of Pneumatic Booster Valve with Energy Recovery. Mathematical Problems in Engineering, 2016.
[54] Bridson, R. Fluid simulation for computer graphics. AK Peters/CRC Press. (2015)
[55] James, A. F. (1994). Introduction to fluid mechanics. Cambridge: MIT Press, MA.
[56] Nikuradse, Johann. Strömungsgesetze in rauhen Rohren. VDI-Verlag, 1933.
[57] Colebrook, C. F., Blench, T., Chatley, H., Essex, E. H., Finniecome, J. R., Lacey, G., ... & Macdonald, G. G. (1939). Correspondence. turbulent flow in pipes, with particular reference to the transition region between the smooth and rough pipe laws.(includes plates). Journal of the Institution of Civil engineers, 12(8), 393-422.
[58] McKeon, B. J., Zagarola, M. V., & Smits, A. J. (2005). A new friction factor relationship for fully developed pipe flow. Journal of fluid mechanics, 538, 429-443.
[59] 渡嘉敷ルイス, 藤田壽憲, & 香川利春. (1997). 管路を含む空気圧シリンダシステムのシミュレーション. 油圧と空気圧, 28(7), 766-771.
[60] Manning, J. R. (1968). Computerized method of characteristics calculations for unsteady pneumatic line flows. Journal of Basic Engineering, 90(2), 231-240.
[61] Cai Maolin, Kenji Kawashima, and Toshiharu Kagawa : Power assessment of flowing compressed air. Journal of fluids engineering 128.2, 402-405 (2006)
[62] 蔡茂林, 藤田壽憲, & 香川利春. (2001). 空気圧駆動システムにおけるエネルギー消費とその評価. 日本油空圧学会論文集, 32(5), 118-123.
[63] Harris, P.G.; O’Donnell, G.E.; Whelan, T. Modelling and identification of industrial pneumatic drive system. Int. J. Adv. Manuf. Technol. 2012, 58, 1075–1086.

[64] Li, J.; Kawashima, K.; Fujita, T.; Kagawa, T. Control design of a pneumatic cylinder with distributed model of pipelines. Precis. Eng. 2013, 37, 880–887.

[65] Belforte, G., Mattiazzo, G., Mauro, S., & Tokashiki, L. R. (2003). Measurement of friction force in pneumatic cylinders. Tribotest, 10(1), 33-48.

[66] SMC Corporation [Online], Available: http://ca01.smcworld.com/catalog/ja/actuator/CG1-CDG1-Z/6-2-1-p0287-0362-cg1/data/6-2-1-p0287-0362-cg1.pdf, Accessed Jan 2020.

[67] SMC Corporation [Online], Available: http://www.smcworld.com/products/select_guide/ja-jp/actuator/aircylinder_data.html, Accessed Jan 2020.

[68] HITACHI [Online], Available: https://library.hitachi-ies.co.jp/assets/pdf/HC-268.pdf, Accessed Jan 2020.

[69] SMC 株式会社 [Online], Available: http://ca01.smcworld.com/catalog/BEST-5-5-jp/pdf/5-p0921-0943-vba.pdf, Accessed Jan 2020.

[70] 株式会社 IHI 原動機 [Online], Available: https://www.ihi.co.jp/ips/enviro/eco_action/2013/ecor2013-7.pdf, Accessed Jan 2020.

[71] TEPCO [Online], Available: http://www.tepco.co.jp/ep/notice/news/2019/1516230_8907.html, Accessed Jan 2020.

[72] TEPCO [Online], Available: http://www.tepco.co.jp/ep/corporate/plan_h/plan03.html, Accessed Nov 2019.

[73] 株式会社 IHI 原動機 [Online], Available: https://www.ihi.co.jp/var/ezwebin_site/storage/original/application/8ec544b497c5be38775eaa7a8d54b922.pdf, Accessed Jan 2020.

[74] 経済産業省資源エネルギー庁 [Online], Available: https://www.enecho.meti.go.jp/about/whitepaper/2013html/2-1-2.html, Accessed Jan 2020.

[75] グローバルエネルギ統計イヤーブック [Online], Available: https://yearbook.enerdata.jp/electricity/electricity-domestic-consumption-data.html, Accessed Jan 2020.

[76] ISO, I. (1989). 6358: 1989 Pneumatic fluid power-Components using compressible fluids-Determination of flow-rate characteristics. International Organization for Standardization Std.

Thanks

Time flies like an arrow. I still remember the scene when I walked into the Suzukakedai campus for the first time. In this three year, there are so many people helped me, and I have learned a lot of both study and life. Firstly, I want to thank my families for their love to me. Without their supports, I could not finish my doctoral course. Secondly my advisor, Associate Prof. Tadano, is an outstanding engineer and academic, who gave me precious guidance and advices in research and help me to finish the doctoral program. Thirdly, I also want to thank Prof. Kagawa for helping and giving me advices even though he is not formal advisor.

In Tadano lab, Zhou san has much experience in Tadano lab and helped me. Saito san is a very interesting people, and we have good two-year life. Jeong san is a student from Korea as the same as me, and we helped each other a lot, as well as enjoying several parties. The graduated doctoral student Yoshiki san is also a great and fun person.

The undergraduate and master students of Tadano Lab are excellent people. Funami san, Takayama san, Ishida san, Yamaguchi san, Konno san, Kimura san, Shiozaki san, Takeishi san, Mizuno san, Aizawa san, Sasajima san, Nakamori san, Hayakawa san, Takeyama san, Irie san, Miyata san, Uematsu san and Aoyama san.

I feel fortunate to have the great three years in Tadano Lab. Also, I am looking forward to the challenging future.